Dissertation zur Erlangung des Doktorgrades
der Fakultät für Chemie und Pharmazie
der Ludwig-Maximilians-Universität München

Effects of abiotic stimuli and the phytohormone ABA on the expression of the aquaporin gene family in maize roots

Chuanfeng Zhu

aus

Henan, VR. China

2005

Erklärung

Diese Dissertation wurde im Sinne von § 13 Abs. 3 bzw. 4 der Promotionsordnung vom 1. Juni 2001 von PD Dr. Anton R. Schäffner betreut.

Ehrenwörtliche Versicherung

Diese Dissertation wurde selbstständig, ohne unerlaubte Hilfe erarbeitet.

München, am 15.03.2005

(Chuanfeng Zhu)

Dissertation eingereicht am: 15.03.2005

1. Gutachter: PD Dr. Anton R. Schäffner
2. Gutachter: Prof. Dr. Stefan Weiss

Mündliche Prüfung: 23.05.2005

INDEX

Abbreviation

A. Introduction 1

1. Water uptake and transport in plants 1
1.1. Water uptake and transport in plants 1
1.2. Transmembrane water transport 2

2. Effect of abiotic stimuli and ABA on plants 3
2.1. Salt stress 3
2.1.1. Effect on water relation 4
2.1.2. Reduced growth 4
2.1.3. Ionic homeostasis 5
2.1.4. Osmolyte biosynthesis 6
2.1.5. Molecular response to salt stress 7
2.2. ABA 8
2.2.1. ABA and its physiological effects 8
2.2.2. Molecular response to ABA 9
2.3. Effect of nutrient-deficiency on plants 10
2.3.1. Nitrate deficiency 10
2.3.1.1. Stimulation of root growth 11
2.3.1.2. Effect on plant water relation 11
2.3.2. K^+-deficiency 12
2.3.2.1. Cell extension 12
2.3.2.2. Stomatal movement 13
2.3.2.3. Water uptake of roots 13

3. Aquaporins in plants 14
3.1. History of aquaporin 14
3.2. Structure and function of aquaporins 14
3.3. Expression of AQP 16
3.4. Regulation of aquaporin 17
3.5. ZmMIPs 18
4. Goal of the project 20

B. Material and Methods 22

1. Materials 22
1.1. Biological Material 22
1.1.1. Plants 22
1.1.2. Bacteria 22
1.1.3. Enzyme and antibody 22
1.1.4. Vectors and oligonucleotides 22
1.2. Chemicals 23
1.3. Molecular biology kits 23
1.4. Apparatus and software 23
1.4.1. Apparatus and equipment 23
1.4.2. Software and internet address 24

1.5.	Solutions and nutrient medium	24
1.5.1.	Solutions	24
1.5.2.	Bacterial medium	26
1.5.3.	Plant medium	27
1.5.4.	Consumed materials	27
2.	**Methods**	27
2.1	Nucleic acids	27
2.1.1.	Isolation of total RNA from maize roots	27
2.1.1.1.	Extraction of total RNA using Trizol reagent	27
2.1.1.2.	Isolation of total RNA using Qiagen RNeasy Plant Mini Kit	28
2.1.2.	Isolation of genomic DNA from maize	28
2.1.3.	Preparation of plasmid DNA	29
2.1.4.	Purification of PCR products	29
2.1.5.	Determination of concentration of nucleic acids	29
2.1.6.	Separation of nucleic acid on agarose gel electrophoresis	29
2.1.7.	Digestion of DNA by restriction endonucleases	30
2.1.8.	Ligation and transformation in *E. coli*	30
2.1.8.1.	Preparation of competent cell	30
2.1.8.2.	GATEWAY recombination	31
2.1.8.3.	Transformation of competent cell	31
2.1.9.	PCR (polymerase chain reaction)	31
2.1.10.	Sequence analyses	32
2.2.	Macroarray analysis	32
2.2.1.	PCR amplification and purification of target DNA fragments	32
2.2.2.	Array printing preparation of membranes	33
2.2.3.	Hybridization with reference probe	33
2.2.4.	In vitro transcription	34
2.2.5.	Preparation of complex probes	35
2.2.6.	Hybridization with complex probe	35
2.2.7.	Data evaluation	35
2.3.	Semi quantitative RT-PCR and quantitative RT-PCR	36
2.3.1.	Semi quantitative RT-PCR	36
2.3.2.	Quantitative real time RT-PCR	37
2.4.	Northern analysis	38
2.5.	In situ hybridization	39
2.5.1.	Tissue fixation and embedding	39
2.5.2.	Sectioning	39
2.5.3.	Synthesis of probe	40
2.5.4.	In situ hybridization on sections	40
2.5.5.	Detection of signal	40
2.6.	Microbiological methods	41
2.6.1.	Culture of bacterial in liquid medium	41
2.6.2.	Culture of Bacterial on agar plate	41
2.6.3.	Glycerol culture	41
2.7.	Protein isolation and detection	41
2.7.1.	Isolation of protein	41
2.7.1.1.	Extraction of microsomal fractions from maize roots	41
2.7.1.2.	Isolation of protein from *E.coli*	42
2.7.2.	Purification of GST-fusion protein	42
2.7.3.	Measurement of activity of GST-fusion protein	42

2.7.4.	Determination of protein concentration	43
2.7.4.1.	Bradford method	43
2.7.4.2.	Lowry method	43
2.7.5.	SDS-PAGE	43
2.7.6.	Staining of SDS-PAGE gel	44
2.7.6.1.	Coommassie brilliant blue (CBB)	44
2.7.6.2.	Pro-Q Diamond	44
2.7.6.3.	Sypro-ruby	44
2.7.7.	Western analysis	45
2.7.7.1.	Transfer of protein from gel to nitrocellulose membranes	45
2.7.7.2.	Immunological detection of ZmPIP proteins	45
2.8.	Culture of plants and physiological methods	46
2.8.1.	Culture of plants	46
2.8.2.	Treatment of plants by NaCl and ABA	47
2.8.3.	Measurement of water content in maize leaves	47
2.8.4.	Assay of ABA concentration in maize roots	47
2.9.	Statistical analysis	47
C.	**Results**	48
1.	**Design of *ZmMIP* array**	48
1.1.	Selection of target sequences for *ZmMIP* array	48
1.2.	Data analysis and normalization	50
1.3.	Reproducibility of *ZmMIP* DNA array	51
2.	**Expression of *ZmMIPs* transcripts in maize primary root.**	52
2.1.	Expression of *ZmMIP* transcripts in longitudinal zones	53
2.2.	Expression of *ZmMIPs* transcripts in cortex and stele	54
3.	**Effects of salt stress on physiological parameters and expression of aquaporin**	57
3.1.	Physiological responses of maize seedlings plants to NaCl stress	57
3.1.1.	Effect of salt stress on water content of maize leaves	58
3.1.2.	Effect of salt stress on ABA concentration	58
3.2.	Effect of NaCl on gene expression of maize MIP genes	59
4.	**Effect of ABA on the expression of *ZmMIP* genes**	61
5.	**Response to the deficiency of K^+ and NO^-_3**	64
5.1.	Growth of plants affected by K^+- and NO^-_3-deficiency	64
5.2.	Effects of nutrient limitation on the transcripts of ZmMIPs	65
6.	**Antisera against ZmPIP1 and ZmPIP2**	67
6.1.	Selection of the epitopes with potential antigenicity	67
6.2.	Immunization of rabbits and chicken with GST-fusion proteins	67
6.3.	Antisera against ZmPIP epitopes	68
7.	**Effect of NaCl and ABA on ZmPIP1 and ZmPIP2 at the protein level**	69
7.1.	Amount of ZmPIP1 and ZmPIP2 proteins	69
7.2.	Phosphorylation of ZmPIP proteins	71

D.	**Discussion**	75
1.	**Diversity and abundance of aquaporins in maize roots**	75
2.	**Location of aquaporin members in primary roots**	77
3.	**Effects of salt stress**	80
3.1.	Immediate and early effects at the onset of salt stress (shock)	80
3.2.	Later effects: 9 h until 24 h	84
3.3.	After 48 h	86
4.	**Effect of ABA on aquaporins**	86
5.	**Effect of salt stress and ABA on aquaporin at protein level**	87
6.	**Nutrient deficiency and *ZmMIP* expression**	88
6.1.	K^+-deficiency	88
6.1.1.	Effect of K^+ on hydraulic conductivity and water relation	88
6.1.2.	Effect of K^+ on growth	89
6.1.3.	AQP expression	90
6.2.	NO_3^--deficiency	90
6.2.1.	Effect of N-starvation on water relations	90
6.2.2.	Influence of NO_3^--deficiency on growth	91
6.2.3.	Repression of aquaporin expression by NO_3^--deficiency	91
7.	**Perspectives**	92
E.	**Summary**	94
F.	**References**	96
G.	**Supplement**	115
	Acknowledgement	124
	Curriculum Vitae	126

ABBREVIATION

ABA	abscisic acid
ABRE	abscisic acid-responsive element
BSA	Bovine serum albumin
cDNA	complementary DNA
cRNA	complementary RNA
ddH_2O	double distilled water
DEPC	Diethyl pyrocarbonate
DMSO	Dimethylsulfoxid
DNA	Deoxyribonucleic acid
dNTP	Deoxynucleotid-5'-triphosphate
DRE	dehydration-responsive element
DTT	dithiothreitol
EDTA	ethylene diamine tetraacetic acid
EST	expressed sequence tag
GST	Glutathion-S-transferase
L_p	Hydraulic conductivity
L_{pr}	Hydraulic conductivity of roots
L_{pcell}	Hydraulic conductivity of cells
MIP	major intrinsic protein;
mRNA	messenger RNA
MS	Murashige und Skoog
NASC	Nottingham *Arabidopsis* Stock Centre
NIP	NOD26-like intrinsic protein
PCD	Programmed cell death
PCR	polymerase-channel reaction
PIP	plasma membrane intrinsic protein
PM	Plasma membrane
P_{os}	osmotic water permeability
RNA	Ribonucleic acid
ROS	reactive oxygen species
rpm	Rotations per minute
RT-PCR	reverse transcription-PCR
SD	Standard deviation
SDS	Sodium dodecyl sulfate
SIP	small and basic intrinsic protein
ssDNA	Salmon sperm DNA
TAE	Tris-acetate-EDTA
TBE	Tris-boric acid-EDTA
TE	Tris-EDTA
TIP	tonoplast intrinsic protein
UTR	untranslated region
UV	Ultraviolet
v/v	volume per volume
Vol	volume
w/v	weight per volume
wt	Wild type

A. INTRODUCTION

1. Water uptake and transport in plants

1.1. Water uptake and transport in plants

Water is major component in the plant cell, which amounts to 70-95% of plant fresh weight. It is also a prerequisite for uptake and transport of micro- and macro-elements. Furthermore water functions as reactant in many biochemical reactions such as photosynthesis. Water is essential for maintaining of cell structure via turgor pressure, elongation and growth of plant cells. Tropic or nastic movements of plants are a result of water moving into or out of the plants. Transport of water across membranes occurs by diffusion, protein-mediated permeation or co-transporter with active solute transport.

To produce one kilogram organic matter plants consume up to 500 kg water, which is lost via transpiration through stomata on the aerial plant organs. In full sun light, leaves can transpire water equivalent to their weight in 1 h. Plants develop various mechanisms to prevent water loss, for example by wax production and regulation of the gas exchange through stomata.

Water lost by transpiration is replaced by water taken up by roots and the force that drives water from soil through plants to air is generated by water potential gradient. Water potential is the chemical potential of water and is a measure of the energy available for reaction or movement (Bidwell, 1974). It is made up of osmotic potential ($?_s$), pressure potential ($?_p$) and gravity potential ($?_g$). The gradient of negative hydrostatic pressure in the xylem vessel acts as main driving forces, when stomata open during the day; osmotic gradient acts as the main driving force at night, when stomata close. Solutes are actively absorbed by roots, leading to the reduction of osmotic potential in the xylem of roots.

Thus, the root is the most important organ for uptake of water and nutrients. According to their morphology and function, roots contain various zones, i.e. meristematic zone, elongation zone, and root hair zone. Each region depicts different function in capacities of water uptake.

Root cell growth is achieved by cell division occurring in the meristematic zone, followed by cell enlargement in the elongation zone. Meristematic cells contain numerous small vacuoles. Water flows into the expanding vacuole and cytoplasm depending on an osmotic gradient between the vacuole and cytoplasm. The mature plant cells have a large central vacuole surrounded by a thin layer of cytoplasm appressed against plasma membrane and cell wall. In order to increase water uptake efficiently, roots may amplify their surface in contact with the soil and medium.

The movement of water into roots occurs either by apoplastic pathway or by cell-to- cell pathway (Fig. 1). Cell-to-cell pathway contains two components, transmembrane pathway

and symplastic pathway, which cannot be separated experimentally. It is generally known that hydrostatic pressure plays an important role in contribution of driving force during the day with high transpiration rate, whereas the contribution of cell to cell pathway is high at night when hydraulic force generated by transpiration is almost absent (Steudle *et al.*, 1995).

In the roots water must travel through exodermis, cortex, endodermis, pericycle and vascular parenchyma to reach the xylem vessel by radial flow. Water transport via apoplastic path or cell to cell pathway during radial water transport, as radial cell walls of exodermis and endodermis may contain barriers such as the Casparian band, which is impermeable to water (Fig. 1). Water flows by cell-to-cell pathway before and across endodermis.

The radial flow in roots is much slower and is considered as speed limiting step of water transport. In contrast, the transport of water along the xylem vessel is much faster because of the lower resistance to water flow.

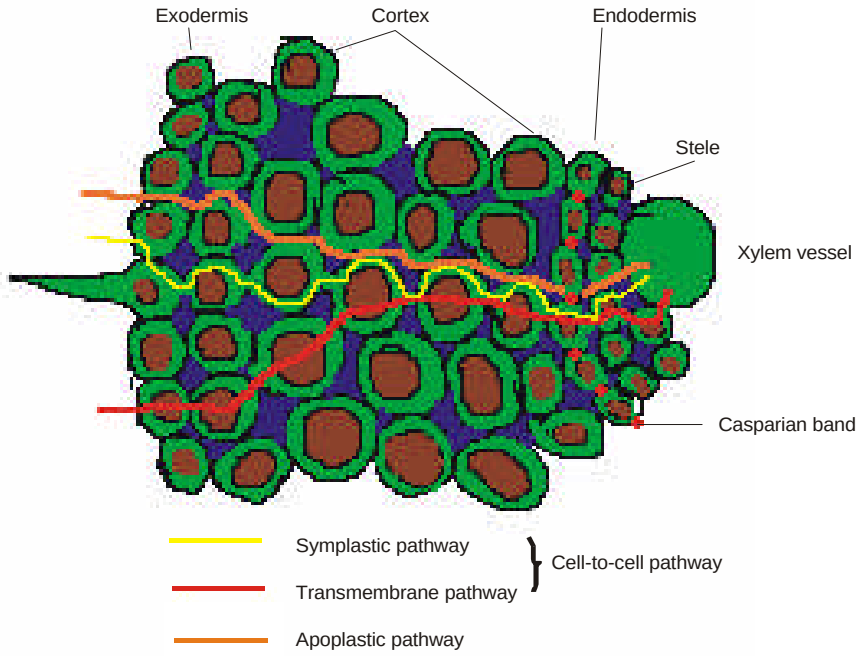

Fig 1. Three different pathways of radial water flow. The apoplastic, the symplastic, and transcellular pathway through a root are depicted.

1.2. Transmembrane water transport

Water may permeate across biological membranes by two ways:

i) by diffusion. The diffusional water permeability P_d is a measure of the free diffusion of water across the membrane in the absence of any imposed gradient;

ii) by following a potential gradient, which is built up by either osmotic or hydrostatic differences. The resulting water permeability P_f refers to the directional flow of water across the membrane.

In a pure lipid bilayer, P_d is more or less equal to P_f, whereas P_f is greater than P_d in many biological membranes. The notion of P_f is related to that of the hydraulic conductivity (L_p), according to the following equation: $P_f = L_pRT/V_{w,}$ where R is the universal gas constant, T is absolute temperature, and V_w is the partial volume of water.

In order to describe the different contributions of water movement and transport in plants as well as their driving forces and ways for experimental assessment the following terms are used generally and throughout this work:

- 'Water potential' consists of osmotic potential and pressure potential and gravity potential (see above). It can be determined by psychrometer and pressure chamber. One can measure osmotic potential and pressure potential by cryoscopic osmometer and pressure probe respectively, and calculate the water potential.
- 'Water flux (flow)' means the sum of water transported through a tissue. Water flux from roots to shoots is usually measured as the xylem sap exuding from the detopped roots or stems under application of pressure or suction, or without any external force. The latter situation is also referred to as pure 'exudation'.
- 'Hydraulic conductivity L_p' is the water flux (volume/ time) per area and driving force. 'Hydrostatic conductivity' is determined by application of pressure in the root pressure chamber to provoke root exudation or by suction to simulate the negative hydrostatic pressure that results from transpiration. It is dominated in many plants by the apoplastic pathway. 'Osmotic hydraulic conductivity' is determined from the variation of water flux (usually with detopped plants) upon changing the external osmotic pressure using a non-permeating solute (PEG). According to the explanations above, it is dominated by the cellular pathway of water.
-Accordingly, 'hydrostatic hydraulic conductivity' and 'osmotic hydraulic conductivity' are distinguished depending on the conditions and method for their determination.
- 'Cellular water permeability' can be measured by cell pressure probe in intact plants or excised plants (Azaizeh *et al.,* 1992) or for isolated plant cells by measuring the change in volume of protoplasts after osmotic changes in the medium (Morillon *et al.,* 2002).

2. Effect of abiotic stimuli and ABA on plants

2.1. Salt stress

The acquisition of water may be problematic when plants experience environmental stress such as high salinity, drought, cold, or high temperature. It is estimated that salinity affects at least 20% of world arable land and more than 40% of irrigated land to various degree (Rhoades *et al.,* 1990).

Salinity imposes ionic and osmotic stress. Plants exhibit a wide range of responses at the molecular, cellular, organ and whole plant level (Bohnert *et al.,* 1999; Hasegawa *et al.,* 2000). These include morphological changes such as inhibition of growth, ion homeostasis by uptake, extrusion, or sequestration of ions, and metabolic changes such as the synthesis of compatible solutes. Primary signals from salt stress causes secondary effects such as the synthesis of phytohormones (abscisic acid (ABA), salicylic acid), reactive oxygen species (ROS) and other intracellular signals (phospholipids), which are transported from stress perception site to other parts of the plants to coordinate the whole plant response to the stress.

2.1.1. Effect on plant water relation

Salt stress affects plant water status via reduction of stomatal conductance and hydraulic conductivity of roots (Martinez-Ballesta *et al.,* 2003). The osmotic and hydrostatic hydraulic conductivity of roots are both decreased in maize plants treated with high salinity (Azaizeh *et al.,* 1991). Azaizeh *et al.* (1992) found the reduction of the cellular permeability of root cortical cells by high salinity using the cell pressure probe.

The low value of root hydraulic conductivity during salt stress was not affected by addition of $HgCl_2$, whereas the hydraulic conductivity of control plants decreased by $HgCl_2$ and reversed by DTT (Martinez-Ballesta *et al.,* 2003). This implies that high salinity reduced the activity or amount of proteins, which were sensitive to $HgCl_2$ (see below, chapter 3.2).

2.1.2. Reduced growth

Like other abiotic stresses salt stress inhibits growth of plants. Salt stress exerts osmotic stress on roots and causes roots to generate phytohormone ABA, which is transported from roots to shoots to result in stomatal closure, thus hampering the entry of CO_2, which results in the reduction of photosynthesis and thereby limits the acquisition of new resources for growth (Hasagawa *et al.,* 2000).

The high level of ABA in roots induced a cyclin-dependent-protein kinase inhibitor (ICK1), which might hinder cell division by reducing the activity of cyclin-dependent protein kinase that is known to be involved in driving cell cycles (Wang *et al.,* 1998).

Disorder of ion homeostasis (see below) during salt stress also inhibits plant growth. Salt stress causes reduction of growth of primary maize roots that was accompanied by reduction in the length of the root tip elongation zone, length of epidermis cells, and in the apparent rate of cell production. Extra Ca^{2+} reverses each of these reductions (Zidan *et al.,* 1990). High ratio of Na^{+}/Ca^{2+} during salt stress inhibits growth of plant crops (Kent *et al.,* 1985). Slow growth is an adaptive feature for plants to survive salt stress because it allows plants to rely on multiple resources to combat salt stress.

2.1.3. Ionic homeostasis

Salt stress imposed by NaCl results in perturbation of ionic steady state not only for Na^+ and Cl^-, but also for K^+ and Ca^{2+}. External Na^+ impacts negatively K^+ influx, thus affecting the enzyme reactions, which need K^+ as a cofactor.

High NaCl causes increase in cytosolic Ca^{2+} that acts as a general stress signal (Lynch *et al.*, 1989). It is not clear if this increase in cytosolic Ca^{2+} is an effector of salt tolerance. Increase in cytosolic Ca^{2+} mediates salt adaptation is transitory. In the general view, salt stress induces Ca^{2+} deficiency and lowers activity of Ca^{2+} (Cram *et al.,* 1981). Supplement Ca^{2+} can ameliorate the inhibition of salt stress on root elongation.

Intracellular ion homeostasis is important for the normal function of cells. To accumulate essential ions and to expel surplus ions plant cells employ transporters, cotransporters and channels in the plasma membrane and vacuolar membrane.

Na^+ may enter plant cells through high affinity K^+ transporter (HKT1) (Maser, 2002) and through non-selective cation channels (Amtmann *et al.,* 1999). However, Berthomieu *et al.* (2003) reported contrasting evidence, that AtHKT1 is not involved in Na^+ uptake by roots in *Arabidopsis* but in recirculation on Na^+ from aerial parts to the roots via the phloem.

In some species such as rice, Na^+ leakage into the transpiration stream via apoplast can account for high levels of Na^+ entry into plants (Yeo *et al.,* 1999). Higher concentration of Na^+ in the cytosol is toxic, and plants have developed a mechanism to reduce Na^+ concentration by efflux and sequestration into vacuoles. Experimental evidence implicated Ca^{2+} to function in salt adaptation. Externally supplied Ca^{2+} reduces the toxic effect of NaCl, presumably by facilitating higher K^+/ Na^+ selectivity of roots (Liu *et al.* 1997; Läuchli *et al*., 1989). High salinity also results in increased cytosolic Ca^{2+} that is acquired from the apoplast and intracellular compartments (Knight *et al*., 1997). In addition to the effect on channel selectivity, a transient Ca^{2+} increase acts as a signal and facilitates adaptation to salt stress, e.g. by affecting the SOS pathway. In *Arabidopsis* Na^+/H^+ antiporter on the plasma membrane is responsible for Na^+ efflux out of cells. Na^+/H^+ antiporter is encoded by *SOS1* gene (Shi *et al.*, 2000; Qiu *et al.*, 2002), which is expressed in stressed plants. The greatest activity of *SOS1* promoter was found in epidermal cells in the root tip and parenchyma cells of vascular tissue (Shi *et al.*, 2002). The Na^+/H^+ antiporter SOS1 is specific for Na^+ and excludes Li^+ or K^+. It is activated by the SOS3-SOS2 complex. SOS3, a myristoylated calcium binding protein, senses Ca^{2+} in the cytosol, interacts with and activates the SOS2 kinase, which phosphorylates and activates SOS1 (Quintero *et al.,* 2002). SOS2 and SOS3 are also necessary for *SOS1* mRNA accumulation and functional protein accumulation under salt stress (Qiu *et al.,* 2002), indicating that SOS2 and SOS3 participate in the regulation of activity of SOS1.

Another method to lower Na^+ in cytosol is by sequestration of Na^+ into vacuole. Na^+ in vacuole can act as osmoticum to participate in osmotic adjustment. Na^+/H^+ antiporters in

the tonoplast function in Na^+ compartmentation. AtNHX1 and AtNHX2 Na^+/H^+ antiporter were found to reside in the tonoplast and their transcription levels are influenced by ABA and osmotic stress (Yokoi *et al.,* 2002). Overexpression of AtNHX1 was reported to enhance plant resistance to salt stress (Apse *et al.,* 2002).

The movement of Na^+ into xylem and transport to shoots is another strategy for lowering the Na^+ concentration in roots. The process is active due to high electrochemical potential gradient between parenchyma and xylem sap (Deboer *et al*., 1999). In *Arabidopsis SOS1* gene encoding Na^+/H^+ antiporter was reported to be expressed preferentially at the xylem symplast boundary of roots (Shi *et al*., 2002). SOS1 is proposed to function in active transport of Na^+ into xylem because *sos1* mutants accumulate the less Na^+ in the shoot. However, during high transpiration Na^+ efflux into xylem may also passively follow the electrochemical gradient towards the xylem using other channels if the concentration of Na^+ in the stellar parenchyma cells is higher than the concentration in xylem sap.

Recirculation of Na^+ to the roots by the phloem has been reported in several species, including lupin (Munns *et al.*, 1988), sweet pepper (Blom-Zadstra *et al.*, 1998), maize (Lohans *et al.*, 2000), and *Arabidopsis thaliana* (Berthomieu *et al.*, 2003).

The extent of the recirculation is related to the tolerance of plants to salinity in tomato (Perez-Alfocea, *et al.,* 2000), the higher recirculation of Na^+ into roots was found in salt-tolerant tomato.

2.1.4. Osmolyte biosynthesis

Salt stress reduces the external osmotic potential. As one measure to cope with these changed envirnoment, plant cells may synthesize metabolites that act as “compatible solute” (Yamcey *et al.*, 1982; Hasegawa et al., 2000). Their accumulation is proportional to the change in the external osmolarity. Frequently the observed compatible solutes are sugars (trehalose, raffinose, sucrose, and fructose), sugar alcohols (glycerol), ions (K^+) and charged metabolites (glycerine betaine, proline etc). These compatible solutes are necessary for intracellular osmotic adjustment during salt stress. Several carbon compounds and nitrogenous compounds are compartmented in cytosol, whereas ions (K^+, Cl^-, and Na^+) are sequestrated in the vacuoles. Cellular osmotic potential is adjusted to maintain water uptake during salt stress and to contribute to the salt tolerance (Delauney *et al.,* 1993).

Organic compatible solutes are typically hydrophilic and replace water at the surface of proteins and membranes, thus acting as osmoprotectants and low-molecular-weight chaperones. Some osmolytes are also viewed as sinks of reducing power following metabolic disturbance. They might be mobilized as sources of carbon and nitrogen after stress is relieved (Greenway *et al.,* 1980).

2.1.5. Molecular response to salt stress

With the availability of the microarray technology it is possible to monitor gene expression in genome scale. Seki *et al.* (2001) examined 1300 genes of *Arabidopsis* under drought and cold stress. The expression of more genes in *Synechocystostis, Saccharomyces cerevisiae, Aspergilus nidulans, Dunaliella salina, Mesembryanthemum crystallinum, Oryza sativa, Arabidopsis* (Bohnert *et al.,* 2001), and rice (Kawasaki *et al.,* 2001) was analysed during salt stress. Genes that are up-regulated by salt stress belong to several groups based on functions. These genes encode the LEA proteins, enzymes involved in biosynthesis of osmolytes, hormones, detoxification and general metabolism, transporters (ion transporter, ABC transporter), regulatory molecules such as transcriptional factors, protein kinases and phosphorylases as well as aquaporins.

Salt stress exerts three major impacts on plant cells such as ionic, osmotic and mechanic impacts, which have their own features. To respond to various impacts plant cells may have specific extracellular and/ or intracellular receptors, which operate independently or cooperatively to initiate down-stream signalling events. The multiplicity of signal sensing accounts for the complexity of the signalling pathway that is ascribed as “crosstalk” (Xiong *et al.,* 2001).

Until now, only few stress sensors have been identified in plants. The information about signal sensors was mostly obtained in bacteria and yeast. For example, the two-component systems consist of a sensory histidine kinase and response regulation function as stress sensor in bacteria and yeast. In yeast, SLN1 (osmosensory histidine kinase) senses osmotic stress and activates the HOG1 (high-osmolarity glycerol response 1) mitogen-activated kinase (MAPK) cascade (Maeda *et al.,* 1994). The yeast double mutant sln1/shol1 is defective in osmosensing. The *Arabidopsis thaliana* histidine kinase *ATHK1* is up-regulated at the transcriptional level during salt stress (250 mM NaCl). When expressed in yeast, *ATHK1* can complement sln 1/shol and confers a high degree of osmolarity tolerance to the double mutant, indicating ATHK1 as a candidate for an osmosensor (Urao *et al.,* 1999).

Signal transduction pathways are complex in plant cells owing to the multiplicity of signals and sensors. Three major signalling types have been associated with salt stress:

I. Osmotic/oxidative stress signal that makes use of MAPK modules.
II. Ca^{2+} -dependent signalling that lead to the activation of LEA gene (such as DRE/CRT classes of genes)
III. Ca^{2+}-dependent SOS signalling that regulates ion homeostasis (Xiong *et al.,* 2002)

Several MAP kinases that are activated by hyperosmotic stress have been identified in plants such as alfalfa, tobacco and *Arabidopsis* (Mikolajczyk *et al.,* 2000; Munnik *et al.,* 1999; Hoyos *et al.,* 2000).

Signals (salt stress or water stress) were perceived and transduced by MAPKKK, MAPKK and MAPK, which offer the scope for cross-talk between different signals (Ligterink *et al.*, 2000). Members of the MAP kinase pathway were increased at the transcriptional level in response to osmotic or other stress treatments (Mizoguchi *et al.*, 2000). This signalling contributes to the production of compatible solutes (proline, sugar, glycine betaine, polyols, etc.) and antioxidants (ascorbic acid, glutathione, thioredoxin, carotenoids). Reactive oxidative species (ROS) are eliminated by scavenging enzyme such as superoxide dismutase, glutathione peroxidase, and catalase, which are activated via MAPK module (Xiong *et al.*, 2002; Tsugene *et al.*, 1999). These targets of the MAPK pathway help establish osmotic homeostasis, stress damage protection or repair mechanism.

Ca^{2+} serves as a second messenger during abiotic stress signalling (Knight *et al.*, 2000). Ca^{2+} signalling changes depending on the nature of the stress, the rate of stress development (Plieth *et al.*, 1999) and tissue type (Kiegle *et al.*, 2000). Recent studies showed that Ca^{2+}-channels are implicated in the regulation of cytosolic Ca^{2+}. Pharmacological studies have shown that cyclic ADP-ribose-gated Ca^{2+}-channel is involved in ABA induced gene expression in tomato (Wu *et al.*, 1997). IP3-gated Ca^{2+}-channels have been implicated in induction of cytosolic Ca^{2+} elevation during dehydration and salt stress (Dewald *et al.*, 2001).

Intracellular Ca^{2+} initiates a protein phosphorylation cascade. CDPK (Ca^{2+}-dependent protein kinase) is implicated in this signalling pathway, which induces and activates transcription factors, the expression of LEA–like proteins, such as RD29A, or enzymes for ABA synthesis (Xiong *et al.*, 2003). These proteins function in the detoxification or alleviation of damages. Sheen (1996) demonstrated the involvement of CDPK in stress-induced gene transcription using a maize leaf protoplast transient expression system.

In addition to CDPKs, *SOS3* is induced by Ca^{2+} involved in the SOS pathway, which is specific for regulation of ionic homeostasis, which has been illustrated above (2.1.3 ion homeostasis).

2.2. ABA

2.2.1. ABA and its physiological effects

ABA accumulates when plants are subjected to abiotic stress (e.g. high salinity, drought, osmotic stress). The factors inducing ABA accumulation include reduced water potential, decreased turgor pressure, changes in cellular volume and /or conformational changes of cellular macromolecules (Hsiao, 1973). Jia *et al.* (2001) provided the evidence that the initiation of ABA accumulation related to the weight loss of tissues or changes in cellular volume.

ABA was first identified and characterized by Okhuma *et al.* (1963) in studying compounds responsible for the abscission of cotton fruits. Two compounds called abscisin

I and II were isolated. The same compounds were discovered in studying bud dormancy in wooden plants (Eagles *et al.,* 1964). The compound was called abscisic acid (Addicott *et al.,* 1968). Later, it was shown that ABA is synthesized through the carotenoid biosynthetic pathway (Taylor *et al.,* 2000; Milborrow *et al.,* 2001).

The phytohormone ABA plays regulatory roles in many physiological processes in higher and lower plants (Davies *et al.,* 1991; Wilkson *et al.,* 2002). ABA mediates water stress tolerance response in higher plants and regulates stomatal aperture in concert with other plant regulators. ABA is implicated in the regulation of the process such as abscission of leaves and fruits, induction and maintenance of dormancy of seeds and buds, inhibition of growth in shoots and promotion of growth in roots (Ober *et al.,* 2003).

The role of ABA on the regulation of stomatal gating has been intensively studied (Hetherington *et al.,* 1998). In contrast the information on the effect of ABA on water uptake and transport in roots remains less elaborate. Hartung (1999) found the implication of ABA on anatomic and morphological changes, such as the formation of root hair and lateral root. In addition, ABA affects the root hydraulic conductivity. The increase and decrease of L_{pr} have been reported. The hydraulic conductivity at root level and root cell level was increased by ABA in maize (Hose *et al*., 2002; Wan *et al.*, 2004). These findings are consistent with the previous reports (Glinka *et al.,* 1971, 1973, 1977; Ludwig *et al.,* 1988; Quintera *et al.,* 1998), but the decrease of L_{Pr} was also found in other studies (Fiscus *et al.,* 1981; Karmoker *et al.,* 1988; Van Seveninck *et al.,* 1988).

2.2.2. Molecular response to ABA

High salinity and drought enhance ABA accumulation. Exogenous application of ABA can have similar effects on gene induction to salt stress or drought. It is reasonable and widely accepted that ABA is involved in osmotic stress response. Seki *et al.* (2002) monitored the expression of 7000 *Arabidopsis* genes under drought, salt, cold stress, and ABA treatment using a full length cDNA microarray. Many ABA inducible genes were also enhanced under drought and salt stress, indicating that ABA mediated the response of gene expression to salt stress and drought.

ABA response is initiated by ABA perception. Despite many attempts to characterize the ABA binding proteins, there is not much known about an ABA sensor. ABA regulates the opening and closure of stomata in the leaves by two separated processes: ABA-inducible closure and inhibition of stomatal opening. GTP binding proteins (G-protein) might be responsible for sensing of ABA and ABA-induced inhibition of stomatal opening because the genetic disruption of G-protein alpha subunit (GPA1) gene reduced the response (Wang *et al.,* 2001a). The role of G-protein associated receptors perceiving ABA during abiotic stress has yet to be demonstrated in plants.

Electrophysiological studies of isolated plasma membrane patches from *Vicia* have demonstrated that ABA mediated activation of Ca^{2+}-channel and increase of intracellular

Ca^{2+}, which depends on ATP hydrolysis. The inhibition of protein phosphatase 2C and ABA increases the probability that this channel is open (Kohler *et al.,* 2002). Ca^{2+}-channel is also implicated in regulating the concentration of intracellular Ca^{2+} during abiotic stress (Kiegle *et al.,* 2000). Ca^{2+} signal is perceived and transduced by CDPK, activating a protein phosphorylation cascade, which regulates ABA responsive gene expression. The signal transduction of ABA is overlapping with the CDPK-mediated signalling of salt stress.

ABA-responsive genes contain ABRE, DRE, and/or MYC and MYB *cis*-elements in their promoters (Zhu, 2002), which are regulated by ABA-signalling active transcriptional factors such as ABREB (b-zip), DREB/CBF, or MYC/B, respectively. For example, CBF4 is a DREB1-related transcriptional factors in *Arabidopsis*, which is up-regulated by drought and ABA but not by cold stress. Over-expression of CBF4 resulted in constitutive expression of CRT/DRE containing stress-responsive genes, enhancing tolerance to drought and freezing stresses (Haake *et al.,* 2002). MYC and MYB recognition sequences of *Arabidopsis* are involved in regulating the expression of ABA-induced genes in response to severe water stress. The dehydration-responsive gene *rd22* contains both of these elements. The gene coding the MYC related DNA binding protein rd22 BP1 is suppressed by water stress and ABA treatment (Abe *et al.,* 1997).

Several b-zip factors that bind ABA-responsive element (ABREs) have been identified as ABA-responsible transcription factors that induced gene expression under dehydration and/or higher level of ABA. These transcription factors induced wheat *EmBP1* (Guiltinam *et al.,* 1990), tobacco *TAF-1* (Oedak *et al.,* 1991) and rice *OSBZB* (Nakagawa *et al.,* 1996), *Arabidopsis AB15* (Ruth *et al.,* 2000). Rock *et al.* (2000) found that Arabidopsis contains at least 58 genes that encode b-zip factors. These proteins may form homo- or hetero-dimer, indicating possible mechanism of positive and negative regulation of genes containing binding sites such as the G-box-half site.

2.3. Effect of nutrient-deficiency on plants

2.3.1. Nitrate deficiency

Nitrogen is an essential macro-element for plant growth, development and productivity, comprising 1.5 - 2% of plant dry matter and 16% of protein (Frink *et al.,* 1999). Plants can use a variety of N species as nitrogen sources such as NO_3^-, NO_2^-, NH_3, NH_4^+, NO_x and peptides. NO_3^- is an important N source (Crawford *et al.,* 1998). NO_3^- is absorbed by roots and stored in vacuoles as osmoticum, contributing to maintaining cation-anion balance and osmoregulation, NO_3^- can be also transported to aerial parts. For biosyntheses of e.g. amino acids, nucleic acids, nucleotides and chlorophyll, NO_3^- must be reduced through NO_3^-/NO_2^- reductase to NH_4^+ and glutamine.

N-deficiency occurs in the agriculture because of high requirement of N sources. A typical N-deficiency symptom is stunted growth; in addition, N-deficient plants may have

markedly slender and often woody stems due to an excess of carbohydrate because they cannot be used in the synthesis of amino acids and other nitrogen-containing compounds. As N is highly mobile within plants, the symptom of N-deficiency tends to occur earlier in older leaves.

2.3.1.1. Stimulation of root growth

In similarity to P- and S-deficiency, N-deficiency causes stunted growth of shoots, but stimulates the elongation of roots. N-limitation allocates a great proportion of the photosynthetic products to roots and facilitates the root growth (Robinson *et al.*, 1994). Root growth may be advantageous for plants to adapt to nutrient deficiency because root growth can maximize resource capture below the ground. Moreover, local sources of N elicit local root proliferation in media which are generally deficient in nutrients (Drew *et al.*, 1975). Such a proliferation can compensate for deficiency in other areas. In contrast to the effect of N-deficiency, K-limitation elicits neither the increase of the root to shoot ratio nor local proliferation of roots, indicating that plants have different mechanisms in response to N- and K^+-deficiency.

2.3.1.2. Effect on plant water relation

NO_3^- also functions as osmoticum. NO_3^- is absorbed and transported actively into the xylem vessel; build–up of NO_3^- in the vessel increased the water potential difference between external medium and xylem vessel. NO_3^- affects the water flow through change in water driving force.

In contrast, N-deficiency may reduce the water driving force, affecting water flux in a negative way. The reduction of xylem water flux during N-deficiency supports the inference. Water flow depends on water driving force and hydraulic conductivity. Thus, the question arises, whether N-deficiency affects the hydraulic conductivity. Indeed, an effect of NO_3^--deficiency on hydraulic conductivity was reported in many species (Carvajal *et al.*, 1996; Barthes *et al.*, 1995, 1996). N-deprivation decreased the hydraulic conductivity of excised maize roots (Lp_r). The low value of Lp_r during N-deprivation was not sensitive to $HgCl_2$, and after N-resupply, Lp_r recovered. This suggests that N-deficiency may reduce Hg-sensitive aquaporin-mediated water transport. Furthermore, the amplitude of a marked diurnal fluctuation in hydraulic conductivity was significantly reduced by N-deficiency, but remained detectable (Carvajal *et al.* 1996).

Measurements using the cell pressure probe showed that the permeability of cells (Lp_{cell}) was smaller than 85% in cotton root cortical cells during N-deficiency (Radin *et al.*, 1989). Larsson et al. (1987) analysed the rate of shrinkage of plasma membrane vesicles from wheat roots grown in hydroponics using stopped-flow spectrophotometer. They found that rate of shrinkage of plasma membrane (PM) vesicles of N-deprived roots was lower than

that of control PM vesicles. Addition of $HgCl_2$ reduced the shrinkage rate of control PM vesicles but not that of PM vesicle from N-deprived wheat roots.

These results indicated that N-deficiency reduced Lp at different level. Although the (toxic) $HgCl_2$-studies were often interpreted as an indication for the involvement of Hg-sensitive aquaporins, it remained unknown whether aquaporins are implicated in changes of hydraulic conductivity in response to N-deprivation.

2.3.2. K^+-deficiency

Potassium is the most abundant inorganic cation in plants, comprising up to 10% of plant dry weight (Leigh *et al.,* 1984). K^+ is an important macronutrient for plants, which carries out vital function in metabolism, growth and stress adaptation. K^+ concentration is high and stable in cytosol and some organelles and essential for enzyme activation, stabilization of protein synthesis and neutralization of negative charges on proteins. On the other hand, K^+ movement leads to osmotic changes that drive water movement in plants such as stomatal movement or light-driven movements of organs.

K^+ was recognized as an impotent nutrient early in agriculture (Laegreid *et al.,* 1999). The symptoms of K^+ deficiency were well described (Marschner, 1995). K^+ starvation leads to the arrest of growth, impaired nitrogen and carbon metabolism and increased susceptibility of pathogens.

2.3.2.1. Cell extension

Cell extension depends on the extensibility of cell wall and water potential difference between the cell and the apoplast. In most cases cell extension is a consequence of K^+ accumulation in the cell, which reduces the osmotic potential. In association with inorganic and organic ions, K^+ is the main solute which is implicated in the osmotic adjustment in the vacuoles. This process accompanies water influx into vacuoles, facilitating enlargement of vacuoles and cell extension.

The stimulation of stem elongation by gibberelic acid (GA) is dependent on supply of K^+. K^+ and GA act synergistically. Highest elongation was obtained when both K^+ and GA were applied. Reducing sugars and K^+ functioned in complementary manner to produce cell turgor required for cell extension (Guardia *et al.* 1980). In the absence of K^+, auxin-induced elongation declined and ceased in *Avena* coleoptiles (Haschka *et al.,* 1975). These results showed that K^+ is essential for cell extension.

2.3.2.2. Stomatal movement

K^+ and counter-anions are responsible for turgor change in the guard cells during stomatal movement. An increase of K^+ in the guard cells reduces cellular osmotic potential resulting in uptake of water from adjacent cells. A corresponding increase of turgor leads to stomatal opening. In contrast, closure of stomata is induced by darkness and ABA, efflux of K^+ and anions from the guard cell. Stomatal closure accompanies the increase of K^+ and Cl^- in the apoplasm of guard cell (Schröder, 2002). E.g. in *Commulina communis* stomata, 3 mM K^+ and 4.8 mM Cl^- were determined for in closed stomata, whereas up to 100 mM K^+ and 33 mM Cl^- were present in open stomata (Bouling *et al.*, 1987). Although sugar can partially replace K^+ in the regulation of stomatal movement (Tallman *et al.*, 1998), during K^+-deficiency sugar-loaded guard cells resulted in incomplete opening and closure of stomata (Hsiao *et al.*, 1986). Maize stomata are apparently very sensitive to K^+-deficiency, being inhibited prior to other K^+ deficient symptoms (Peaslee, 1996). It is concluded that K^+ plays an important role in the regulation of stomatal movement.

2.3.2.3. Water uptake of roots

The relation between K^+ transport and water flow was investigated by applying hydrostatic forces or suction on root systems to simulate transpiration. Most results showed that water flow caused solute flow, which lacked transport selectivity for K^+ over Na^+. In addition, K^+ flow in intact plants was found to be much lower than that in excised roots subjected to pressure (Salim *et al.*, 1984). These evidences demonstrate that K^+ transport does not affect water flow during high transpiration.

Under the conditions of low transpiration, K^+-influx into roots and active release to the xylem cause an inward water potential gradient, along which water moves osmotically (Läuchli *et al.*, 1979). Mengel *et al.* (1973) found that exudation decreased quickly after transfer of sunflower plants from K^+-sufficient to K^+-deficient solution. This implies that K^+ deficiency affects water flux during low transpiration.

Besides its osmotic role, K^+ may affect hydraulic conductance of roots by other mechanisms. Graham *et al.* (1972) found that root conductance to water flow under pressure gradient was reduced significantly 8 days after transfer from 4 mM K^+ solution to K^+ free solution.

In *Arabidopsis*, addition of K^+ to K^+-starved *Arabidopsis* seedlings induced the expression of several aquaporin genes in the roots and shoots (Armengaud *et al.*, 2004). This indicated that K^+ regulating aquaporin expression might relate to the regulation of hydraulic conductivity of roots by K^+-deficiency. The information about aquaporin expression in maize during K^+-deficiency is unknown and remains to be established.

3. Aquaporins in plants

3.1. History of aquaporin

Preston *et al.* (1992) extracted an abundant protein found in erythrocyte membranes and demonstrated a specific water transport activity of this protein. It was named CHIP28 (channel-forming integral protein, 28 kDa) and later renamed AQP1 (aquaporin1). AQP1 showed homology to MIP (major intrinsic protein) in the membrane of eye lens fibre cells. Therefore, the gene family is generally named MIP family after this prototypal protein. MIP proteins are found in bacteria (Baker *et al.,* 1990; Heller *et al.,* 1980), fungi (Beijer *et al.,* 1993), plants (Kaldenhoff *et al.,* 1993; Maurel *et al.,* 1993; Kammerloher *et al*., 1994; Schäffner, 1998) and animals (Agre *et al.,* 1987; Höfte *et al.,* 1992; Preston *et al.,* 1992).

Arabidopsis ?-TIP, a MIP member located in the tonoplast was the first plant MIP that showed water transport activity when assayed by heterologous expression in *Xenopus laevis* oocytes (Maurel *et al.,* 1993). Later homologues residing in plasma membrane were characterized (Kammerloher *et al.,* 1994; Daniels *et al.,* 1994). Since then, many homologues were identified in *Arabidopsis thaliana* (Kaldenhoff *et al.,* 1993), maize (Chaumont *et al.,* 1998; Barrieu et al., 1998), wheat (Niemietz *et al.,* 1997) , rice (Lian *et al.,* 2004), tomato (Uehlein *et al.,* 2001), barley (Katsuhara *et al.,* 2002), tobacco (Fray *et al.,* 1994; Maurel *et al.,* 1997), potato (Heymann *et al.,* 1999), ice plant (Yamada *et al.,* 2000), sunflower (Sarda *et al.,* 1997), cauliflower (Reisen *et al.,* 2003) and radish (Sagu *et al.,* 2002). Thirty-five and 34 isoforms of aquaporin have been found in *Arabidopsis* (Quigley *et al.,* 2001) and in maize (Chaumont *et al.,* 2001), respectively.

According to sequence homologies the plant MIP family has been classified into four groups, PIPs (plasma membrane intrinsic protein), TIPs (tonoplast intrinsic protein), NIPs (NOD 26-like intrinsic protein), and SIPs (small and basic intrinsic protein) (Johanson *et al.,* 2001). The assignment of plant MIPs to specific membrane locations has been experimentally proven for several isoforms; it was further extended based on sequence homology. However, this is not necessarily true in all cases; e.g. as some PIP antigens reacted with both purified plasma membrane and an uncharacterised, other membrane fraction (Barkla *et al.,* 1999; Kirch *et al.,* 2000).

3.2. Structure and function of aquaporins

MIPs share typical structural properties. They possess a molecular mass of 25-30 kDa, they have 6 membrane-spanning helices and 5 loops with N- and C-termini residing in the cytosol. Loop B and loop E are characterised by the presence of highly conserved, duplicated signature motif asparagine–proline-alanine (NPA) in both loops, which fold into the membrane forming half a helix each that is lining the channel.

Murata *et al.* (2000) analysed and refined the structure of AQP1 and proposed the first atomic model for AQP1. AQP1 exists as a tetramer with each subunit containing its own

pore. The pore narrows to approximately 3 Å in diameter, which constraints the transport of large uncharged molecules through aquaporin. At the narrow center of the pore, the highly conserved Asn76 and Asn192 in the NPA motif are juxtaposed. Except the two Asn residues the constraint points are hydrophobic. Therefore, the interaction of the oxygen atom of water with these Asn residues reorients the two hydrogen atoms when water passes through this constraint. Thus, the formation of hydrogen bonds with adjacent water molecules is prevented, which contributes to the exclusion of proton-permeation through hydrogen bonds. Furthermore, constriction points are surrounded by residues Phe56, His180, Cys189, and Arg195. Arg195 was found to be conserved in all members of aquaporins and position at the narrowest segment of channel. At low pH His180 becomes protonated. The positive charges of Arg195, His180 display a positive dipole from the pore helixes, providing strong repelling charge against the passage of protons during water permeation.

Recently real time molecular dynamics simulation demonstrated this predicted rotation of water during passage of the juxtaposed Asn76 and Asn192 of the NPA motif (de Grot *et al.*, 2001). All structures are in accordance with a bidirectional water flow across the aquaporin.

Mercurials may inhibit many sulfhydryl-containing proteins including aquaporins. In some aquaporin members cystein residues are present either in loops B or E or at the surface of a transmembrane helix facing the pore (Agre *et al.*, 1995; Daniels *et al.*, 1996). Daniels *et al.* (1996) found two mercury-sensitive aquaporins in *Arabidopsis*, which have different position of cysteine residues from in animal aquaporin (Preston *et al.*, 1993). The substitute of cysteine residue makes aquaporin to lose the sensitivity to mercury. The mercury-insensitive AQP RD28 of *Arabidopsis* can acquire mercury sensitivity by introduction of a cysteine residue next to the NPA from the extracellular side of the membrane (Daniels *et al.*, 1994).

Some members of MIP were characterized to transport water. They were called aquaporins. In addition, water may diffuse as a small uncharged molecule across the lipid layer of biological membranes resulting in constitutive background water permeability.

There are no sensitive techniques to detect water permeation similar to the recording of currents due to ion transfer as water does not carry any charge. However, the analysis of the function of individual aquaporin can be performed by expression in *Xenopus laevis* oocytes. The water permeability of aquaporins in the oocytes can be studied by analysing the swelling and increase in volume after transfer into a defined, hypotonic medium. In addition to *Xenopus laevis* oocytes, yeast and amoeba expression systems are applied to characterize the function of aquaporins in a similar way (Chaumont *et al*., 1997).

In addition to water some MIPs are permeable to other molecules such as glycerol (Weig *et al.*, 2000), urea (Gaspar *et al.*, 2003), formamide (Whittembury *et al.*, 1997), ammonia (Niemietz *et al.*, 2000), boric acid (Dordas *et al.*, 2000), or CO_2 (Nakhoul *et al.*, 1998;

Prasad *et al.,* 1998; Uehlein *et al.,* 2003). Some members of MIPs that transport water and other small uncharged molecules are named aquaglyceroporin. GlpF, a MIP member from *E. coli* which transports only glycerol, is called glyceroporin (Maurel, *et al.,* 1994).

3.3. Expression of AQP

Since transport properties of several MIP members have usually been characterized in oocytes, the function of most AQP and their physiological relevance in whole plants are unknown. One important aspect to gain insight into their function is to learn about their spatial expression pattern.

AtTIP1;1 and *AtPIP1;2* were highly expressed in the elongation zone of roots (Ludevid *et al.,* 1992; Kaldenhoff *et al.,* 1995), where cells are vacuolated and increase in volume. An increase in aquaporin expression and thereby increased water permeability of membrane could assist these processes.

High expression of *AtPIP* and *AtTIP* was also observed in vascular tissue and surrounding cells (Yamada *et al.,* 1995; Kaldenhoff *et al.,* 1995; Daniels *et al.,* 1996). The presence of aquaporin may raise water permeability and facilitate water transport from symplast to apoplast in the roots and assist the opposite phenomenon in the aerial parts of plants.

TIP7 and *TIP20* of *Helianthus* were expressed in guard cells (Sarda *et al.,* 1997). Expression studies using RT-PCR revealed higher expression of aquaporin in guard cells of *Vica faba* compared to other leaf cell types (Sun *et al.,* 2001). *SsAQP2* was expressed in the pulvini motor cells of *Samea samen, SsAQP2* transcript fluctuated under circadian control and accounted for physiological function of rhythmic cell volume change (Moshelion *et al.,* 2002). Apparently, high expression of aquaporin indicated the importance of aquaporins for bulk water flow across guard cells or motor cells and therefore for stomata movement or circadian movement.

TIP isoforms can be also used as markers for different types of vacuoles (Neuhaus *et al.,* 1998). During the germination of *Arabidopsis* seeds, vesicles with high density of storage proteins had high expression of α-TIP. Later, α-TIP was replaced by γ-TIP in small vesicles (Maurel *et al.,* 1997). Jaun *et al.* (1999) confirmed the observation using confocal immunofluorescence: vacuoles containing seed type proteins were marked by α- and δ- or α-, γ- plus δ-TIP, whereas vacuoles containing vegetative storage proteins were marked by δ- plus γ-TIP; those labeled by γ-TIP alone were lytic vacuoles.

In addition to the above organ and cellular specific expression of aquaporin, some members of aquaporin are expressed in all tissues and in all organs (Höfte *et al.,* 1992; Daniels *et al.,* 1994). Transcripts of aquaporins were affected not only by developmental factors, but also by phytohormones and environmental factors such as osmotic stress (Yamada *et al.,* 1995; Suga *et al.,* 2002), drought (Fray *et al.,* 1994; Guerrero *et al.,* 1990),

blue light (Kaldenhoff *et al.,* 1993), ABA (Weig *et al.,* 1997), and GA (Phillips *et al.,* 1994).

3.4. Regulation of aquaporin

Change in developmental stage and in environmental condition may require increased or decreased water permeability across membrane. The presence of aquaporin provides the prerequisite for rapid transmembrane water transport and regulates water flux between cells and within the cells. Regulation of aquaporins was observed at transcriptional, post-translational level and process involving targeting of aquaporin.

Transcriptional regulation involves induction, synthesis and activity of transcriptional factors, which affect in turn the induction or repression of aquaporin genes. It has been reported that the transcripts of aquaporin were regulated by phytohormones, developmental stages or environmental cues such as cold, drought, high salinity, anoxia or mineral starvation (Ueda *et al.,* 2004; Bray, 2004; Seki *et al.,* 2002; Klok *et al.,* 2002). The regulation of aquaporin transcripts by developmental stage has been described above (3.3).

Several global and singular studies revealed a deregulation of MIP transcription in response to external stimuli. With the sequencing of genomes and the development of DNA array, the analysis on gene expression can be performed at the genome-wide level. The analysis of transcriptome showed that *AtPIP2-1* was induced after 3 h treatment with chilling (4^oC), mannitol or high salinity in the leaves of Arabidopsis, but the transcripts of another highly expressed member *AtPIP1-2* remained constant at 3 h or 27 h (Kreps *et al.,* 2002).

In rice, the expression profiles were different for two varieties exhibiting different salt-sensitivity; the transcripts of some aquaporins were down-regulated after 15 min salt shock, recovered after 1 h of salt stress, and were up-regulated after 7 d of treatment in the roots of the resistant variety Pokkali. In contrast, in the salt-sensitive variety IR 29, aquaporin genes were transiently induced at 3 h of treatment (Kawasaki *et al.,* 2001). Jang *et al.* (2004) analysed the expression pattern of all 13 members of *AtPIP* under treatment with ABA, high salinity and other stressors using real-time RT-PCR. Differential regulation profiles in the aerial parts and roots were observed. Highly expressed aquaporin members such as *AtPIP1-1*, *AtPIP1-2* and *AtPIP2-7* were induced in the roots by high salinity and ABA. *AtPIP1-5* was repressed by salt stress and ABA. Other aquaporin members were not responsive to ABA and high salinity in such a parallel manner.

This implied that the regulation of aquaporin expression involved ABA-dependent and ABA-independent signalling pathways. These experiments indicated that the expression of aquaporin was affected by the varieties, severity of stressors, duration of treatment and species, developmental stage of plants.

Subsequently protein amounts produced are not only affected by the amount and stability of mRNA, but also by the factors which regulate the activity of enzymes involved in the metabolism of aquaporin.

Phosphorylation is an important regulating mechanism at the posttranslational level. Bean α-TIP was progressively phosphorylated during germination possibly by CDPK (Ca^{2+} dependent protein kinase) (Maurel *et al.,* 1995). The phosphorylation of spinach PM28 depends on a CDPK on the membrane (Johansson *et al.,* 1998), but low water potential in the apoplast induced dephosphorylation of PM28 presumably reducing its activity. The inactivitation of PM28 was interpreted to prevent excess water loss during osmotic stress and allowed cells to undertake protective measures such as osmotic adjustment.

The change in temperature from 5 ^{o}C to 20^{o}C or from 20 ^{o}C to 5^{o}C regulated the opening and closing of tulip petals in the dark. During the opening, when there is water transport towards the petals, a putative aquaporin was phosphorylated by CDPK and possibly activated. On the other hand, dephosphorylation and inactivation of aquaporin was associated with the closing of tulip petals (Azad *et al.,* 2004).

Relocation of AQP2 regulated by vasopressin was observed in the collecting duct of kidney. Vasopressin induced targeting of AQP2 containing vesicles to plasma membrane (Deen *et al.,* 1995). Vasopressin bound to an adenylyl cyclase-coupled vasopressin receptor (V2), resulting in the increase in cAMP and activation of PKA, which in turn phosphorylated AQP2 located in the intracellular vesicles. The phosphorylation at Ser256 of C terminus was found to trigger fusion of these vesicles to plasma membrane (Nielsen *et al.,* 1995). Regulation of a tonoplast MIP by vesicles shuttling was reported in ice plant (Vera-Estrella *et al.,* 2004). Osmotic stress (mannitol) induced expression of McTIP protein, which was distributed to other membrane fractions. The redistribution of McTIP1;2 was also influenced by factors such as aquaporin glycosylation and cAMP-dependent signal pathway.

3.5. ZmMIPs

Chaumont *et al.* (2001) screened 470000 maize ESTs representing 215 maize cDNA libraries and found 33 different complete nucleotide sequences. They belong to the PIPs (13), TIPs (12), NIPs (5), and SIPs (3) (Fig. 2). They share the common features, i.e. six putative transmembrane helices and the double NPA motives in loops B and E. The sequences have high similarity within each subgroup. For example, PIP proteins are very closed related to each other and have 64%-100% identity. However, their relation to other three groups are very less, only 16% to 35% of amino acid are conserved with members of other groups.

The transport function of ZmMIP was investigated using *Xenopus laevis* oocytes. ZmPIP1-5, ZmPIP2-1, ZmPIP2-4, ZmPIP2-5, ZmTIP1-1, and ZmTIP2-3 were characterised to

transport water, ZmPIP1-1 and ZmPIP1-2 were found to have low or no water permeability (Gaspar *et al.*, 2003; Chaumont *et al.*, 2000; Fetter *et al.*, 2004; Lopez *et al.*, 2004). However, ZmPIP1-2 provokes an increase of osmotic permeability in oocytes when it was co-expressed with ZmPIP2 members, indicating a synergistic function and/ or the formation of active heteromers. ZmPIP1-5 has capacity to transport urea (Gaspar *et al.*, 2003). The transport function of other members is unknown.

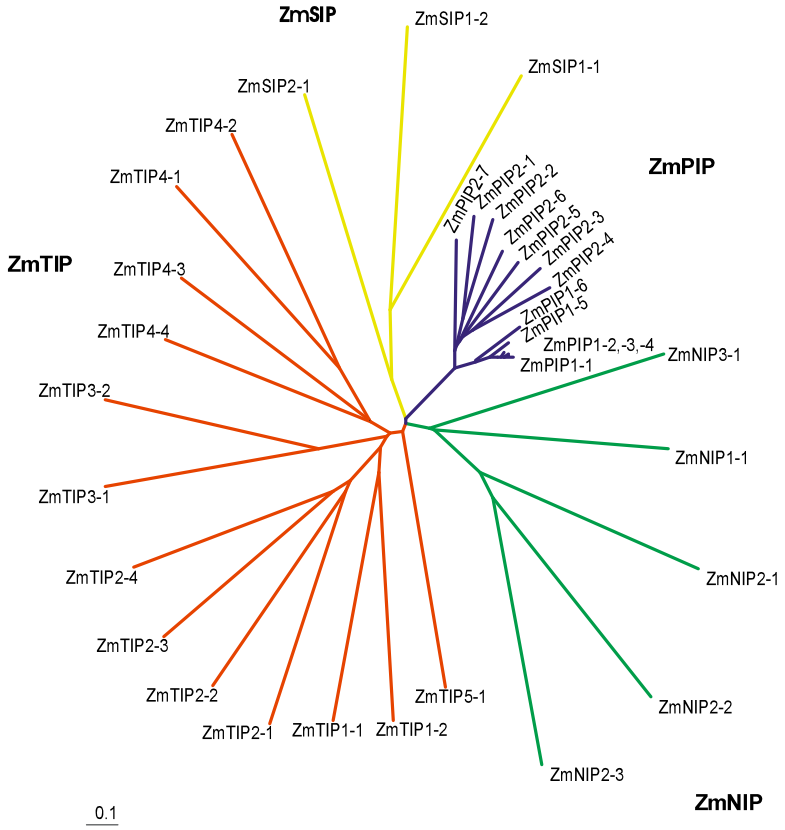

Fig. 2. Phylogenetic analysis of 34 maize MIP proteins. The bar represents the evolutionary distance, expressed in the number of substitutions per amino acid.

Most of *ZmMIPs* are expressed in roots, reproductive organs and aerial vegetative tissue. Some members are transcribed in all organs, such as *ZmPIP1-1, ZmPIP1-2, ZmPIP1-3, ZmPIP2-1, ZmTIP1-1 and ZmTIP2-1*. Other aquaporin genes are expressed only in specific organs*; ZmPIP2-2* is expressed primarily in reproductive organ tissue, whereas *ZmPIP2-4, ZmPIP1-5* and *ZmTIP2-3* are expressed exclusively in roots (Chaumont *et al.*, 2001; Gaspar *et al.*, 2003; Lopez *et al.*, 2004). The expression of *ZmPIP1-1* and *ZmPIP2-4* correlated with the permeability of cells in the primary roots of maize, which affected the extension of growth of roots (Hukin *et al.*, 2002). Whether other members of aquaporins are related to the permeability of cells, elongation and water uptake of roots is unknown.
The expression of a few *ZmMIP* genes was also studied at tissue level (Chaumont *et al.*, 1998, 2000; Barrieu *et al.*, 1998). *ZmTIP1-1* was highly expressed in the root epidermis, root endodermis, small parenchyma cells sounding the mature xylem vessel in the roots and stems, phloem companion cells and a ring of cells around the phloem strand in the

stems and leaf sheath. *ZmPIP1-1, ZmPIP1-2* and *ZmPIP2-5* were expressed in the meristematic zone and zone of cellular elongation, tips of primary and lateral roots, leaf primordia, and male and female inflorescence meristems. Hukin *et al.* (2002) reported higher expression of *ZmPIP1-2* and *ZmPIP2-4* in subapical zone than in apical zone; there was no difference in *ZmTIP1-1* transcripts in both zones.

The oscillation of transcripts of several aquaporin genes such as *ZmPIP1-1, ZmPIP1-5, ZmPIP2-1, ZmPIP2-5* and *ZmTIP2-3* during day and night cycle was observed (Gaspar *et al.*, 2003; Lopez *et al.*, 2003, 2004).

The effect of abiotic stress on the expression of maize aquaporins has been also investigated. Lopez *et al*. (2004) examined *ZmTIP2-3*, which was induced salt and water stress, but not by ABA. A more extended study has been performed by Wang *et al.* (2003). After application of 150 mM NaCl to hydroponically grown maize seedlings, seven *ZmPIP*s and two *ZmTIP*s were found to be repressed after 12 h. However, these authors used a cDNA microarray harbouring EST clones with amplicon of at least 400 bp, which cannot differentiate between homologous members; e.g. the target sequence of "*ZmPIP1-3*" *(ZmPIP1-1* according Chaumont *et al*., 2001) may cross-hybridize with *ZmPIP1-4, ZmPIP1-3 and ZmPIP1-2*[1], their *ZmPIP2-4* target may cross-hybridize with *ZmPIP2-3, ZmPIP2-5, ZmPIP2-1* and *ZmPIP2-2*[2].

Gaspar *et al.* (2003) found that *ZmPIP1-5* was induced after addition of KNO_3 into NO_3^--deficient maize seeding. Chilling repressed all PIP genes but the amount of ZmPIP1 proteins increased and that of ZmPIP2 proteins was constant (Aroca *et al.*, 2005).

To overcome the limitations of these studies, I initiated a systematic analysis of all *ZmMIP* members using gene-specific DNA targets for hybridizations.

4. Goal of the project

Maize is one of most important crops, ranking second to wheat as grain and feed among the world cereal crops (FAO, 1986). Plant water relation affects growth, development and productivity. In plant water relations, aquaporins may play an important role in regulation of transmembrane transport of water, which affects uptake, transport and loss of water. The expression of aquaporins responds to developmental and environmental factors. In maize it was specifically shown that the root hydraulic conductivity was deregulated by salt treatment, application of the phytohormone ABA or nutrient deficiency. Therefore, the aim of this project was to approach the involvement of aquaporins in these changes by assessing the whole complement of the aquaporin-encoding *MIP* gene family from maize.

[1] The target sequence of ZmPIP2-4 exhibited 98%, 96%, 91% and 88%homology with ZmPIP2-3(over 240 nt), ZmPIP2-5 (over182 nt), ZmPIP2-1 (over 163nt) and ZmPIP2-2 (over 159 nt) respectively. [2.] The target sequence of ZmPIP1-3 had 88%-85% homology with ZmPIP1-4 , ZmPIP1-3 and ZmPIP1-2 (over 204 nt).

To perform global expression analysis of the homologous MIP members, a DNA array had to be designed harboring specific target sequences of *ZmMIPs* and control genes.

Using this tool, I wanted to study *ZmMIP* transcription in different zones of the root that are implicated mainly in cell division, cell elongation, water uptake, transcellular transport and long distance transport. Such an analysis of *ZmMIPs* expression in roots can help to elucidate and relate the function of specific aquaporin isoforms in these processes.

Abiotic stimuli and ABA have been identified to affect the hydraulic conductivity of roots. The underlying mechanism and an involvement of aquaporins is not clear. Therefore, the level of aquaporins in the roots of maize undergoing salinity stress was to be analyzed to understand the implication of aquaporin in effect of salt stress on plant water relation. It is also well known that the level of ABA increases upon salt stress. There exist two pathways mediating signalling during salt stress, ABA-dependent or independent pathways. The study on expression of aquaporins in roots applied with exogenous ABA can shed light on whether ABA mediates effect of salt stress on aquaporin expression. In addition, the ABA experiments were of particular interest because a collaborating laboratory had previously identified the up-regulation of water permeability by exogenous application of ABA (Hose *et al.*, 2002; Wan *et al*., 2004).

Until recently, most of the analysis on aquaporin expression was conducted at transcriptional level. Only marginal evidence exists regarding the expression and their regulation at protein level. Therefore, two antisera, discriminating ZmPIP1 or ZmPIP2 isoforms, were used to investigate the level of ZmPIP protein in response to salt stress and treatment with ABA.

Furthermore, it has been reported that hydraulic conductivity of roots and root cells was regulated by nutrient deficiency such as NO_3^-- and K^+-deficiency (pp. 10-13). Whether and how aquaporins are mediating the effects of NO_3^- and K^+ on hydraulic conductivity is unknown. Analysis of aquaporin expression was conducted during K^+- or NO_3^--deficiency to address that issue.

B. MATERIAL AND METHOD

1. Materials

1.1. Biological Material

1.1.1. Plants

Zea mays Helix (KWS, Einbeck, Germany) was used for all analyses.

1.1.2. Bacteria

E. coli DH-5α
E. coli BL21
E. coli BL21- Gold (DE3)

1.1.3. Enzyme and antibodies

1.1.3.1. Enzymes

HindIII (10 U/µl	MBI Fermentas GmbH, St. Leon-Rot
Protease	Sigma, Louis, USA
Proteinase K	Invitrogen GmbH, Karlsruhe, Germany
RNase A	Boehringer Mannheim, Mannheim
RNase-Inhibitor RNasin (35-50 U/µl)	MBI Fermentas, St. Leon-Rot
Superscript TM II RNase H – Reverse Transcriptase (200 U/µl),	Invitrogen, Life Technologies, Groningen
T4 Polynucleotid Kinase (10 U/µl)	MBI Fermentas, St. Leon-Rot
Taq-DNA-Polymerase (5 U/µl)	Qbiogene, Heidelberg

1.1.3.2. Antibodies

Alexa647 goat anti-chicken	Molecular Probe Inc. Eugene, USA
Alkaline phosphatase-coupled anti-Digoxigenin	Roche, Mannheim, Germany
anti chicken Ig conjugated with alkaline phosphatase	Promega Madison, USA
anti Rabbit Ig conjugated with alkaline phosphatase	Promega Madison, USA
Chicken antiserum against ZmPIP2	Pineda-Antikörper-service, Berlin, Germany
IRDye800 goat anti-rabbit	Rockland Inc, Gilbertsville, USA
Rabbit antiserum against ZmPIP1	H. Sieber & A. Schäffner; raised by Prof. Bernd Kaspers, Tiermedizin, LMU München

1.1.4. Vectors and oligonucleotides

Oligonucleotides (see supplement)	
pDEST 15 vector	Invitrogen , Karlsruhe, Germany
pDON 221 vector	Invitrogen, Karlsruhe, Germany
pGEM-T-easy Vector System	Promega GmbH, Mannheim
SP1, SP3 and SP4	NASC, Nottingham, UK

1.2. Chemicals

(±)-cis, trans-Abscisic acid	Sigma-Aldrich, Steinheim, Germany
Agar	USB, Cleveland
Agarose SEA KEM LE	FMC Biochemicals, Maine, USA
Ampicillin	Roche, Mannheim, Germany
BSA (Fraction V)	SIGMA Aldrich Chemie, Steinheim
Chloroform	Merck, Darmstadt
DEPC (Diethylpyrocarbonat)	SIGMA Aldrich Chemie, Steinheim
Dithiothreitol (DTT)	Invitrogen, Life Technologies, Groningen, NL
EDTA (Ethylendiamintetraacetat)	SERVA, Heidelberg
Ethidiumbromid	SIGMA Aldrich Chemie, Steinheim
Ficoll Typ 400	Amersham Pharmacia Biotech, Freiburg
Glycerin	Roth, Karlsruhe
Herring sperm DNA	Boehringer Mannheim, Mannheim
IPTG (Isopropyl b-D-thiogalactopyranoside)	SIGMA Aldrich Chemie, Steinheim
Kanamycin	Roche, Mannheim
MES (2-[N-Morpholino] ethansulfon acid)	SIGMA Aldrich Chemie, Steinheim
MOPS (3-[N-Morpholino] propansulfon acid)	SIGMA Aldrich Chemie, Steinheim
Murashige and Skoog (MS) Medium	SIGMA Aldrich Chemie, Steinheim
Nucleotide (dATP, dCTP, dTTP, dGTP)	MBI Fermentas, St. Leon-Rot
Oligo-dT	Invitrogen, Life Technologies, Groningen, NL
pAW109 RNA	Applied Biosystems, Foster City, CA, USA
Polyvinylpyrrolidon MW 360.000 (PVP-360)	Roth, Karlsruhe, Germany
Polyvinylpyrrolidon MW 40.000 (PVP-40; K30)	SIGMA Aldrich Chemie, Steinheim
Rubidium chlorid	Merck, Darmstadt
Spermidin	SERVA, Heidelberg
Tris (hydroxymethyl)-aminomethyl	Biomol Feinchemikalien GmbH, Hamburg
Tween 20	SIGMA Aldrich Chemie, Steinheim
X-Gal (5-bromo-4-chloro-3-indolyl ß-D-galactopyranoside)	Boehringer Mannheim
Xylencyanol FF	SIGMA Aldrich Chemie, Steinheim

1.3. Molecular biological kits

Absolute™ QPCR SYBR® Green ROX Mix	ABgene, Surrey, UK
CSPD reagent	Roche, Mannheim, Germany
Detection buffer for Northern analysis	Roche, Mannheim, Germany
QIAprep Spin Miniprep Kit	Qiagen, Hilden, Germany
QIAquick Gel Extraction Kit	Qiagen, Hilden, Germany
QIAquick PCR Purification Kit	Qiagen, Hilden,Germany
Ribo-Probe in vitro Transcription	Promega, Madison, USA)
RNeasy Plant Mini Kit	Qiagen, Hilden, Germany
StripAble™ cDNA probe Synthesis and Removal Kit	Ambion, Texas, USA
Trizol® reagent	Invitrogen, Karlsruhe, Germany
Wash buffer 1, 2, 3 for Northern analysis	Roche, Mannheim, Germany

1.4. Apparatus and software

1.4.1. Apparatus and equipment

Applied Biosystem PE-7700	Applied Biosystem, Foster, USA
Bio-Rad Gel Doc 2000	Bio-Rad Lab GmbH, Munich, Germany
Microm HM 355	MICROM international GmbH, Walldorf, Germany
FLA-3000 image reader	Fuji, Düsseldorf, Germany

Halbmikro-Osmometer TYP M 1KG	Dr. Herbert Knauer, Berlin, Germany
Microgrid II	BioRobotics, UK
Microm HM 355	MICROM international GmbH, Walldorf, Germany
Mikrotiterplatten-Centrifuge 4K15C	Sigma GmbH, Osterode, Germany
MultiCycler PTC-200	Biozym, Oldenburg, Germany
Rotary Kilns for Hybridization	Bachofer GmbH, Munich, Germany
Scintillation counter	Beckman Coulter GmbH, Ramsey, USA
Speed-Vac Concentrator SVC-100 H	Bachofer GmbH, München, Germany
Spectrophotometer DU640	Beckman Coulter GmbH, Unterschleißheim, Germany
UV Stratalinker	Stratagene, La Jolla, USA
Vibratome 1000 classic, CE	Vibratome company, St.Louis, USA

1.4.2. Software and internet addresses

AIDA array evaluation	http://www.raytest.de
Array vision	http://www.imagingresearch.com/
Array vision 5.0	InterFocus, Mering, Germany
Haruspex	http://euklid.mpimp-golm.mpg.de/gxdb/
Multianalyst software	Bio-Rad, Munich, Germany
NCBI/Blast	http://www.ncbi.nlm.nih.gov/BLAST/
Photoshop	Adobe, Sanjase, USA
Primer3	http://frodo.wi.mit.edu/cgi-bin/primer3
Sequencing	http://www.e-sequence.medigenomix.de/
TIGR Maize Gene index	http://www.tigr.org

1.5. Solutions and nutrient medium

1.5.1. Solution

10 x NTE buffer	5 M NaCl 100 mM Tris/HCl pH7.5 10 mM EDTA
10 x salt	3 M NaCl 0.1 M Tris/HCl pH6.8 0.1 M $NaPO_4$-buffer 50 mM EDTA
10 x TBS buffer	1 M Tris/ HCl pH 7.5 1.5 M NaCl
100x Denhardt-solution	2 % (w/v) Ficoll Typ 400 2 % (w/v) PVP-360 2 % BSA steril filtrated
12% resolving gel	ddH_2O 1.674 ml 4x separate buffer pH8.8 1.250 ml 30% Rotiphorese 2.0 ml 10% APS 25 µl TEMED 2.5 µl Total 5 ml
1x running buffer	25mM Tris/HCl pH8.3 200mM glycine Add SDS to 0.1% before use
1x TAE	40 mM Tris-acetate pH 8.0 1 mM EDTA

1x TE	10 mM Tris/HCl pH 8.0 1 mM EDTA
20 x SSC	3 M NaCl 0.3 M Na_3Citrat pH 7.0
4x Separate buffer	1.5M Tris /HCl pH 8.8 0.4% (w/v) SDS
4x Stock buffer	5 M Tris/HCl pH 6.8 0.4% (w/v) SDS
5X loading buffer	30 % Glycerine (v/v) 0.25 % Bromphenolblau (w/v) 0.25 % Xylencyanol FF (w/v)
6% stack gel	ddH_2O 1.25 ml 4x stock buffer pH6.8 0.625 ml 30% Rotiphorese 0.5 ml 10% APS 20 µl TEMED 10 µl Total 2.5 ml
Coommasie solution	0.05% Coommasie brilliant blue R-250 50% methanol 10% acetic acid
DEPC-treated ddH_2O	0.1 % (v/v) DEPC, autoclaved
Destaining solution for staining of protein	10% methanol 10% acetic acid
Destaining solution for detection of phosphor-protein	50 mM NaAc pH 4.0 20% Acetonitrile
Lambda DNA	MBI Fermentas, Leon-Rot, Germany
Herring sperm DNA	10 mg/ml, autoclaved
Homogenization buffer A for isolation of fusion protein	2.5 ml Bugbuster TM HT protein 2.5 µl Mecaptolethanol 50 µl Lysozym (0.5 mg/ 50µl in 0.1M Tris/HCl pH 8.0) 125 µl Complete Protease Inhibitor Cocktail (Roche, Manheim, Germany);
Homogenization buffer B for isolation of fusion protein	30 ml 1X PBS 30 µl ß-Mercaptolethanol
Homogenization buffer for isolation of microsomal fractions	50 mM HEPES-KOH pH 7.5 5 mM EDTA pH8.0 5 mM EGTA pH 8.0 0.5 M Sucrose 50 mM NaF 1 mM Na_3VO_4 5 mM ß-glycerol phosphate Complete, Mini Tablets (Roche, Germany) 0.5 µM K252a 2 mM DTT 1 mM PMSF 0.5% (w/v) PVPP
Laemmli buffer (Laemmli, 1970)	10% (w/v) SDS 30% (v/v) glycerin 100 mM Tris/HCl pH 6.8 5% 2-mercaptoethanol (add before use)
Prestained protein marker (Biolab, New England)	MBP-ß-galactosidase (175 kDa) MBP-paramyosin (83 kDa) Glutamic dehydrogenase(62 kDa) Aldolase (47.5 kDa) Triosephosphate isomerase (32.5 kDa) ß-Lactoglobulin A (25 kDa) Lysozyme (16.5 kDa) Aprotinin (6.5 kDa)

Resuspension Buffer	0.33 M sucrose 5 mM KPO_4 buffer 4 mM KCl 5 mM NaF 1 mM Na_3VO_4 10 mM ß-glycerol phosphate 5 mM EDTA 5 mM EGTA pH 8.0 Complete Mini Tablets (Roche, Germany) 0.1 µM K252a
TBS	10 mM Tris/HCl pH 7.4 150 mM NaCl 1 mM $MgCl_2$
TBST	1X TBS buffer 1% dried milk powder 1% BSA 0.5% Tween 20
TFB 2	10 mM Pipes pH 6.42 75 mM $CaCl_2$ 10 mM $RbCl_2$ 15% (w/v) glycerol The pH was regulated to 6.5 with 1 M KOH solution was sterile using 0.45µm filter
TFB 1	100 mM RbCl 30 mM KOA_C 10 mM $CaCl_2$ 50 mM $MnCl_2$ 15% (w/v) Glycerol The pH was regulated to 5.8 with 0.1 M acetic acid
Transfer buffer	25 mM Tris 192 mM glycine 0.1 % SDS Before use 20% SDS was added until the concentration of SDS is 0.01%
X-Gal	100 mg in 2 ml N,N'-Dimethyl-formamide

Radiochemicals

α-[^{33} P]-dATP (>2500 Ci/mmol)	Redivue Amersham Pharmacia Biotech, Freiburg
?-[^{33} P]-ATP (>2500 Ci/mmol)	Redivue Amersham Pharmacia Biotech, Freiburg

1.5.2. Bacterial medium

LB-Medium	2.5 % (w/v) Miller´s Luria Broth Base (Sigma) 60 µl 5 M NaOH/100 ml Medium
LB-Platte	1.25 % (w/v) Bacto Agar (Difco Laboratories, Detroit, USA) 2.5 % (w/v) Miller´s Luria Broth Base (Sigma) 60 µl 5 M NaOH/100 ml Medium
RB-Medium	1 % (w/v) Trypton (Difco Laboratories, Detroit, USA) 0.5 % (w/v) yeast-extract (Difco Laboratories, Detroit, USA) 0.5 % (w/v) NaCl 2 ml 1 M NaOH/l medium
SOC medium	0.5% (w/v) yeast extract (Difco Laboratories, Detroit, USA) 2% (w/v) Trypton (Difco Laboratories, Detroit, USA) 10 mM NaCl 2.5 mM KCl 10 mM $MgCl_2$ 10 mM $MgSO_4$ 20 mM glucose pH 7.5

1.5.3. Plant medium

type	Control medium	K-deficient medium	NO_3-deficient medium
Macro-element	1.5 mM KH_2PO_4	1.5 mM NaH_2PO_4	1.5 mM KH_2PO_4
	2.0 mM KNO_3	2.0 mM $NaNO_3$	2.0 mM KCl
	1.0 mM $CaCl_2$	1.0 mM $CaCl_2$	1.0 mM $CaCl_2$
	1.0 mM $MgSO_4$	1.0 mM $MgSO_4$	1.0 mM $MgSO_4$
Micro-element	18 µM FeNaEDTA	18 µM FeNaEDTA	18 µM FeNaEDTA
	8.1 µM H_3BO_4	8.1 µM H_3BO_4	8.1 µM H_3BO_4
	1.5 µM $MnCl_2$	1.5 µM $MnCl_2$	1.5 µM $MnCl_2$

1.5.4. Consumed materials

AutoSeq ™ G-50	Amersham Pharmacia Biotech, Freiburg, Germany
Hybond-N+ Nylon membrane (15 mm x 73 mm)	Amersham Pharmacia Biotech, Freiburg,Germany
Hybridization tubes (50 mm x 150 mm)	ThermoHybaid, Heidelberg,Germany
Imaging plate BAS-IP 2340	FUJI Photo Film Co., LTD, Japan
MicroSpin TM G-25 columns	Amersham Pharmacia Biotech, Freiburg
MicroSpin TM S-400 HR columns	Amersham Pharmacia Biotech, Freiburg
Miracloth-Filter	Calbiochem, La Jolla, USA
Multiscreen plates	Millipore, Bedford, Ma, USA
nylon membrane	Roche, Mannheim, Germany
PCR-reaction tube (single and plate)	Biozym, Hess. Oldendorf, Germany
Phospho-image	Fuji Photo film Co., Tokyo, Japan
stone woollen (Grodan)	Grodania A/S, Hannover, Germany
Whatman-paper	Schleicher &Schuell, Dassel, Germany

2. Methods

2.1. Nucleic acids

2.1.1. Isolation of nucleic acids

2.1.1.1. Isolation of total RNA from maize roots

2.1.1.1.1 Extraction of total RNA using Trizol® Method

Maize roots were harvested, briefly rinsed with in distilled H_2O, dried with paper towel, put immediately in liquid nitrogen and stored in the freezer of –80^oC. For disruption using a mortar and pestle or dismembrator, frozen material was ground or homogenized to a fine powder under liquid nitrogen; the powder was transferred into liquid nitrogen pre-cooled falcon and stored in –80 ^oC freezer.

For isolation of total RNA Trizol® reagent (Invitrogen, Karlsruhe, Germany) was used following manufacturer's instruction. One hundred mg root powder was weighed and put in pre-cooled Eppendorf tube and nitrogen was let to evaporate without allowing sample thawing. Then it was mixed with 1 ml Trizol® reagent and it was shaken for 10 min by hand. After extraction with 200 µl chloroform and centrifugation the upper, aqueous phase containing RNA was recovered into a fresh Eppendorf tube. The RNA was precipitated by 500 µl isoprophanol and washed with 70% ethanol. RNA was dissolved in 30-50 µl DEPC-treated water.

2.1.1.1.2. Isolation of total RNA using Qiagen RNeasy Plant Mini Kit

For isolation of total RNA from maize roots RNeasy® Plant Mini Kit (Qiagene, Hilden, Germany) was used according to the manufacturer's protocol. Buffer RLC was added in maize root powder for lysis. A short incubation at 56°C was not needed to disrupt tissue and therefore omitted because it could degrade total RNA.

Trizol® reagent or Qiagen RNAeasy® Kit isolated total RNA contained usually genomic DNA, which will cause errors in semi- or real time quantitative RT-PCR. Therefore, contaminated DNA was to be removed. Two purification methods were applied in the project and had same efficiency for purification.

One was digested with RNase free DNase (Roche, Mannheim, Germany) followed by Phenol extraction and ethanol precipitation (2.1.2.1). 12.5 µl 10X digestion buffer (400 mM Tris-HCl pH 7.5 and 60 mM $MgCl_2$), 1 µl RNase free DNase and 1 µl RNase inhibitor were added into about 50-100 µg RNA sample, final volume was adjusted to a volume of 125 µl with DEPC-treated water, the solution was incubated at 37°C for 15 min. Another was on-column DNase digestion, followed by RNA cleanup with RNeasy Kit (Qiagene, Hilden, Germany).

The concentration of total RNA was determined by measuring the absorption at 260 nm in a spectrophotometer**.** 10 mM Tris/HCl pH 7.5 was used to zero the spectrophotometer; the ratio of A260/280 was calculated to estimate the purity of total RNA with respect to contaminants that absorb in the UV, such as protein. The ratio of A260/280 of purified total RNA was 1.8-2.0.

2.1.2. Isolation of DNA

Genomic DNA was extracted from etiolated maize seedlings according to the method of Dellaporta *et al.* (1983) modified by Fabri and Schäffner (1994). The DNA was used as template for amplification of target sequences.

1-1.5 g material powder (2.1.1.1.1) was extracted in 15 ml extractions buffer (1 mM Tris/HCl pH 8.0, 50 mM EDTA pH 8.0, 500 mM NaCl, 10 mM 2-Mercaptoethanol) with 60 µl 20 µg/ml proteinase K, incubated in water bath at 65°C for 10 minutes. Five ml of 5 M potassium acetate was added, mixed and placed on ice for 20-30 min, followed by centrifugation at 25000 g for 20 min at 4°C. The supernatant was filtered through two layer of miracloth into a clean 50 ml centrifuge tube. 10 ml 2-propanol was added, mixed gently by inversion and left at -20°C for 40 min to precipitate DNA, then centrifuged at 20000 *g* for 20 min at 4°C. The supernatant was discarded; the pellet was allowed to drain for 5 min and resuspended in TE buffer and transferred to an Eppendorf tube.

DNA was incubated at 37°C for 1 h with 7 µl RNAse A (10mg/ml) stock solution, one volume Tris saturated phenol was added and mixed, followed by centrifugation at 20000g

for 5 min. The upper aqueous phase was transferred into a new Eppendorf tube, mixed with 460µl phenol: chloroform: isoamyl alcohol = 25:24:1, centrifuged 20000g for 5min. One volume chloroform: isoamyl alcohol (24:1) was added in water phase and centrifuged 20000g for 5min. 1/10 volume 3 M pH 5.2 sodium acetate and 0.6 volumes of 2-propanol were added in water phase, mixed and allowed to stand ambient temperature for 5 min, centrifuged at 15000g for 15 min, the pellet was washed with 500 ml 75% ethanol, and spun for 5 min, the pellet was drained for 5 min and resuspended in 200 µl TE buffer and stored at 4^{o}C.

The concentration of DNA was measured using spectrophotometer. The purity of DNA was estimated with the ratio of A260/A280. The ratio of isolated DNA was about 1.8 indicating high quality DNA. Contaminations by protein would lower the ratio, whereas RNA would increase it.

2.1.3. Preparation of plasmid DNA

Plasmid DNA was prepared with help of Qiaprep® Spin Miniprep Kit (Qiagen, Hilden, Germany), according to manufacturer' protocol. Up to 20 µg of high copy plasmid DNA could be obtained from 1-5 ml overnight cultures of *E. coli* in LB medium.

2.1.4. Purification of PCR products

After PCR reaction or other enzymatic reaction DNA fragments were purified from primer, nucleotides, polymerase and salt. The purification was performed with Qiaquick® PCR Purification Kit (Qiagen, Hilden, Germany) following manufacturer's instruction.
To purify the target fragment from unspecific fragments from standard or low melting agarose Qiaquick® Gel Extraction Kit (Qiagen, Hilden, Germany) was applied according to the protocol. The method was appropriate for extraction and purification DNA of 70 bp to 10 kb.

2.1.5. Determination of concentration of nucleic acids

The concentration of total RNA was determined by measuring the absorption at 260 nm in a spectrophotometer**.** 10 mM Tris/HCl pH 7.5 was used to zero the spectrophotometer; the ratio of A260/280 was calculated to estimate the purity of total RNA with respect to contaminants that absorb in the UV, such as protein.

2.1.6. Separation of nucleic acids on agarose gel electrophoresis

The integrity and size distribution of total RNA purified with two methods was checked by agarose gel electrophoresis and ethidium bromide staining. The respective ribosomal bands appeared as sharp bands on the stained gel.

To check the quality and length of DNA fragments nucleic acid was separated on agarose gel (0.5- 2% in TAE buffer) according to size of nucleic acid; to visualize the fragment under UV lighter till to 0.5 µg/ml ethidium bromide was added into 1X TAE running buffer, to quantify RNA the same concentration of ethidium bromide should be added in the agarose gel. 5X loading buffer was mixed with nucleic acid, the samples and DNA standard marker were loaded in the gel and run at 5-10 V/cm for 1-2 h.

2.1.7. Digestion by restriction endonucleases

To check the length of insert in plasmid the plasmid was cleaved by restriction endonuclease, the sort of chosen restriction endonuclease depended on the sequence of nucleic acid that insert was franked.

Digest contained 0.2 µg plasmid DNA, 1X reactive buffer, ca. 5 units of restriction endonuclease, ddH_2O was added to the volume of 20 µl. The mixture was incubated at 37^oC for 1 h or overnight. The enzyme was deactivated at 65^oC for 10 min. The fragments sizes were checked by agarose gel electrophoresis.

2.1.8. Ligation, recombinantion and transformation of DNA fragments

2.1.8.1. Preparation of competent cell

A single colony of bacteria was inoculated into 2.5 ml of rich Broth (RB) in a plating tube and cultivated at 37°C with moderate shaking (230 rpm) over night. 2.5 ml of culture was subcultured in 250 ml RB with 20 mM $MgSO_4$, and grown to OD = 0.4-0.6.
The suspension was centrifuged at 5000 rpm for 5 min at 4^oC. The supernatant was discarded, the bacteria pellet was resuspended carefully in 100 ml of ice cold TFB I and kept on ice for 5 min. The bacteria suspension was centrifuged at same speed, the pellet was resuspended gently in 10 ml cold TFB2 and incubated on ice for 15-60 min, 100µl was aliquoted in ice-cold Eppendorf tubes then frozen quickly in liquid nitrogen and stored at -80^oC.
To assure the efficiency of transformation the prepared competent cells must be tested. Plasmid DNA containing 100, 10, 1 and 0.1 pg were added in 100 µl *E. coli* DH-5α competent cell and placed on the ice for 20 min, incubated at 37^oC for 45 sec and left on the ice for 2 min. 900 µl SOC medium was added in every tube and incubated at 37^oC for 1.5 hr with shaking (230 rpm). The medium was centrifuged at 4000 g for 5 min. The supernatant was discarded, the pellet was re-suspended in rest medium, and the culture was plated on the LB medium agar plate with 100 µg/ml, ampicillin/ 800 µg IPTG/ 800 µg X-Gal, which was incubated at 37^oC overnight.

2.1.8.2. GATEWAY recombination

DNA fragments encoding different ZmPIP2 epitopes were polymerized by PCR using primers with 29mer attachments allowing recombination according to the GATEWAY

system. PCR fragments were recombined in a 5 µl reaction (1/4 the recommended volume) into pDONR221 (Invitrogen). The inserts were confirmed by sequencing. Using a secondrecombination, the inserts were transferred to their final destination pDEST15 allowing the expression as a GST fusion proteins in E.coli.

2.1.8.3. Transformation of competent cell

Ligation was performed following the manufacture's instruction with slight modification. The reaction was set up in 5 µl ligation solution containing 1x rapid ligation buffer, 0.5 µl pGEM® T easy, 300 ng PCR product and 0.5 µl T4 DNA ligase. The ligation was incubated at room temperature for 1 h. The procedure for transformation of different vectors such as pGEM® T-easy, pDEST15, pDON221 was same as that for testing the transformation efficiency of competent cells.
In case of GATEWAY-based vectors containing the ccdB gene *E. coli* DB3.1 were used.

2.1.9. PCR (polymerase chain reaction)

The purpose of a PCR is to make a huge number of copies of a DNA fragment. This is necessary to have enough starting template for sequencing. There are three major steps in a PCR, which are repeated for 25 or 40 cycles. This is done on an automated cycler, which can heat and cool the tubes with the reaction mixture in a very short time.
a. Denaturation at 94°C:
During the denaturation, the double strand melts open to single stranded DNA, all enzymatic reactions stop.
b. Annealing at lower temperature depending on primer sequence:
The primers bind to complementary sequence of the template, the polymerase can attach and starts copying the template. Once there are a few bases built in, the base-pairing is so strong between the template and the primer, that it does not break anymore.
c. Extension at 72°C.
This is the ideal working temperature for the polymerase. The bases (complementary to the template) are coupled to the primer on the 3' side, polymerase adds dNTPs from 5' to 3', reading the template from 3' to 5' side, and bases are added complementary to the template.
20 ng of plasmid DNA or 100 ng genomic DNA were mixed with 1µl forward primers and reverse primer, 2.0 µl of 10 x reaction buffer, 0.2 µl 20 mM dNTP, ddH_2O and 0.1 µl 5 U/µl Unit of Taq polymerase to an end volume of 20 µl. The PCR tubes were placed into PTC-200 Peltier Thermal Cycler (MJ Research).

The PCR was performed as followed:
95°C / 2 min 1 cycle
95°C / 30 sec ⎫
xx°C / 30 sec ⎬ 25-40 cycles
72°C / 45sec ⎭
72°C / 5 min 1 cycle
4°C / ∞
PCR products were analyzed by electrophoresis on a 2% agarose gel.

2.1.10. Sequence analyses

All MIP target sequences were confirmed by sequencing. Samples (Plasmid–DNA) were sent to the company TopLab or MediGenomix and sequenced. Eighteen control gene targets were not sequenced.

2.2. Macroarray analysis

2.2.1. Construction of target DNA sequence

To produce gene-specific probes 3'-UTR sequences were selected from cDNA sequences. In addition to maize *MIP* genes, 18 constitutively expressed genes were selected from maize EST data according to their expression in roots documented by EST frequency (www.tigr.org) to normalize data. Primer pairs for aquaporin and constitutive genes were designed according to primer 3 (http://frodo.wi.mit.edu/cgi-in/primer3/primer3_www.cgi).

Target sequences from aquaporins and constitutive genes were amplified using specific primer pairs and genomic DNA (2.1.9) from etiolated maize seedling as template. PCR products were tested on 2% agarose gel to confirm whether length of PCR products was corresponding. PCR products were purified using Qiaquick PCR Purification kit (2.1.4) and Qiaquick gel extraction Kit (2.1.4) (Qiagen GmbH, Hilden, Germany). Purified PCR products were ligated into pGEM T-easy vector (Promega, Madison, USA) and transformed DH-5α component cell (2.1.8). Bacterial were plated on LB agar plate containing with ampicillin / IPTG/X-Gal and grown at 37^{o}C overnight, and white clones were picked into reagent tube containing 5 ml LB liquid medium with ampicillin. After overnight growth plasmid DNA were prepared from bacterial (2.1.3) using QIAprep spin Miniprep Kits (Qiagen GmbH, Hilden, Germany). Plasmid-DNA was sequenced (2.1.10) to confirm rightness of target sequence using blasting (NCBI).
Specific target sequences were amplified using $M13^{+}$ and $M13^{-}$ primers and plasmid DNA as template. The first round PCR products were diluted to 50 folds. The second round PCR was performed using T7 and SP6 primers and diluted PCR products as template. The following reactions and program were used:

PCR mix:

2 µl plasmid DNA (200µg/µl Plasmid DNA was diluted 100 fold)	
10x PCR buffer	2 µl
20 mM dNTP	0.2 µl
10 µM $M13^{+}$	1 µl
10 µM $M13^{-}$	1 µl
Taq DNA polymerase (5 U/µl)	0.1 µl
Add ddH_2O to 20 µl	

PCR program

95^{o}C	2min

95°C	30s	⎫
56°C	30s	⎬ 30cycles
72°C	60s	⎭

The second round PCR:
PCR mix

First PCR product (50fold diluted)	10 µl
10x PCR buffer	10 µl
20 mM dNTP	1 µl
10 µM T7	5 µl
10 µM SP6	5 µl
Taq DNA polymerase	2 units
Add ddH_2O to 100µl	

PCR program

95°C	2 min	
95°C	30 s	⎫
52°C	30 s	⎬ 35 cycles
72°C	60 s	⎭

600 µl PCR products (from six parallel reactions) were concentrated using Multiscreen plates (Millipore, Bedford, Ma, USA), resuspended in 200 µl distilled water in 96 well plates. The quality, size and quantity were determined by electrophoresis (2% agarose gel). The estimated concentration was in a range of 150 to 250 ng/ µl.

2.2.2. Array printing and preparation of membranes.

Concentrated PCR products were spotted in duplicate on to Hybond-N^+ nylon membranes (Pharmacia, Freiburg, Germany) using MicroGrid Robot (400 µm pins, 10 repeats per spot to transfer sufficient amount of DNA; BioRobotics, Cambridge, UK) (Fig. 3). After spotting nucleic acids were UV-cross-linked to the membrane using standard conditions of the UV-Stratalinker (Stratagene, La Jolla, USA). Membranes were denatured on 0.5 M NaOH/1.5 M NaCl soaked Whatman paper for 5 min, neutralized on 0.5 M Tris/HCl pH 7.5/ 1.5 M NaCl Whatman paper and finally on 2x SSC-soaked Whatman. Afterwards the membranes were rinsed with 2x SSC until pH of solution was lower than 8.

2.2.3. Hybridization with reference probes

T7 probes were prepared, the mixture for each membrane contained 2.5 µl 10 µM T7 primer , 1.25 µl polynucleotide kinase buffer, 1µl ?-^{33}P-ATP (Amersham, UK), 1 µl polynucleotide kinase. 6.75 µl distilled water was added to total volume 12.5 µl. The mixture was incubated at 37°C for 30 min. After incubation 37.5 µl of distilled water was added in the mixture. T7 probe was purified using G-25 Sephadex column (Amersham

Pharmacia Biotech, Freiburg, Germany) following manufacture's instruction, 1 µl T7 probe was measured by liquid scintillation counter (Beckman, Ramsey, USA).

The membranes were pre-hybridized at 38°C for 3 h in pre-hybridization solution containing 5x SSC, 5x Denhardt´s solution, 0.5% SDS, 100 µg/ml denatured Salmon sperm DNA and hybridized at 38°C overnight after addition of the labeled T7 probe into the prehybridization solution. The membranes were washed at 38°C for 20 min with 2x SSC/ 0.1% SDS and at 38°C for 20 min with 0.2x SSC/ 0.1% SDS. The membranes were wrapped with 2x SSC soaked Whatman 3MM paper in plastic film and exposed to imaging plate (Fuji Photo film Co, Tokyo, Japan) for 18 h. Care was taken to prevent drying of the membranes because this would interfere with the stripping of the T7 probe. Primary data were required using a FLA 3000 image reader (Fig. 3; Fuji, Düsseldorf, Germany).

Labelled probes were completely removed from filters by two washes with 0.4 M NaOH for 30 min. Then membranes were rinsed several times with 2x SSC until pH of washing solution was lower than 8. Removal of the labelled probes was controlled by a hand-held monitior and exposure (1 day) of the filters.

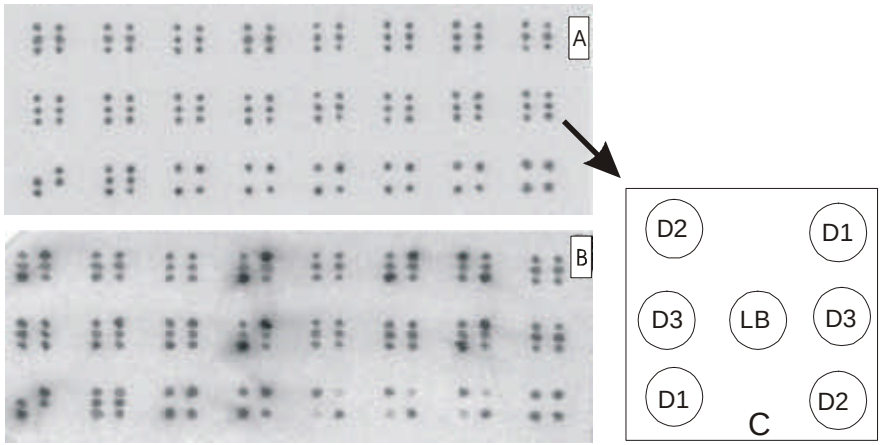

Fig.3. Reference hybridization (A), complex hybridization (B) and distribution of probes on the DNA macroarray (C). Reference hybridization and complex hybridization occur with radioactive marked T7oligonucleiotide and complex respectively. D1, D2 and D3 show three macrotiter plates. LB, local background.

2.2.4. In vitro transcription

Plasmids containing spiking control genes SP1, SP3 and SP4 (NASC, Nottingham, UK) were used as templates and amplified using specific primer pairs (see supplement). After purification of PCR products using Qiaquick PCR Purification kit (Qiagen GmbH, Hilden, Germany) (2.1.1.2), in vitro transcription was performed using Ribo-Probe in vitro Transcription (Promega, Madison, USA) following manufacture's instruction. Plasmid DNA was degraded with RNase-free DNase and RNA was purified using RNeasy mini Kit

(Qiagen GmbH, Hilden, Germany) and quantified by spectrophotometer. The quality of RNA was controlled on 1% agarose gel.

SP1, SP3 and SP4 RNAs were diluted to the final concentration of 10 ng/µl, aliquoted, and separately stored at -80^{o}C. Before preparation of complex probes SP1, SP3 and SP4 RNAs were mixed at the ratio of 100 pg : 50 pg : 50 pg and added to each plant RNA sample for reverse transcription. To assure the accuracy and precision of experiments new mixture of spiking RNA were used for each hybridization.

2.2.5. Preparation of complex probes

For synthesis of cDNA complex probes using StripAble^{TM} cDNA probe Synthesis and Removal Kit (Ambion, Texas, USA), 10 µg total RNA (purified using Qiagen kit) was mixed with the mixture of in-vitro transcribed RNA from human genes SP1, SP3, SP4 (2.2.4) and 2 µl 10 x oligo (dT) primer, DEPC-treated water was added to volume of 11 µl. The mixture was heated at 65^{o}C for 5 min and quenched on ice.
The reaction mixture containing 2 µl 10x RT-buffer, 2 µl 10x Nucleotide Mix, 1 µl 200 U/µl MMLV-Reverse Transcriptase and 4 µl α-^{33}P-dATP (> 40 µCi) (Amersham Pharmacia, UK) was added to RNA sample and incubated at 40^{o}C for 90 min. cDNA probe was denatured with 1 µl 0.5 M EDTA pH 8.0 and added with ddH2O to the final volume of 100 µl. One µl cDNA probe was measured using scintillation counter. The intensity of cDNA probes should be 15-25 x 10^{6} cpm/100 µl. All cDNA probes were denatured at 100^{o}C for 2 min and quenched on ice before use.

2.2.6. Hybridization with complex probes

All the procedures for prehybridization and hybridization with cDNA complex probes were identical to those with T7 reference probes, except that hybridization was performed at 68^{o}C in hybridization tubes in a rotary hybridization oven. The membranes were washed at 68^{o}C for 20 min with 2x SSC/ 0.1% SDS and at 68^{o}C for 20 min with 0.2x SSC/ 0.1% SDS.
After data were obtained the filters were stripped using StripAble^{TM} cDNA probe Synthesis and Removal Kit (Ambion, Texas, USA). The filters were incubated with 1x degradation buffer and 1x degradation dilution buffer at room temperature for 5 min each with gentle shaking, and then with 0.2% SDS and 1x Blot reconstitution buffer at 68^{o}C for 20 min in a water bath. The removal of complex probes was controlled by a hand-held monitor and exposure to an imaging plate.

2.2.7 Data evaluation

The spot detection and quantification of hybridization signals from the phosphoimager data were analyzed using the Array Vision 5.1 (InterFocus, Mering, Germany) software.

The local background signal of each subgrid was subtracted from all related spot intensities. If the signal intensity of the spot was lower than 2 folds of local background, it was replaced by local background (lb) value. This value was labeled by a negative sign to indicate this instance (i.e. lower than twofold the local background). Furthermore, the lb value was subtracted from all signal values, which were more than 2 folds of local background value. For normalization, the signal intensities were divided by the mean of the signal measured for three internal standard transcripts (SP1, SP3 and SP4) (internal normalization) or by the mean of all signal values of the array for normalization (Haruspex) (http://euklid.mpimp-golm.mpg.de). The same procedure was used for the reference (T7 oligonucleotide) and complex (cDNA) hybridization signals.
The ratio of normalized complex value / normalized reference value was calculated. As there were two replicates on each array, the average values of this technical replicates were taken as the gene activity.
To compare two different scenarios, the ratio of the corresponding gene activities was obtained by dividing the gene activity of treated sample by the value of untreated sample. If both gene activities of treated and untreated samples were labelled “negative”, the gene was considered as not detected (n.d.). If the gene activity of either the treated sample or the untreated sample was negative, the ratio was included as a positive value. These values were considered as estimates for the real induction or repression, since one of the values was indicated as below detection limit.
The experiment was repeated three times, from which the mean value of ratio was calculated. The result was tested by t-test (expected value) (Precht *et al.*, 1993).

$$to = \frac{\bar{x} - \mu o}{s/\sqrt{n}}$$

H_o: $\mu = \mu_o$ (μ_o=1)
H_1: $\mu < \mu_o$, if $t_o < -t_{n-1;\,1-\alpha.}$ (one side hypothesis)
$\mu > \mu_o$, if $t_o > t_{n-1;\,1-\alpha.}$ (one side hypothesis)
then H_o was rejected at significant value α=0.05.
With $\bar{x}$ mean value, μo expected value, s, standard deviation; n, number of samples.

2.3. Semi-quantitative RT-PCR and quantitative RT-PCR

2.3.1. Semi-quantitive RT-PCR

For semi-quantitative RT-PCR cDNA was synthesized from 2 µg of total RNA (Qiagen kit) using oligo (dT)12-18 and Superscript™ RNase (Gibco Life Technologies, Gaithersburg, USA). Amplification of cDNA by PCR was performed using gene-specific primers with Taq DNA polymerase (Qbiogene, Heidelberg, Germany). Gene-specific primers were designed for *Rab17* and *Dbf1*; for several *ZmPIP* genes primers designed by Eli Hose and Anton Schäffner were used (Supplement 1.1). PCR reactions were optimized for each gene to obtain products in the linear amplification range. For all genes tested 30 cycles were optimal. As an internal standard 10^6 copies of the synthetic RNA pAW109

(Applied Biosystems) was added to total RNA. At least three reactions were carried out for each gene. PCR products were run on 1.5% (w/v) agarose gel and quantified using Multianalyst software (Bio-Rad, Munich, Germany). The relative transcript values of gene was signal intensity normalized using the pAW109-derived signal.

Total RNA	2 µg
DEPC-H_2O	12.2 µl
5x first strand buffer	8 µl
RNA inhibitor (50 U/µl)	2 µl
DTT (100 mM)	4 µl
20mM dNTP	1 µl
Oligo $(dT)_{12-18}$ (0.05 µM)	6.8 µl
pAW109 mNA (10^6 copy)	1 µl

Add DEPC-H_2O to 38 µl

Incubation at room temperature for 10 min.

SUPERSCRIPT™ Rnase (200U/µl, 1:3 dilution with 1x first strand buffer)	2 µl

Temperature program

42°C	30 min
50°C	40 min
94°C	5 min
4°C	10 min

2.3.2 Quantitative real time RT-PCR

For detection of mRNA of *ZmMIP*s in samples real-time RT-PCR was conducted in the Applied Biosystem PE-7700 (Applied Biosystem, Foster, USA) using Absolute™ QPCR SYBR® Green ROX Mix (ABgene, Surrey, UK).

Total RNA was isolated and purified to remove genomic DNA (2.1.1.1.1 and 2.1.2.4). The amounts of RNA were equalized according to the ethidiumbromide fluorescence encompassing the bands of 28S to 18S rRNA.

The cDNA was prepared as follows. Twelve µl containing 2 µg total RNA, 10^6 copies pAW109 (Applied Biosystems, Foster City, CA, USA), 0.5 µg oligo$(dT)_{15}$ and RNase-free water were incubated at 70°C for 10 min and chilled on ice. A cocktail containing 1X first strand buffer, 500 µM dNTP Mix (MBI Fermentas, St. Leon-Rot), 0.01 M DTT, 25 units RNase inhibitor, 200 units Superscript ™ RNase (GIBCO-BRL, Gaithersburg, USA) was mixed with the denatured total RNA in a total volume of 20 µl. After incubation at 42°C for 60 min and at 70°C for 15 min, the cDNA solution was used directly for qPCR or stored at -20°C.

For each RNA sample another reverse transcription was performed without Superscript™ reverse transcriptase to check the contamination of genomic DNA. For real-time PCR analysis cDNA sample was diluted to 50 fold with distilled water. The reactive mixture (25µl) for real-time PCR contained 4 µl of diluted cDNA, 0.5 µM primers (Supplemental Tab. 1), 12.5µl Absolute™ QPCR SYBR® Green ROX Mix (ABgene, Surrey, UK) and distilled water.

PCR products produced melting curves with sharp, single transition, indicating high purity and homogeneity of PCR products, optimal temperature for data collection of every gene could be obtained. After real time RT-PCR, PCR products were run on 2% agarose gel, only one band or signal was observed in all samples. No band or signal was observed when either template of the reverse transcription was omitted.

The expression of gene was calculated based on the comparative C_t method ($2^{-\Delta\Delta Ct}$). First, the transcripts of target genes were normalized by that of a reference gene or internal standard gene, then the expression rate was obtained by division of treated value by untreated value.

The program for real time RT-PCR.

95°C 15 min 1 cycle for enzyme activation
95°C 15 sec ⎫
55°C 25 sec ⎬ 40 cycles
72°C 45 sec ⎭
81°C or 78°C 10 sec for data collection.

Different temperature were used to assure specific measurement of the gene-derived PCR products, e.g. contaminating, short PCR products melted earlier.

Gene	Data collection
ZmPIP1-2	78°C
ZmPIP1-1, ZmPIP2-4, ZmPIP1-5, Paw109	81°C

The primers used for ZmMIP qRT-PCR were identical to those used for target sequence preparation (Tab. 1)

Melting curve program

Temperature (°C)	Incubation time	Temperature transaction rate (°C/s)	acquisition mode
95	0 s	20	No
60	15 s	20	No
95	0 s	0.1	Yes

2.4. Northern blot analysis

For Northern analysis 10 µg total RNA (2.1.1.1; Trizol method)) was denatured with a mixture of 0.05% formaldehyde and 42% formamide at 95°C for 5 minutes, and fractionated in a denaturing formaldehyde 1.2% agarose gel and blotted overnight onto nylon membrane (Roche, Mannheim, Germany) by capillary transfer using 20x SSC. The

membranes were air-dried and nucleic acids were fixed using standard settings of a UV cross-linker (Stratalinker, Stratagene). Northern blots were pre-hybridized for 1 h at 50°C with 10 ml pre-hybridization buffer (Roche). The membrane was probed with DIG-labelled PCR products of *ZmPIP1-1* and *ZmPIP1-2* (Roche, Mannheim, Germany) according to the manufacturer's protocol. Hybridizations were carried out overnight at same solution at 50°C with addition of 5 µl of denatured Digoxigenin-labelled DNA probe. After hybridization, the membrane were washed twice for 5 min at room temperature with 2x SSC/ 0.1% SDS, then washed twice for 15 min at 50°C with 0.1x SSC/ 0.1% SDS. After washing for 2 min with wash buffer 1 (Roche, Mannheim, Germany), Northern blots were blocked for 30 min with 1% block buffer (Roche, Mannheim, Germany), followed by incubation for 30 min at room temperature with 1 : 10000 alkaline-phosphatease-coupled anti-digoxigenin antibody in 1% blocking buffer. After two times washes for 15 min with wash buffer 1 (Roche Mannheim, Germany) and once for 2 min with detection buffer, CSPD reagent (Roche) was used as substrate to perform chemiluminescent detection as recommended by the manufacture (Roche). An X-ray film was exposed for 30-60 min.

2.5. In situ hybridization

2.5.1. Tissue fixation and embedding

0.5 cm root pieces were sampled from zone 10-20 mm from the tip of primary roots grown in wetted paper for 4 days and immediately placed overnight at 4°C in a freshly prepared fixation solution containing 4% formaldehyde in 1X PBS buffer pH 7. After two washes at room temperature for 30 min with 1X PBS, the samples were dehydrated in a series of solution of increasing ethanol concentration (50%, 70%, 85%, 95%, 100%) for 60 min each. Then, ethanol was gradually replaced by Histoclear (Roth, Karlsruhe, Germany) and Paraplast Plus chips (Roth, Karlsruhe, Germany) were added at the ratio1:1. Samples were incubated at 60°C for 2 h before the Histoclear/ Paraplast mix was replaced by melting Paraplast after two changes everyday for 3 days at 60°C. Samples were embedded in Paraplast Plus block and stored at 4°C before section.

2.5.2. Sectioning

The embedded tissues were sectioned into 8 µm thick slices and placed on Superfrost/ Plus slides (Roth, Karlsruhe, Germany). Sections were dried and affixed to the slides by incubating the slides in the hot plate at 42°C overnight, dewaxed with histoclear, and hydrated by passing through an ethanol series with 0.85 % NaCl.

The sections were washed with 1x PBS, then treated with 0.2 M HCl for 20 min and with 10 µg/ml proteinase K (Sigma, Louis, USA) in 100 mM Tris/HCl pH 7.5 and 50 mM EDTA for 30 min. The protease was blocked by incubation with 0.2% glycine for 2 min and subsequent washing with 1X PBS for 2 min. Subsequently, the sections were treated

with 4% formaldehyde in 1X PBS for 10 min, after wash with 1X PBS the sections were treated with 0.5% acetic anhydride in 0.1 M triethanolamine pH8.0 for 10 min. Finally, the sections were dehydrated through an ethanol series (30%, 50%, 70%, 85%, 95%) to 100% ethanol.

2.5.3. Synthesis of probe

Plasmid DNA containing *ZmPIP1-1* specific sequences were used as template. PCR was performed using T7 promoter containing adaptor primer and another specific primer (2.1.8). PCR products were purified using Qiaquick PCR Purification kit (Qiagen GmbH, Hilden, Germany) (2.1.2.2), in vitro transcription was performed using Ribo-Probe in vitro Transcription (Promega, Madison, USA) following manufacture's instruction.

The reaction mixture contained 4 µl 5x buffer, 2 µl 100 mM DTT, 0.5 µl (20-40 u) RNase inhibitor, 4 µl NTP (1 µl ATP, 1 µl CTP, 1 µl GTP, 0.6 µl UTP and 0.4 µl DIG-UTP, 2.5 mM each), 1 µl T7 RNA polymerase (15-20 u), and incubation at 37^{o}C for 2 h. Plasmid DNA was degraded with 1 µl RNase-free DNase (Roche, Manheim, Germany) and stopped with 2 µl 0.2 M EDTA pH 8.0.

The in vitro transcribed RNA was purified by LiCl and ethanol precipitation and washed with 70% ethanol and resuspended in DEPC-treated water. The concentration of RNA was determined by spectrophotometer. The quality of RNA was controlled on 1% agarose gel.

2.5.4. In situ hybridization on sections

The sections were pre-hybridised with SPB solution containing 1x salt, 40% deionized formamide, 10% dextransulphate, 1 mg/ml tRNA and 1x Denhardt at temperature for 0.5 h and 50^{o}C for 1.5 h in box containing 50% formamide wetted paper. The sections were hybridised at 50^{o}C overnight with SPB solution with sense or antisense probes in the same box. After hybridization the sections were washed twice at 50^{o}C for 45 min, with 2 x SSC/50% formamide and twice at 37^{o}C for 5 min with 1x NTE buffer The sections were treated with 20 µg/ml RNase A in 1x NTE buffer at 37^{o}C for 30 min, then washed subsequently two times with 1x NTE at room temperature for 5 min, once with 2x SSC/ 50% formamide at 50^{o}C for 1 h, with 1x SSC for 5 min and 1 x PBS for 5 min, briefly with 1x TBS buffer.

2.5.5. Detection of signal

The slides were incubated successively for 40 min in TBS buffer with 0.5% blocking reagent (Roche, Manheim, Germany) and for 40 min in TBS buffer with 1% BSA and 0.3% Triton X100. The sections were incubated for 1 h in same solution containing alkaline-phosphatase conjugated anti-digoxigenin at 1: 3000 dilutions, then washed three

times for 15 min with TBS buffer plus 1% BSA and 0.3% Triton X 100, shortly with detection buffer containing 100 mM Tris /HCl pH 9.5, 100 mM NaCl and 50 mM $MgCl_2$.

The transcripts were detected by incubating the slide in detection buffer with NBT/BCIP (Roche, Mannheim, Germany) according to manufacture's instruction. The reaction was checked under a microscope (Zeiss). After colour development the reaction was stopped by washing slides two times for 5 min in distilled water.
Photograph of sections were made using microscope (Zeiss) with Canon G2 digital camera (Canon, Japan). The images were processed (background subtraction) using photoshop (Adobe, Sanjase, USA).

2.6. Microbiological methods

2.6.1. Culture of bacterial in liquid medium

E.coli was grown in LB medium at 37^{o}C for 12-16 hr with shaking at 230 rpm in shaking incubator. According to different plasmid corresponding antibiotics were added into medium.
Ampicillin 50 µg/ml (stock solution 100 mg/ml), kanamycin 50 µg/ml (stock solution 50 mg/ml)

2.6.2. Culture of bacteria on agar plates

Autoclaved LB medium with 1.25% (w/v) Agar was cooled to 50^{o}C, ampicillin or kanamycin were added to final concentrations of 100 µg/ml and 50 µg/ml, respectively. Agar solution was poured into sterile Petri dishes. These agar plates were stored at 4^{o}C. The bacteria were plated on the agar plates and incubated at 37^{o}C for 12-16 hr.

2.6.3. Glycerol culture

For long term storage of bacterial strains 190 µl 80% glycerol was added to 810 µl bacterial culture, mixed well, incubated on the ice 5 – 10 min, then stored at -80^{o}C.

2.7. Protein chemical methods

2.7.1. Isolation of protein

2.7.1.1. Extraction of microsomal fractions from maize roots

About 0.5 g roots were ground to a fine powder and mixed with 20 ml homogenizing buffer. The homogenate was filtered through two layers of miracloth into pre-chilled centrifuge tube (SS-34) and centrifuged at 8000x g for 10 min at 4^{o}C, the supernatant was

filtered through a layer of miracloth into ultra centrifuge tubes and centrifuged at 110,000x g for 40 min at 4 C. The supernatant fraction was discarded. 100 µl of suspending buffer was added in the pellet and incubated on ice for 30 min, then resuspended using douncer. The resuspension solution was stored at -80^{o}C.
For determination of phosphoproteins, the homogenizing and resuspending buffers contained phosphatase (glycerol phosphate) and kinase (K252a, NaF, Na_3VO_4) inhibitor (see 1.5.1).

2.7.1.2. Isolation of protein from *E. coli*

The transformed BL-21 (DE 3) were grown in LB medium with 100 µg/ml ampicillin at 37^{o}C and 250 rpm until OD_{600}= 0.6. IPTG was added in the medium to the final concentration 0.1 mM. After 5 h induction the culture was centrifuged at 9000 g for 10 min, the sediment was frozen at –80^{o}C for isolation of GST-fusion proteins. Before and after addition of IPTG 2 ml of culture were sampled for assay of GST activity.
2.5 ml homogenization buffer A per 50 ml culture was added to the frozen *E. coli* cell pellet. The sample was shaken at room temperature for 15 min. Three ml of buffer B with 1% Triton was added in lysate and shaken softly. The lysate was centrifuged at 10000 rpm for 10 min at 4^{o}C. The supernatant was collected; 10 µl of supernatant was used for assay of activity of GST and analysis of fusion-protein by SDS-PAGE.

2.7.2. Purification of GST-fusion protein

300 µl Glutathione Sepharose^{TM} 4B (Amersham Bioscience AB, Uppsala, Sweden) equilibrated by 1x PBS was added into the supernatant and shaken at room temperature for 30 min, and then centrifuged at less than 1000 rpm for 5 sec to sediment Glutathione Sepharose^{TM} 4B beads. The supernatant was discarded; the pellet was transferred to column. The fusion protein was washed three times with 1x PBS and eluted by 2x 300 µl glutathione (20 mg/3 ml in 0.1 M Tris/HCl pH 8.0). 20 µl of eluate was sampled for assay of activity of GST and SDS-PAGE analysis.

2.7.3. Measurement of activity of GST-fusion protein

The following solutions 100 µl 0.1 M KH_2PO_4 pH6.5, 10 µl 100 mM 1-Chloro-2,4 Dinitrobenzene (CDNB), 10 µl 100 mM glutathione and 880 µl distilled water were mixed in two cuvette labelled by blank and sample. Two cuvettes were covered with wax film and inverted to mix.
Fifty-five µl of the sample (supernatant or eluate) was added into sample cuvette and mixed. The reading at 340 nm was recorded at 1 min interval for 5 min by first blanking the spectrophotometer. The activity of GST (glutathione S-transferase) was calculated as A340 nm/ min/ ml.

2.7.4. Determination of protein concentration

2.7.4.1. Bradford method

800 µl samples containing 2.5 to 20 µg BSA in 0.1 M Tris/HCl pH 8.0 were mixed with 1x Bradford solution, incubated at room temperature for 15 min, the 595 nm absorption reading of samples were measured using a spectrophotometer.

2.7.4.2. Modified Lowry method

The determination of microsomal fraction protein was performed according to modified Lowry method (Markwell *et al*., 1978), to eliminate the interference of resuspension buffer (2.7.1.1), 5 µl of resuspension buffer was added in 0-50 µg BSA solution for preparation of a standard curve of absorbance.

2.7.5. SDS-PAGE

This gel system uses the method described by Laemmli (1970). The protein sample is denatured and coated with detergent by heating in the presence of SDS and a reducing agent. The SDS coating gives the protein a high net negative charge that is proportional to the length of the polypeptide chain. The sample is separated on a polyacrylamide gel containing SDS by electrophoresis. Since a net negative charge taken by proteins is roughly proportional to their size, the molecular mass of the proteins can be estimated by comparing the mobility of a band with protein standards.
Resolving and stacking mini-gel solutions for the preparation of two 7 x 10 cm gels with a thickness of about 0.75 mm were prepared. 10% ammonium persulfate and TEMED were added just prior to pouring the gel. The resolving gel mix was poured into assembled gel plates, leaving sufficient space at the top for the stacking gel to be added later.
The gel mix was gently overlaid with water-saturated butanol and the gel was allowed to polymerize for at least 15-30 min. After polymerization, the butanol layer was removed and the surface of the resolving gel was rinsed with water. The remaining space was filled with the stacking gel solution and the comb was inserted immediately. After the stacking gel had polymerized, the comb was removed and the wells were rinsed with water to remove unpolymerized acrylamide. At least 1 cm of stacking gel should be present between the bottom of the loading wells and the resolving gel.

GST-fusion proteins, bacterial lysates or protein markers were denatured with Laemmli buffer at 95^{o}C for 5 min, whereas 10 µg proteins of microsomal fraction were denatured at 56^{o}C for 20 min with Laemmli buffer and 100 mM DTT. To check the oligomerization of aquaporin 0-200 mM DTT were added in 10 µg microsomal fraction before denaturation. The denatured protein samples were loaded onto the gel with a prestained protein standard marker. The gel was run in SDS gel running buffer at 80 mA for approximately 2 h.

2.7.6. Staining of SDS-PAGE

2.7.6.1. Coomassie brilliant blue

To visualize the proteins on the SDS-PAGE the gel was stained in Coomassie dye solution acid for 2 hr, the gel was subsequently destained in destaining solution over night. The gel was photographed and quantified with multi-analyst (Biorad, Germany)

2.7.6.2. Pro-Q Diamond

Pro-Q Diamond phosphoprotein gel stain is a technique providing a means for selectively staining phosphoproteins in SDS-polyacrylamide gels. This proprietary fluorescence stain allows direct in-gel detection of phosphate groups attached to tyrosine, serine or threonine residues; it can detect as little as 1-16 ng of phosphoproteins per band, depending on the phosphorylation state of the protein. For individual phosphoproteins, the strength of the signal correlates with the number of the phosphate groups and is linear over three orders of magnitude. According to the manufacturer, the stain is also compatible with mass spectrometry, allowing analysis of the phosphorylation state by mass spectrometry.
The mini-gel was immersed in 100 ml of 50% methanol and 10% acetic acid and incubated at room temperature with gentle agitation for at least 30 min. The fixation step was repeated once or the gel could be left in the fixation solution overnight to assure all of SDS was washed out. The gel was washed for 10 min two times to remove all methanol and acetic acid from the gel. The gel was stained by Pro-Q Diamond phosphor-protein gel stain in the dark with agitation for 2hr. for destaining the gel was incubated in Destain solution in the dark with gentle agitation for 1 hr three times. The stained gel was visualized on the FLA3000 (532nm/580nm), the signal was quantified by AIDA 1D-evaluation (Raytest, Straubenhardt, Germany).

2.7.6.3. SYPRO-ruby

After staining with Pro-Q Diamond the gel was assayed for total protein with Coomassie brilliant blue stain (CBS) or a SYPRO-ruby stain. SPRO-Ruby offers a quantitative stain with a similar sensitivity than silver stains. It can stain lipoprotein, glycoprotein and other proteins, showing less protein to protein variability; it does not stain nucleic acids. It delivers a linear quantitation range of over three orders of magnitude.
The gel stained by PRO-Q Diamond was washed in distilled water for 10 min. The gel was incubated in SPRO-Ruby for 3 h or overnight in the dark. Subsequently, the gel was washed in 10% methanol and 7% acetic acid for 30 min in the dark. The proteins on the gel were scanned with FLA 3000. The signal was quantified by AIDA 1D-evaluation.

2.7.7. Western analysis

2.7.7.1. Transfer of protein from gel to nitrocellulose membranes

Electrode plates of the semi-dry apparatus (Milliblotting-SDE apparatus) was rinsed with transfer buffer. Nine pieces of Whatmann-3MM paper and one piece of nitrocellulose (Biotrace TM NT, PALL Life Science) or Potran BA 85 cellulosenitrate (E) (Schleicher & Schüll, Dassel, Germany) were cut and submerged in transfer buffer (see 1.5.1) for several minutes, which were exactly the size of the gel. Six pieces of 3MM paper, 1 piece of membrane, SDS-PAGE gel and 3 pieces of 3MM paper were orderly placed on the anode and exactly aligned. Any air bubbles were removed with a pipette by rolling over the sandwich. The upper electrode was placed and electrical leads were connected. A current of 2.5 mA cm^{-2} was applied for 1 h. To check the efficiency of transfer the gel was stained with Coommassie brilliant blue solution or the membrane was stained with Ponceau Red. After blotting the nitrocellulose membrane could be stained or used for immunological visualization of proteins.

2.7.7.2. Quantitative Western analysis

The membrane was blocked in TBST solution with 1% BSA and 3% fatless milk powder at 4^{o}C for 1 h to overnight with gentle shaking. The membrane was incubated with 1 : 1000 rabbit antiserum against ZmPIP1 or 1 : 500 chicken antiserum against ZmPIP2 in TBST solution with 1% BSA for 2 h, then the membrane was washed 3x 10 min in TBST solution, subsequently the membrane was incubated with 1: 4000 anti-rabbit lgG (Fc) alkaline phosphatase conjugate or anti-chicken lgY alkaline phosphatase conjugate in TBST with 1% BSA for 1 hr. The membrane was washed 2X 10 min in TBST solution and once 10 min in TBS solution. The membrane was submerged in Western blot dye (Biorad, Germany), the progress of colour reaction was monitored. When the band was of desire intensity, the reaction was stopped by rinsing the membrane in distilled water. The membrane was stored at room temperature in the dark.

To quantify the amount of protein two colour infrared fluorescent immunoblots was used. The membrane was blocked in 1X PBS solution with 5% fatless milk powder at 4^{o}C overnight with a gentle shake. The membrane was incubated with 1: 1000 antibodies against ZmPIP1 and 1 : 500 antibodies against ZmPIP2 in 1X PBS buffer with 1% fatless milk powder and 0.1% Tween-20 for 1 hr, then the membrane was washed four times 5 min in 1X PBS buffer with 0.2% Tween-20, subsequently the membrane was incubated with 1: 10000 IRDye800 goat anti-rabbit and Alexa647 goat anti-chicken with 1% BSA in 1X PBS buffer with 1% fatless milk powder and 0.1% Tween-20 for 1 hr. The membrane was washed four times for 5 min in 1X PBS with 0.2% Tween-20 and once for 5 min in PBS buffer. The proteins were visualised and quantified by scanning the wet or dry membrane on Odyssey (LiCor) (Fig. 4). Wet membranes give lower signals, but allow

additional washing or stripping. From 2.5 to 20 µg the immunosignals were linearly related to the amount of protein (data not shown).

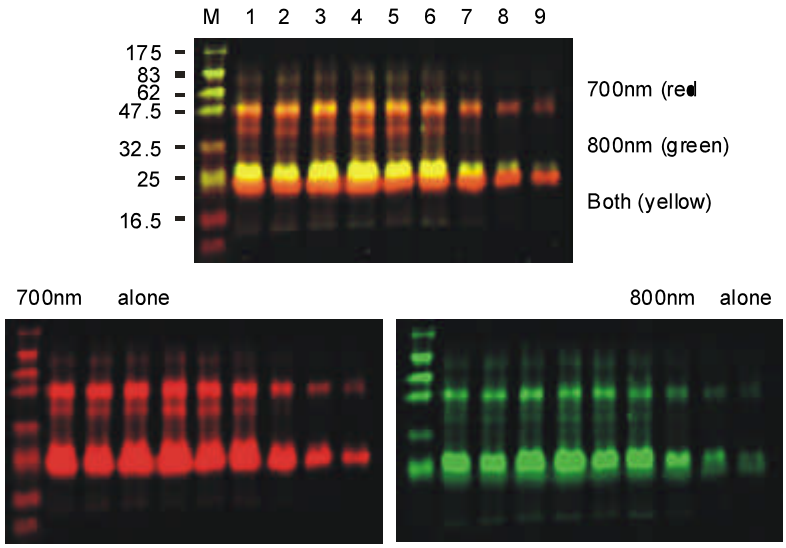

Fig. 4. Measurement of amount of ZmPIP1 and ZmPIP2 using two colour infrared fluorescent immunoblots. Microsomal fractions were isolated from roots treated with ABA. The fractions were separated on the 12% SDS-PAGE and blotted onto nitrocellulose. The membrane was probed with rabbit anti-ZmPIP1 (visible in red) and chicken anti-ZmPIP2 (visible in green). Antibodies bound on the membrane were detected with secondary Alexa680 goat anti-rabbit and IRDye800 goat anti-chicken (Methods). M: protein marker; lane 1: control at 1 h; lane 2: 1 µM ABA at 1 h; lane 3: 100 µM ABA at 1 h; lane 4: control at 24 h; lane 5: 1 µM ABA at 24 h; lane 6: 100 µM ABA at 24 h; lane 7, 8, 9: 10 µg, 5 µg and 2.5 µg samples treated with 100 µM ABA for 24 h. In other lanes 20 µg samples were loaded.

2.8. Culture of plants and physiological methods

2.8.1. Culture of plants

Maize seeds were immersed for 2 h in distilled water and germinated on wetted paper in the dark for 4 days at 24°C. Then the seedlings were transferred in continuously aerated hydroponic medium of Gibeaut *et al.* (1997). Small pieces of rock wool were used to fix the germinated kernels on top of the drillings in the cover plate. Plants were grown for additional seven days under 16/8 h at a photosynthetically active radiation of 180-230 µMol m^{-2} s^{-1}. The temperature was controlled between 22 and 25°C and relative humidity ranged from 45- 60%.

For analysis of spatial expression patterns of aquaporins maize seedling were grown on wetted paper in the above same condition for 6 days. The primary roots were cut in zone 0-3 mm, 3-10 mm,10-20 mm, 20-50 mm, 50-60 mm from the apex. The zone 10-50 mm was separated into two tissues cortex and stele with tweezer. After separation the materials were frozen in liquid nitrogen for further analyses.

2.8.2. Treatment of plants by NaCl and ABA

ABA or high-salinity stress treatments were carried out. For ABA treatments 1 µM and 100 µM (±)-ABA were added in hydroponic medium. Sampling times were 1 h, 6 h and 24 h after addition of the hormone. For high-salinity-stress treatments, 100 mM and 200 mM NaCl were applied in hydroponic solution, after 2 h, 9 h, 24 h and 48 h of treatment probes were harvested. After sampling the probes were frozen in liquid nitrogen for further analyses.

2.8.3. Measurement of water content in maize leaves

Leaf water status was assayed by measuring the fresh weight and dry weight of leaves of seedlings. Dry weight was obtained after drying of leaves at 104^{o}C for 3 h.

2.8.4. Assay of ABA concentration in maize roots

Freeze-dried tissue samples were homogenized and extracted in 80% methanol. Extracts were passed through a Sep Pak C_{18}-cartridge. Methanol was removed under reduced pressure and the aqueous residue partitioned three times against ethyl acetate at pH 3.0. The ethyl acetate of the combined organic fractions was removed under reduced pressure. The residue was taken up in TBS-buffer (Tris buffered saline; 150 mol m^{-3} NaCl, 1 mol m^{-3} $MgCl_2$, 50 mol m^{-3} Tris; pH 7.8) and subjected to an immunological ABA assay (ELISA) as described earlier (Peuke *et al*., 1994). The accuracy of the ELISA was verified for maize in earlier investigations (Hartung *et al*., 1994). All measurements were done at the University of Würzburg by Daniela Schraut and Bianca Dietrich.

2.9. Statistical analysis

In the present study, all experiments except nutrient deprivation analyses were reproduced at least three times and mean value and standard deviation were calculated.

Depending on the problem and data sets, different modes of analyses were applied: Anova (two-factor with replication) was used to detect significance of NaCl on water content of leaves in comparison with that of control. Anova (single factor) was used to evaluate the difference in length of shoots and roots between control plants and nutrient-deprived plants. The correlation coefficient was calculated using program “correlation” in Microsoft office. For correlation between dimer of ZmPIP2 and phosphorylated upper band, and between two methods of normalization of DNA array.

To detect significance of transcript induction or repression t-test for expected value was used. The expected value of expression rate of stressed to unstressed should be 1, if the treatment had no effect. The real data were introduced as the mean value +/- standard deviation of three treatments (ratio treatment *vs*. control for each replica experiment). The probability level for above test methods was assigned $p = 0.05$.

C. RESULTS

1. Design of ZmMIP array

To measure the abundance of gene transcripts several methods can be used such as Northern analysis, quantitative RT-PCR and DNA arrays. In order to comprehensively investigate transcriptional profiles of the major intrinsic protein genes of *Zea mays* (*ZmMIP*) a DNA array harboring gene-specific target sequences for 31 members was established. This allowed the parallel analysis of these genes in a single hybridization.

1.1. Selection of target sequences for ZmMIP array

Eleven *ZmPIPs*, 12 *ZmTIPs*, 3 *ZmSIPs* and 4 *ZmNIPs* cDNA were compiled according to Chaumont *et al.* (2001) and another TIP member named here *ZmTIP2-4* (Finkelstein *et al., 1998*) because it belongs to the *ZmTIP2* subfamily (Tab.1). In order to distinguish highly homologous maize *MIP* cDNAs the *MIP* target sequences were based on their 3´-UTR regions that showed higher sequence divergence. All selected target sequences were 110 to 350 bp in length. They were compared by BLAST analyses to maize cDNA sequences to verify their specificity.

Nineteen target sequences did not detect any other homologous maize genes when analyzed by NCBI BLAST algorithm. The specificity of the remaining 12 target sequences can be considered as follows. Xu *et al.* (2001) and Affenzeller (2003) reported that sequences having lower than 70% identity over a range of at least 70 nt did not considerably cross-hybridize. According to this criterion, four other target sequences having 84-88% homology over 60-67 nt would allow a specific detection of the respective gene transcripts (*ZmPIP1-2*/ *ZmPIP1-3* and *ZmTIP4-1/ZmTIP4-2*). Six target sequences had considerably higher homologies (93-96%), although only within short stretches of 28-48 nt. However, they may be regarded as specific probes as well, because e.g. the pair *ZmPIP2-3*/ *ZmPIP2-4* showed differential hybridization indicating the induction of *ZmPIP2-4* by NaCl or ABA. Instead, the potentially cross-hybridizing *ZmPIP2-3* was not altered (see below, Chapter 3 and 4).

The sequences targeting *ZmTIP3-1* and *ZmTIP3-2* had 84% homology over 98 nt. Thus, a weak cross-hybridization may be possible. The high homology of *ZmTIP2-3* and *ZmTIP2-4* (93.2% for the whole transcript) and *ZmPIP1*-3 and *ZmPIP1-4* (97% for the whole transcript) did not allow designing gene-specific probes. The latter pair may even correspond to the same gene (Chaumont *et al*., 2001). Therefore, a single target sequence was designed in these two cases that detected both gene transcripts. Finally, the partial cDNA sequence annotated as *ZmPIP2-7* does not include a 3'-UTR. Therefore, no gene-specific target could be obtained.

In order to evaluate and normalize the data and control experiments the established maize MIPs array also harbors probes for 18 constitutively expressed cDNAs expressed in roots.

Tab.1 Primers, length and specificity of 3'-UTR target sequences for detection of *ZmMIP*s by DNA array. Forward (f) and reverse (r) primers are given that were used for amplification of the target sequences. The resulting fragments were analyzed by the BLAST algorithm at the NCBI database for cross-hybridization to other maize genes.

cDNA	Acc.	Primer_f	Primer_r	length	analysis for crosshybridization
ZmPIP1-1	X82633	aggtcttaaaggagccgatg	tgaactcttaaagcttgactcg	241	no Maize Gene
ZmPIP1-2	AF131201	ggagaatttaagttattatccatttg	gaaactgaaatcaagaaaaccc	140	23-82 (88%) ZmPIP1-3
ZmPIP1-3	AF326487	tgtaccgagctgtgtgtatg	gatgaaaaatccagctgataga	146	43-110 (88%) ZmPIP1-2
ZmPIP1-4	AF326488	-	-		no separate target sequence possible, detected by ZmPIP1-3
ZmPIP1-5	AF326489	gagccgtgactgattatacg	gggagtcttcttcttaactttca	404	no Maize Gene
ZmPIP1-6	AF326490	gtcatacacggagttctgct	aatgggccttggtatattatg	213	no Maize Gene
ZmPIP2-1	AF326491	cttggctgtggagcaatg	cggaataatcccttgagagt	212	no Maize Gene
ZmPIP2-2	AF326492	cgtgatgagcagagctaaag	cccttggcagcagatatta	264	no Maize Gene
ZmPIP2-3	AF326493	accgatcgatccaagtgta	gaatgcattttgtcacatatacag	180	137-166 (96%) ZmPIP2-4
ZmPIP2-4	AF326494	gcaccgttccgattctgt	gtgatcggataaaaactcacg	190	95-128 (96%) ZmPIP2-3
ZmPIP2-5	AF130975	ggaggcgtgaactgtagata	tttttcattttacccagtcg	212	no Maize Gene
ZmPIP2-6	AF326495	gctattcagctcttcctcct	ttgcattcgtccatctttat	277	no Maize Gene
ZmPIP2-7	AF326496	-	-		no 3`-UTR known, no specific target sequence possible
ZmTIP1-1	AF037061	ccctccaccgactactaaaa	aggcaaatgcacaaatctta	263	no Maize Gene
ZmTIP1-2	AF326500	gcagcagactactgatgacc	ggacaaaataacatcacacaca	204	no Maize Gene
ZmTIP2-1	AF326501	accactccatctccgctc	ggcaaaggcacatcatatt	120	no Maize Gene
ZmTIP2-2	AF326502	gattcagctcatccaacg	cgaaacgaaaatcacctgt	232	no Maize Gene
ZmTIP2-3	AF326503	-	-		no specific target sequence possible, ZmTIP2-3 transcripts detected by ZmTIP2-4
ZmTIP2-4	AF057183	gatccgtctgtgttgatttc	cgaactgtgcattgcatttat	199	1-24 (100%), 91-177 (92%) ZmTIP2-3
ZmTIP3-1	AF326504	aaattgtattgtggggtcgt	cagcatgtacacatcacctg	110	1-99 (84%) ZmTIP3-2
ZmTIP3-2	AF342809	ccgtgtcctgttgtcaaat	ttgtacctggaatttattacat	151	56-84 (93%) ZmTIP3-1
ZmTIP4-1	AF326505	catcagcccctgtgttgt	gcaggaaacccccaaaaa	169	28-95 (84%) ZmTIP4-2
ZmTIP4-2	AF326506	gttcgttacctacaagcatga	aaaaatcacgtccaacgtatag	250	no Maize Gene
ZmTIP4-3	AF326507	gagtgtgacttggtttgagc	ccacaagaaattctgcagtt	157	no Maize Gene
ZmTIP4-4	AF326508	caccgacttctaggcagtag	tgctgcttccattccatt	110	no Maize Gene
ZmTIP5-1	AF326509	cgtttgacaagctagtgtgc	cgtacaacaagctatttaagtacag	181	no Maize Gene
ZmSIP1-1	AF326497	aataagaaatagaggaaggtcac	agcccaaaattacaagtaaaca	130	no Maize Gene
ZmSIP1-2	AF326498	ggatcttcagggctatgttc	ctgggaaccaggaacttatt	148	16-64 (93%) ZmSIP1-1
ZmSIP2-1	AF326499	ctacacacaaggcgaaatgt	tgagtcaactctgagaagcttta	212	no Maize Gene
ZmNIP1-1	AF326483	ccggtaatttagcctacaaaa	ggcacagtacgttttccat	163	no Maize Gene
ZmNIP2-1	AF326484	cgcacttgtttactcctcag	gtcccaaaattaagctccag	187	no Maize Gene
ZmNIP2-2	AF326485	catccacaacactgtcagc	tatttgtgttccgagttcca	350	no Maize Gene
ZmNIP3-1	AF326486	gtacgtgctgtgtctgtgtg	gcaaatcttgttcagaaatca	244	no Maize Gene

They were chosen according to their low (1-10), middle (10-20) or high (20-30) representation as EST sequences derived from maize cDNA libraries. About half of the ESTs of the selected genes had been found in root cDNA libraries (Suppl. 1.2).

In addition, five known ABA-responsive control genes *Rab17*, *Rab28*, *Bz2*, *Fer2*, and *Mlip15* as well as three negative, non-hybridizing human genes (TGF-beta, accession

number M60316; HLA class I histocompatibility, C-4 alpha chain, M11886; BRACHYURY, AJ001699) were included. Three further probes SP1, SP2 and SP3 (NASC: http://arabidopsis.org.uk) could be used as targets for spiking controls in the RNA samples to be hybridized (Methods).

All newly designed target sequences were confirmed by sequencing after cloning into pGEM-Teasy (data not shown). For array production the fragments were amplified by stepwise PCR reactions, purified, and checked by gel electrophoresis. Approximately, 4 ng of DNA per spot was transferred onto a charged Nylon membrane (Methods).

1.2. Data analysis and normalization

All membranes were hybridized with α-^{33}P-labeled T7 oligonucleotide to determine the relative amount of spotted DNA prior to hybridization with cDNA probes. These values were used for a first normalization step (Thimm *et al*., 2002; Methods).

Since the array consisted only of a small number of target sequences, it was crucial to check and compare different methods for data normalization after hybridization with complex cDNA probes. Therefore, two methods were compared for data normalization: the inclusion of several additional and potentially constitutive gene targets for normalization via the total gene signal intensity and the addition of spiking, non-plant mRNAs for normalization.

In both cases, valid signals according to background corrections (Methods) would be divided by the average of all signals or by the average of three spiking gene signals.
To utilize total gene intensity for data normalization 18 genes were chosen, which as a first criterion had different EST frequencies and, secondly, 50% of these ESTs were derived from root cDNA libraries. Data normalization was performed using the Haruspex algorithm (Methods, Thimm *et al.*, 2002).

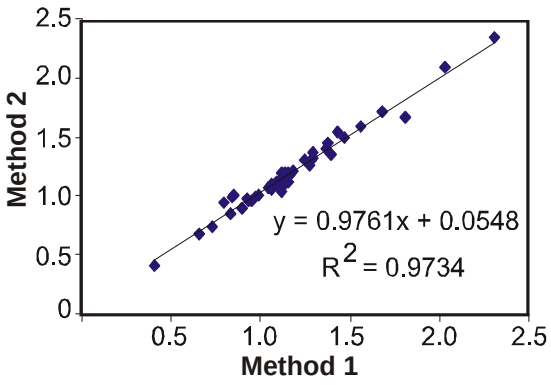

Fig.5. Comparison of two different methods for normalization of array data. Methods 1 or 2 refer to normalization of the data by total gene signal intensity or spiking genes, respectively.

To normalize the data via spiking controls three target sequences provided by the NASC were added to the *ZmMIP* array. These were three non-plant cDNAs, SP1 corresponding to B-cell receptor-associated protein (AF126021), SP3 to myosin light chain 2 (M21812), and SP4 to insulin-like growth factor II (X07868). The plasmids harboring SP1, SP3, and SP4 were used for in vitro transcription of mRNA that was spiked into the plant RNA before labeling (Methods). The summed signal of these three control targets was used for normalization in this case.

To compare and evaluate both methods for data normalization the eventual data of 31 MIP and 18 control gene targets were plotted (Fig. 5). It was shown that two sets of data were well correlated. The coefficient of determination was 0.9734, and the slope was 0.9761.

Despite this good correlation at least under non-stressed conditions, normalization via spiking controls was used in all subsequent analyses. The planned stress treatments with salt or the phytohormone ABA might cause a more substantial shift in the expression of all several genes, which might jeopardize the normalization.

1.3. Reproducibility of ZmMIP DNA array

To check the reproducibility of method, the same RNA sample from cortex of maize primary roots was analyzed twice by DNA array hybridization. The data for 31 MIP and 18 control genes were compared in a scatter plot (Fig. 6). A good correlation (R^2 = 0.9757) was found indicating that the DNA array hybridization resulted in reproducible data.

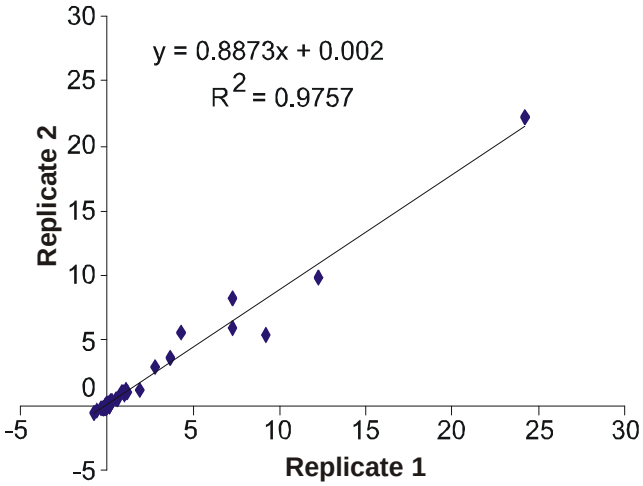

Fig. 6. Analysis on the reproducibility of DNA array hybridization. The cortex and stele were separated from the region 20-50mm of primary roots of 6-day-old seedling cultured on the wetted paper. Total RNA was prepared and two replicates of same RNA from cortex were assayed for gene activity using DNA array.

2. Expression of ZmMIPs transcripts in maize primary root.

To determine the expression of maize *MIP* members in unstressed roots RNA was isolated from 11-day-old roots from hydroponically cultivated plants. The abundance of MIP transcripts in roots was very different. *ZmPIP1-5* and *ZmTIP1-1* showed the by far highest expression. In addition, *ZmPIP1-1*, *ZmPIP2-1*, *ZmPIP2-4*, *ZmPIP2-5*, *ZmPIP2-6*, *ZmTIP2-1*, *ZmTIP2-2*, and *ZmTIP2-4* were highly transcribed in roots (Fig. 7). All other MIP members were expressed at low levels or not detected at all by the DNA array hybridizations (Fig. 7). Therefore, these genes are not transcribed in unstressed maize roots or limited to a specific, minor cell type obviating their detection.

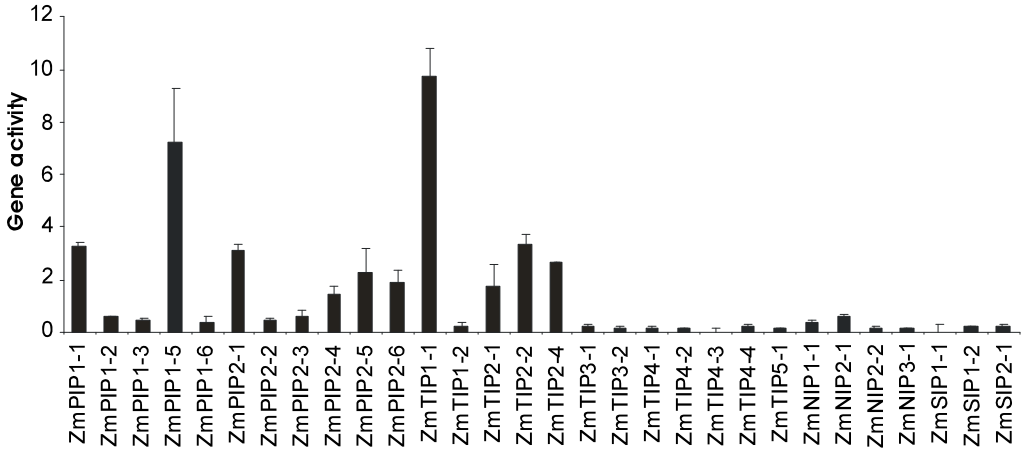

Fig. 7.. Abundance of ZmMIP transcripts in maize roots. Roots were harvested from 11-day old seedlings cultured in hydroponic solution. Total RNA (10 µg) extracted from roots was assayed by *ZmMIP* DNA array for gene activities. Relative gene activities above 0.20 were significantly detected above two fold background values. Signal values were normalized by internal standard (Methods).

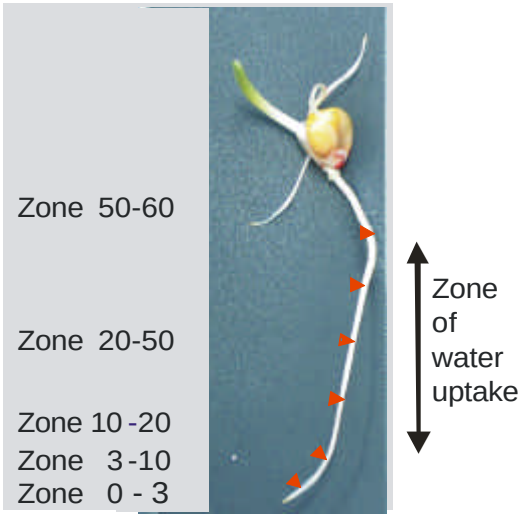

Fig. 8. Different zones of the primary maize root. The primary roots of 6-day-old-seedling were cut in different zones 0-3 mm, 3-10 mm, 10-20 mm, 20-50 mm and 50-60 mm.

2.1. Expression of ZmMIP transcripts in longitudinal zones

Root is important organ taking up water and nutrients. According to their morphology roots can be classified into various zones, such as root tips, elongation zone, root hair zone and lateral root zone, each region depicts different function in capacities of water uptake (Fig. 8).

Analysis on aquaporin expression in different zones of root was performed in order to investigate a relationship between their expression and water uptake.

Maize seeds were germinated on wetted paper for 6 days at 24°C in the dark, primary roots were harvested and cut into 0-3, 3-10, 10-20, 20-50 and 50-60 mm sections starting from the root tips (Fig. 8). Three independently grown materials were analyzed.

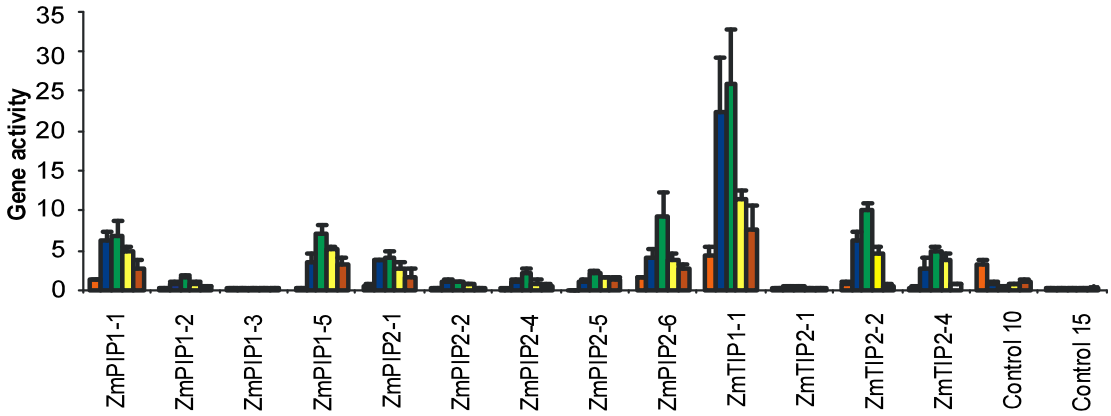

Fig. 9. Expression analysis of *ZmMIP*s in longitudinal zones of maize primary roots by DNA array. Total RNA were isolated from zone 0-3 mm (red), 3-10 mm (blue), 10-20 mm (green), 20-50 mm (yellow), 50-60 mm (magenta). The gene activity of *ZmMIP*s was assayed by DNA array. Three independent experiments were performed, and the bar represents the standard error of the mean. In addition, two control genes are shown; in particular, control 10 indicates higher expression in the root tip in comparison to other zones.

Fig. 9 shows the expression profile of some members of aquaporins *ZmPIP1-1*, *ZmPIP1-5*, *ZmPIP2-1*, *ZmPIP2-6*, *ZmTIP1-1*, *TmTIP2-2* and *ZmTIP2-4*.

The expression levels of all clearly detected *ZmMIP* members, in particular of *ZmPIP1-1*, *ZmPIP1-2*, *ZmPIP1-5*, *ZmPIP2-1*, *ZmPIP2-4*, *ZmPIP2-5*, *ZmPIP2-6* as well as of *ZmTIP1-1*, *ZmTIP2-2*, and *ZmTIP2-4* were high in the 3-50 mm zones, which expression peaked in the region of 10-20 mm (Fig. 9). *ZmPIP2-3* was detected only in zone 10-20 mm, but not in other zones. The transcripts of *ZmNIP3-1* were observed in all zones, the expression peaked in zone 10-20 mm. The transcripts of other members of aquaporin were not detected in all zones. The generally lower expression of *ZmMIP* genes in the root tip is not due to a technical problem, because one control gene showed the opposite behaviour (Fig. 9, control 10).

The expression profiles of highly expressed *ZmPIP* members *ZmPIP1-1*, *ZmPIP1-2*, *ZmPIP1-3*, *ZmPIP2-1*, *ZmPIP2-3*, *ZmPIP2-4*, *ZmPIP2-5*, and *ZmPIP2-6* were corroborated by semi-quantitative RT-PCR, although the decline towards the 50-60 mm zone was less pronounced (Fig. 10).

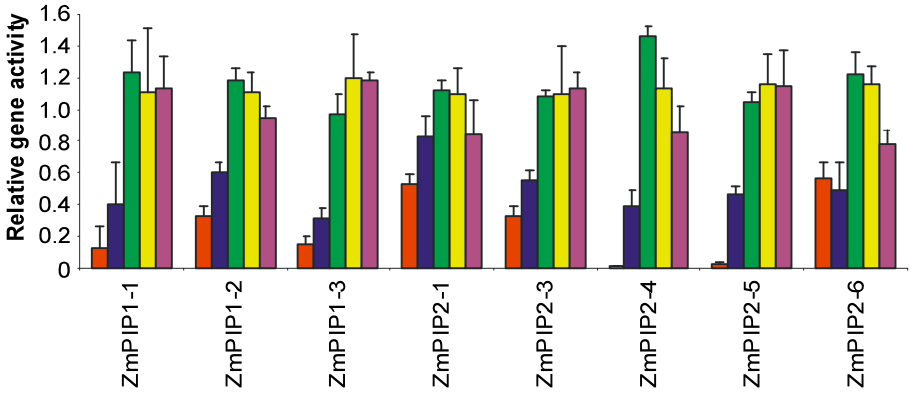

Fig. 10. Expression of ZmMIP in longitudinal zones of maize primary roots by semi-quantitative RT-PCR. Total RNA were isolated from zone 0-3 mm (red), 3-10 mm (blue), 10-20 mm (green), 20-50 mm (yellow), 50-60 mm (magenta). The gene activity of ZmMIPs was assayed by semi-quantitative RT-PCR. Three independent experiments were performed, and the bar represents the standard error of the mean.

Thus, the expression of the indicated *ZmPIP* and *ZmTIP* genes is correlated with and peaks in two regions that are thought to require an increased water supply. The 3-10 mm zone encompasses the differentiation and elongation region where cells need to take up water for their own expansion growth. The adjacent 10-50 mm zone defines the root hair zone where most of the root water uptake takes place.

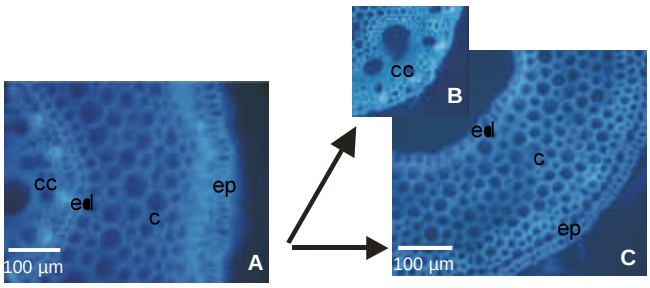

Fig. 11. Transverse sections of maize primary root before (A) and after (B and C) separation of cortex and stele. The root hair region (10-50mm) of 6-day–old primary roots grown in wetted paper or separated cortex and stele tissues were embedded in 4% low-melting agarose. Agarose blocks were cut into 50 µm thick sections using a vibratome. The section was visualized by fluorescence microscopy. (c) cortex; (cc) central cylinder; (ed) endodermis; (ep) epidermis.

2.2. Expression of ZmMIPs transcripts in cortex and stele

In addition to analysis of the expression of aquaporins in longitudinal regions the transcripts of *ZmMIPs* were determined in the transverse dimension by separations into

cortex and stele tissue (Fig. 11). The cortex and stele tissues from 10-50 mm zone of primary roots were separated with help of tweezers (Methods); transverse sections were cut and observed in the microscope before and after separation in order to visualize the separation.

Fig. 11 shows that endodermis hanged onto the cortex cells. The endodermis appear to be intact, however, its integrity was not independently analyzed. Thus, cellular content, in particular RNA might have been partially damaged or lost. The separated tissue were quickly rinsed twice in distilled water and frozen in liquid nitrogen.

Fig. 12 shows the expression of *ZmPIP* and *ZmTIP* genes in both tissues after DNA array hybridization. Interestingly, *ZmPIP1-1, ZmPIP1-5, ZmPIP2-3, ZmPIP2-4, ZmPIP2-5, ZmTIP1-1, ZmTIP2-2 and ZmTIP2-4* were expressed higher in cortex than in stele. In contrast, there was no significant difference in expression of *ZmPIP1-2, ZmPIP1-3 and ZmPIP2-6* between cortical cells and stele. Seven isoforms of *ZmNIPs* and *ZmSIPs* were analyzed; *ZmNIP1-1* and *ZmSIP1-1* were not detected. No difference between cortex and stele was observed; other isoforms *ZmNIP2-1, ZmNIP2-2, ZmNIP3-1* and *ZmSIP2-1* had higher abundance in cortex than in stele.

The same material was analyzed for expression of *ZmPIP1-1, ZmPIP1-2, ZmPIIP1-3, ZmPIP2-1, ZmPIP2-3, ZmPIP2-4, ZmPIP2-5* and *ZmPIP2-6* using semi-quantitative RT-PCR (Fig. 13). *ZmPIP1-1, ZmPIP2-1, ZmPIP2-3, ZmPIP2-4 and ZmPIP2-5* had higher abundance in cortex than in stele, the expression of *ZmPIP1-2,* and *ZmPIP2-6* were expressed almost same in both tissues. The higher abundance of *ZmPIP1-3* in stele than in cortex was observed.

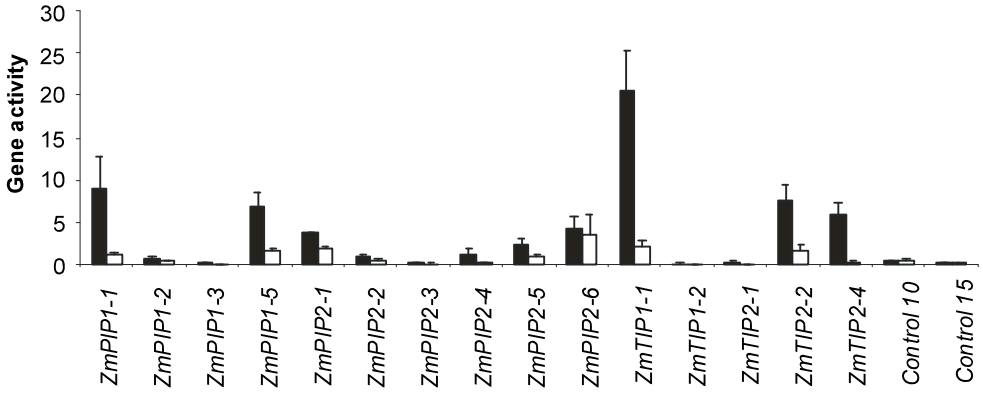

Fig. 12. Expression of ZmMIPs in cortex and stele of maize primary roots by DNA array. Total RNA were isolated from cortex (black) and stele (white). The gene activity of ZmMIPs was assayed by DNA array. Three independent experiments were performed, and the bar represents the standard error of the mean. Two control genes are displayed that were equally expressed in cortex and stele (compare Fig. 9).

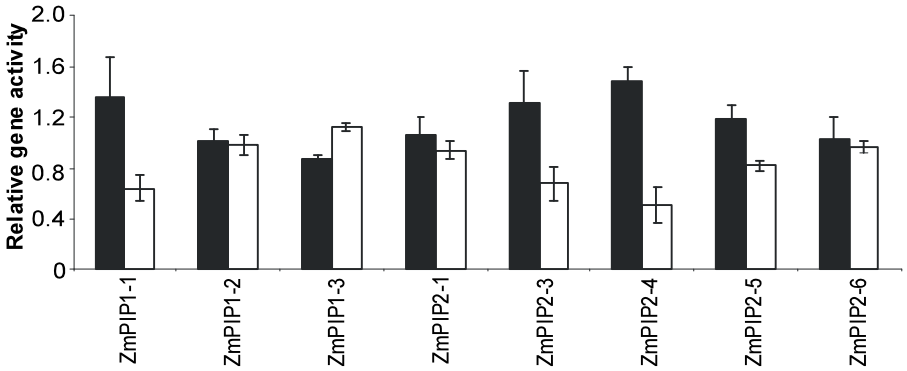

Fig. 13. Expression of ZmMIPs in cortex and stele of maize primary roots by semi-quantitative RT-PCR. Total RNA were isolated from cortex (black) and stele (white). The gene activity of ZmMIPs was assayed by semi-quantitative RT-PCR (Methods). Three independent experiments were performed, and the bar represents the standard error of the mean.

To verify the result of DNA array and semi-quantitative RT-PCR Northern analysis was performed for *ZmPIP1-1 and ZmPIP1-2* (Fig. 14), the result of Northern analysis was correlated well with that of two methods. Northern blot analysis (Fig. 14) showed that ZmPIP1-1 was expressed higher in cortex than in stele, in comparison with ZmPIP1-1 ZmPIP1-2 was expressed weak and had no significant difference in both tissues.

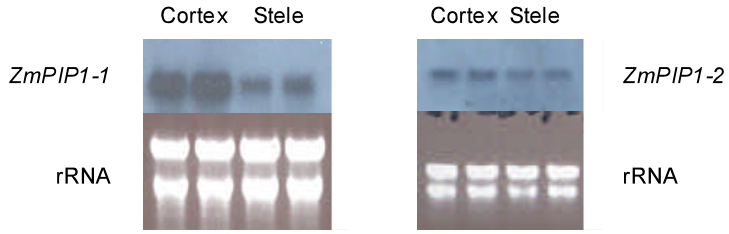

Fig. 14. Northern-blot analysis of *ZmPIP1-1* and *ZmPIP1-2* in the cortex and stele of primary roots. Total RNA (10µg) were isolated from cortex and stele from the region 20-50mm of primary roots of 6-day-old seedlings, and separated by gel electrophoresis. After transfer the blots were hybridized with the indicated probes. rRNA was used as loading control.

In the zones of elongation and root hair the cell wall of endodermis was lignified and suberized and could not permeate to water, apoplastic pathway was blocked in the layer of endodermis, therefore transcellular pathway played a important role in water transport through the layer of endodermis. Aquaporins were implicated in transcellular pathway; so far there were reports that aquaporins were expressed highly in endodermis cells. In our experiments of separation of cortex and stele endodermis cells might have been partially damaged, its RNA might have been lost. It was necessary to localize the aquaporins expression in intact section using in situ hybridization. *ZmPIP1-1* was highly expressed gene among the members of aquaporins was used to investigate the localization of expression at the cellular level by in situ hybridization. Samples were taken 10-20 mm from root tip of maize primary roots (Methods) (Fig. 15). In comparison with the section hybridized with no probe a weak, non-specific signal was detected in root sections hybridized with a sense control probe (Fig. 15 C-D). However, in the root sections hybridized with *ZmPIP1-1* anti-sense probe a stronger signal was present in cortical cells

than in stele (Fig.15. E-F), the same signal intensity was also observed in endodermis and epidermis. The result agreed with that of DNA array, RT-PCR and Northern analysis.

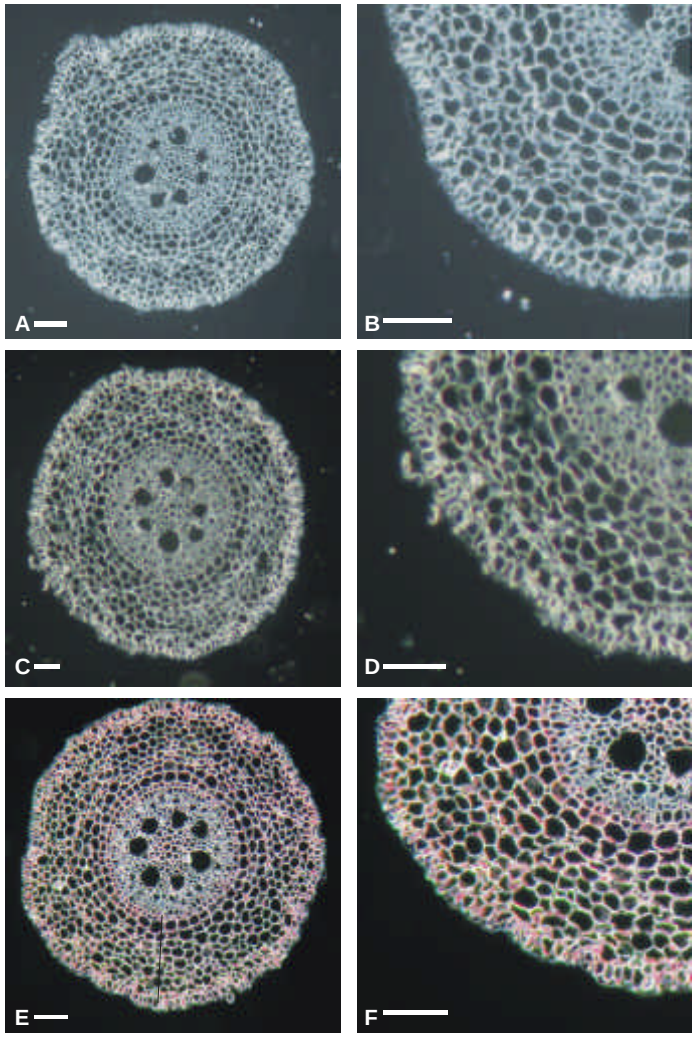

Fig. 15. In situ location of *ZmPIP1-1* mRNA in maize primary roots. Transverse sections of the primary root (10-20 mm from root tip) were hybridized without probes (a and b) and with sense (c and d) and anti-sense (e and f) digoxigenin-labeled *ZmPIP1-1* RNA probes. Bars = 100 µm

3. Effects of salt stress on physiological parameters and expression of aquaporin

3.1. Physiological responses of maize seedlings plants to NaCl stress

Application of NaCl to the root system of maize plants exerts a strong water stress onto the plants resulting in both osmotic stresses by lowering the water potential of the surrounding medium and in an ionic effect of the ions involved. Thus, both water relations are strongly affected by NaCl and toxicity of ions may harm the plants (Hasegawa *et al*., 2000; Zhu, 2001). Application of NaCl to the root system of maize plants affects plant growth and

development by exerting osmotic and toxic effect of ions on the plants, Both pathways could influence the expression of aquaporins.
To investigate the reaction of maize seedlings in response to exogenous NaCl two physiological parameters were recorded after the application of two different NaCl concentrations to 11-day-old, hydroponically grown maize seedlings in addition to the analyses of *ZmMIP* gene expression.

3.1.1. Effect of salt stress on water content of maize leaves

Application of NaCl to the root system of maize plants exerts a strong water stress onto the plants. The physiological reactions of 11-day-old, hydroponically grown maize seedlings to 100 mM and 200 mM NaCl were compared by determining the water content of their leaves.

After addition of NaCl to the hydroponic solution, leaves were harvested after 2, 9, 24, and 48 h. Plants started to wilt after 2 h treatment, however, after one day turgescent leaves indicated recovery in both cases. Application of 100 mM NaCl slightly, but not significantly decreased the water content of leaves in comparison to control plants (Fig. 16). Although not statistically significant, both experiments may reflect a diurnal variation of the water content showing lowest values at 19:00 o´clock 9 h after the addition of NaCl**.** In contrast, 200 mM NaCl rapidly and significantly reduced the water content of leaves in comparison with both control and 100 mM NaCl treatment ($p < 0.05$). A potential diurnal effect was overruled under these conditions (Fig. 16).

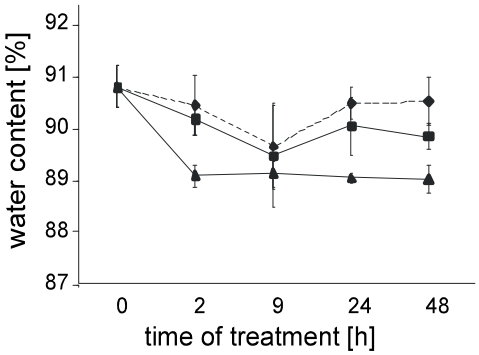

Fig. 16. **Water content of maize leaves after addition of NaCl to roots.** Water content was assayed after treatment of 11-day old seedlings by 0 mM (◆), 100 mM (■), and 200 mM (▲) NaCl for the times indicated. Data are means ± SD of three samples.

3.1.2. Effect of salt stress on ABA concentration

ABA is known to accumulate in response to drought and salt stress. Since differential reactions to two NaCl concentrations were observed for leaf water content in roots, ABA levels in roots were determined in parallel by an immunological assay by D. Schraut in the laboratory of W. Hartung, University of Würzburg (Methods). Indeed, salt stress

significantly induced the amount of ABA in maize roots (Fig. 17). After 2 h ABA accumulated to identical levels in both 100 mM and 200 mM NaCl experiments. However, at later time points there was a clear difference between both treatments. ABA levels were strongly reduced to values slightly above controls in roots treated with 100 mM NaCl, whereas they remained at very high levels throughout the whole period examined after application of 200 mM NaCl (Fig. 17).

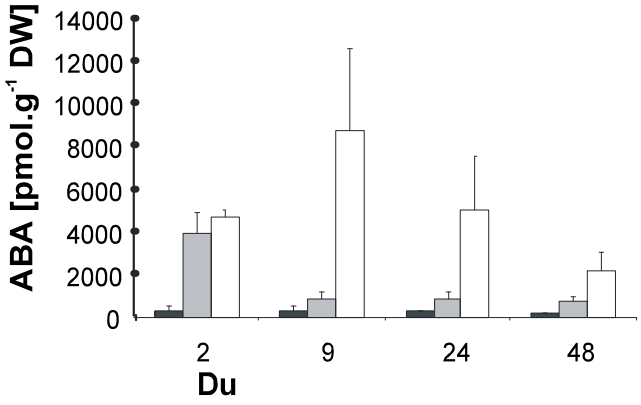

Fig. 17. ABA concentration in maize roots subjected to salt stress. ABA was extracted from roots of 11-day-old seedlings treated by 0 mM (black), 100 mM (white), 200 mM (grey) NaCl at indicated times, and determined by an immunoassay from lyophilized samples taken in parallel to expression analyses (Materials & methods). Data are means ± SD of three independent experiments.

3.2. Effect of NaCl on gene expression of maize MIP genes

Besides the toxic, ionic effect the major and immediate effect of NaCl addition to the root substrate is the lowering of the water potential that may strongly influence plant water relations. Therefore, the expression of maize *MIP* genes encoding known or putative aquaporins in roots of 11-day old seedlings was assayed using the maize MIP DNA array after administration of 100 mM and 200 mM NaCl to the hydroponic solution. In addition to the differential impact on leaf water content the stress- and ABA-responsive maize gene *Rab17* was at most weakly induced by 100 mM NaCl at 24 h, but significantly up-regulated by 200 mM NaCl at 9 h, 24 h and 48 h (Tab. 2). Interestingly, the transcriptional responses of *ZmPIP* and *ZmTIP* genes were also different for both NaCl concentrations. Two hours after addition of 100 mM, but not of 200 mM NaCl a transient and specific induction of the highly expressed *ZmPIP* members *ZmPIP1-1* and *ZmPIP2-4* was observed. In addition, an induction of *ZmPIP1-5* was indicated (Tab. 2). *ZmPIP1-5* showed a statistically significant weak induction (1.56-fold, p-value 0.004), which may be important because this gene was the highest expressed *ZmPIP* member in roots. Quantitative RT-PCR confirmed these results for *ZmPIP1-1*, *ZmPIP1-5*, and *ZmPIP2-4*, as well as the unaltered level of *ZmPIP1-2* transcripts (Fig. 18). Although these inductions are rather weak, it has to be stressed that these *ZmPIP* members were already expressed at higher levels in unstressed maize roots. None of the *ZmTIP* genes was significantly altered 2 h after application of NaCl. In contrast to the induction of the stress-control gene *Rab17* upon 200 mM NaCl, the expression of the *MIP* genes to both NaCl concentrations was not

Table 2. *ZmPIP* and *ZmTIP* transcripts in maize roots subjected to salt stress at different time points. Expression ratios of three independent replicates are given. Inductions are highlighted in red (ratio = 2.0, p = 0.05), orange (ratio = 2.0, 0.05 <p =0.1), light red (ratio = 1.67-2.0, p = 0.05), or yellow (see text). Reductions are indicated in aquamarine (ratio < 0.5, p = 0.05), green (ratio < 0.5, 0.05 < p= 0.10), light green (ratio = 0.50-0.60, p = 0.05) (Materials & methods). Gene activities in unstressed roots are shown for comparison; n.d., not detected. Genes that were not detected in any experiment are not listed (Supplemental Tab. 2). Gene activities in unstressed roots are indicated for comparison, higher expression levels (>1.0 arbitrary units) are printed in bold.

[a] Note that *ZmPIP2-3* was not induced although its target sequence was 96% homologous to *ZmPIP2-4* over a stretch of 29 nt (Suppl. Tab. 1). This underlines the specificity of the target sequences under the stringent hybridization conditions used.

Gene	Gene activity	2h 100mM			9h 100mM			24h 100mM			48h 100mM		
		mean	SD	p	mean	SD	p	mean	SD	p	mean	SD	p
ZmPIP1-1	**3.3**	**1.87**	0.32	0.01	**0.74**	0.15	0.06	**1.32**	0.48	0.18	**1.49**	0.69	0.16
ZmPIP1-2	0.57	**1.18**	0.50	0.35	**n.d.**	n.d	n.d	**1.04**	0.12	0.32	**1.38**	0.55	0.26
ZmPIP1-3	0.41	**1.51**	0.18	0.01	**n.d.**	n.d	n.d	**1.01**	0.52	0.40	**1.20**	0.45	0.34
ZmPIP1-5	**7.2**	**1.56**	0.10	0.004	**1.13**	0.27	0.25	**1.26**	0.37	0.19	**1.71**	0.95	0.14
ZmPIP1-6	0.37	**1.25**	0.10	0.02	**n.d.**	n.d	n.d	**0.97**	0.38	0.38	**1.07**	0.20	0.32
ZmPIP2-1	**3.1**	**1.40**	0.13	0.01	**0.95**	0.30	0.36	**1.20**	0.47	0.29	**1.14**	0.24	0.22
ZmPIP2-2	0.42	**0.84**	0.04	0.01	**n.d.**	n.d	n.d	**1.89**	0.86	0.10	**1.19**	0.66	0.41
ZmPIP2-3	0.58	**1.06**	0.15	0.33	**n.d.**	n.d	n.d	**1.02**	0.40	0.48	**1.32**	0.65	0.33
ZmPIP2-4	**1.4**	**1.97**	0.67	0.04	**1.17**	0.33	0.25	**1.03**	0.28	0.49	**0.95**	0.04	0.17
ZmPIP2-5	**2.3**	**1.10**	0.31	0.35	**1.04**	0.39	0.49	**0.94**	0.38	0.34	**1.10**	0.26	0.31
ZmPIP2-6	**1.9**	**1.92**	0.73	0.06	**0.73**	0.27	0.37	**0.81**	0.52	0.22	**0.83**	0.25	0.16
ZmTIP1-1	**9.7**	**1.29**	0.04	0.00	**0.68**	0.07	0.01	**0.81**	0.23	0.15	**1.02**	0.56	0.42
ZmTIP1-2	0.25	**1.52**	0.44	0.07	**n.d.**	n.d	n.d	**0.94**	0.30	0.39	**n.d.**	n.d.	n.d.
ZmTIP2-1	**1.7**	**1.10**	0.33	0.38	**0.88**	0.07	0.12	**1.00**	0.43	0.41	**0.93**	0.22	0.28
ZmTIP2-2	**3.4**	**0.91**	0.27	0.28	**0.85**	0.27	0.21	**1.62**	0.71	0.14	**1.07**	0.06	0.09
ZmTIP2-4	**2.6**	**1.36**	0.17	0.03	**1.01**	0.07	0.39	**1.81**	0.56	0.05	**1.69**	0.39	0.04
RAB17	0.09	**1.41**	0.29	0.06	**n.d.**	n.d	n.d	**2.50**	1.19	0.07	**n.d.**	n.d.	n.d.
Gene	**Gene activity**	**2h 200mM**			**9h 200mM**			**24h 200mM**			**48h 200mM**		
		mean	SD	p	mean	SD	p	mean	SD	p	mean	SD	p
ZmPIP1-1	**3.3**	**1.31**	0.54	0.27	**1.02**	0.16	0.48	**0.91**	0.36	0.29	**1.70**	0.05	0.001
ZmPIP1-2	0.57	**1.32**	0.36	0.13	**n.d.**	n.d.	n.d.	**0.58**	0.10	0.01	**1.47**	0.71	0.26
ZmPIP1-3	0.41	**1.10**	0.28	0.36	**n.d.**	n.d.	n.d.	**0.72**	0.29	0.12	**1.14**	0.01	0.02
ZmPIP1-5	**7.2**	**0.87**	0.22	0.20	**0.92**	0.38	0.33	**0.50**	0.18	0.03	**1.14**	0.36	0.34
ZmPIP1-6	0.37	**0.93**	0.10	0.18	**n.d.**	n.d.	n.d.	**0.31**	0.08	0.01	**0.83**	0.64	0.33
ZmPIP2-1	**3.1**	**0.96**	0.16	0.34	**0.74**	0.35	0.18	**1.01**	0.58	0.39	**0.99**	0.12	0.41
ZmPIP2-2	0.42	**0.86**	0.07	0.04	**n.d.**	n.d.	n.d.	**1.20**	0.88	0.45	**1.60**	1.10	0.24
ZmPIP2-3	0.58	**0.87**	0.05	0.09	**n.d.**	n.d.	n.d.	**n.d**	n.d	n.d	**1.45**	0.49	0.20
ZmPIP2-4	**1.4**	**1.08**	0.31	0.42	**1.00**	0.10	0.49	**0.32**	0.03	0.001	**1.00**	0.43	0.45
ZmPIP2-5	**2.3**	**0.92**	0.20	0.27	**0.64**	0.23	0.07	**0.31**	0.03	0.001	**0.68**	0.26	0.09
ZmPIP2-6	**1.9**	**1.08**	0.54	0.47	**1.10**	0.26	0.33	**0.53**	0.14	0.02	**0.71**	0.19	0.07
ZmTIP1-1	**9.7**	**0.76**	0.05	0.01	**0.92**	0.29	0.31	**0.55**	0.20	0.04	**0.77**	0.17	0.08
ZmTIP1-2	0.25	**1.11**	0.18	0.28	**n.d.**	n.d.	n.d.	**0.52**	0.06	0.04	**1.15**	0.55	0.43
ZmTIP2-1	**1.7**	**0.92**	0.13	0.21	**0.69**	0.27	0.19	**0.35**	0.11	0.02	**0.67**	0.42	0.13
ZmTIP2-2	**3.4**	**0.80**	0.16	0.09	**0.33**	0.16	0.02	**0.12**	0.03	0.03	**0.56**	0.33	0.11
ZmTIP2-4	**2.6**	**0.96**	0.27	0.36	**1.07**	0.60	0.43	**0.59**	0.28	0.10	**1.14**	0.63	0.48
RAB17	0.09	**1.37**	0.78	0.38	**26.15**	9.54	0.03	**39.41**	26.94	0.01	**42.07**	32.82	0.07

significantly altered after 9 h. However, the situation completely changed when assayed 24 h after NaCl addition. With 100 mM NaCl added no significant inductions or suppressions were detected. Instead, multiple *ZmPIP* and *ZmTIP* transcripts were reduced by 200 mM NaCl after 24 h (Tab. 2). Importantly, the repressed genes included highly transcribed members of both *PIP* subfamilies, *ZmPIP1-2*, *ZmPIP1-5*, *ZmPIP1-6* as well as *ZmPIP2-4*, *ZmPIP2-5*, and *ZmPIP2-6*, and most *ZmTIP* genes.

Interestingly, other highly expressed *ZmPIP* members, *ZmPIP1-1* and *ZmPIP2-1*, were not affected. After 48 h, transcriptional deregulation of all *ZmPIP* and *ZmTIP* genes was basically abolished for both NaCl concentrations indicating the recovery of homeostasis in both cases. Nevertheless, the ABA-responsive marker *Rab17* stayed induced in the 200 mM NaCl treatment until 48 h. The differential responses of *ZmPIP1-1*, *ZmPIP1-2*, *ZmPIP1-5* and *ZmPIP2-4* to 200 mM NaCl after 24 h were confirmed by qRT-PCR (Fig. 18A-D).

Data for *ZmSIP* and *ZmNIP* were collected as well (Supplement), but will not be discussed here because of their low expression, which renders expression ratios less certain and because of their unknown role in water relations.

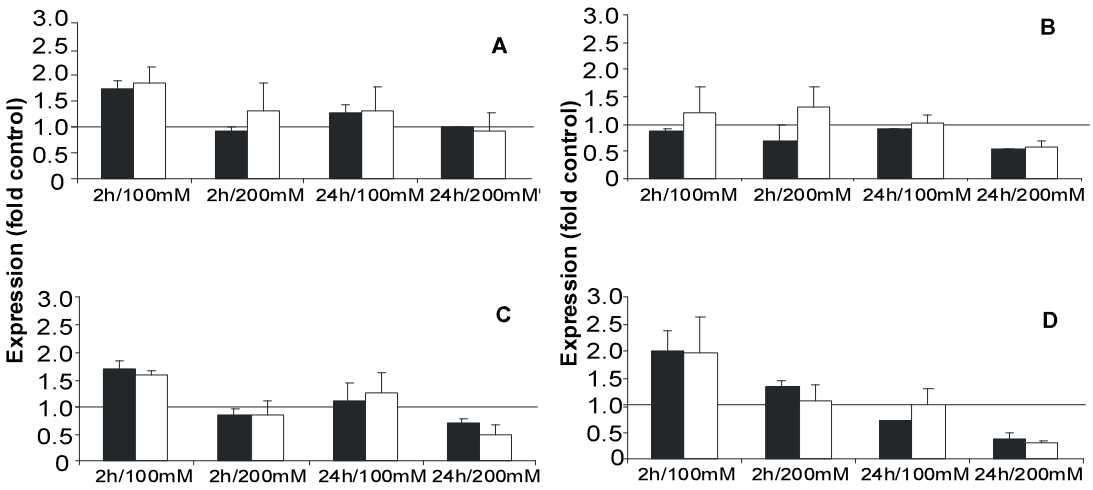

Fig. 18. Comparison of real-time quantitative RT-PCR and DNA array. Total RNA were isolated from roots of 11-day-old seedlings subjected to treatment with 100 mM, 200 mM NaCl and 0 mM (control) at indicated times, and assayed for relative expression ratio of *ZmPIP1-1* (A), *ZmPIP1-2*(B), *ZmPIP1-5*(C) and *ZmPIP2-4*(D) using real-time quantitative RT-PCR (black) and DNA array (white). The transcripts level of each *ZmMIPs* in the roots was plotted as the relative expression (fold) of the non-stressed control plants.

4. Effect of ABA on the expression of ZmMIP genes

Since NaCl increased the ABA concentration in roots we were interested whether the transcriptional reaction of *ZmMIP* genes to NaCl was mediated by ABA. Therefore, 11-day-old, hydroponically grown maize seedlings were subjected to 1 µM and 100 µM ABA for 1 h, 6 h and 24 h. These two concentrations were chosen because 1 µM ABA roughly

reflects the physiological level and up to 100 µM ABA is frequently used in the study of ABA-dependent expression, although such a high, concentration may exert a non-physiological, toxic effect.

Furthermore, considering a possible delay of ABA biosynthesis after NaCl application in comparison with the direct effect of exogenously added ABA, the first two time points in the ABA experiments were chosen earlier than in the NaCl experiments.

The analysis of transcripts was performed using the *ZmMIP* DNA array. The ABA-responsive genes *Rab17* and *Dbf1* served as controls (Kizis *et al*., 2002). *Rab17* was weakly induced by 1 µM ABA after 24 h and significantly up-regulated by 100 µM ABA in accordance with published data (Tab. 3). This enhancement measured by DNA array analyses was also confirmed by semi-quantitative RT-PCR (Fig.19). Since *Rab17* was induced later and mostly by the higher ABA concentrations, the early induction of *Dbf1* by both concentrations of ABA confirmed the responsiveness of the plants used in this study (Fig. 19).

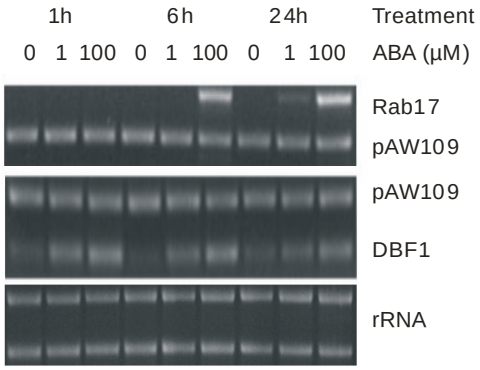

Fig. 19. Independent analyses of ABA responses of *Rab17* and *DBF1* control genes. Semi-quantitative RT-PCR analyses of *Rab17* and *DBF1* transcription in response to ABA (Methods). Staining of rRNA by ethidium bromide was used as a control for the amount of RNA used in the analyses.

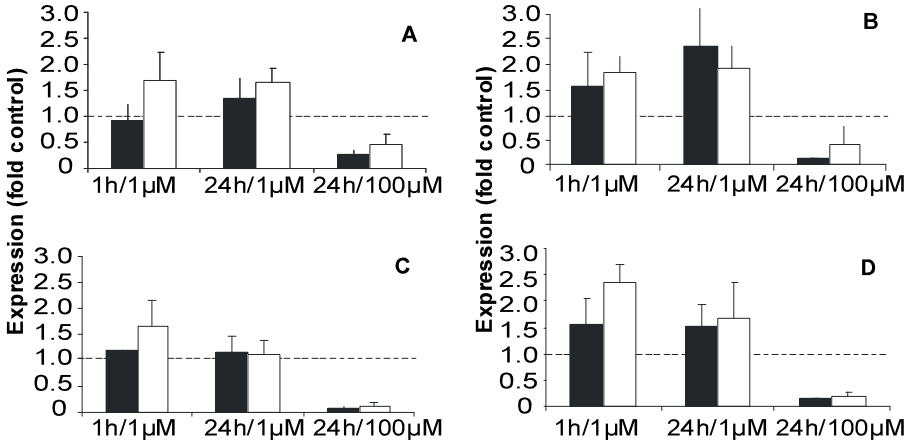

Fig. 20. Comparison of real-time quantitative RT-PCR and DNA array. Total RNA were isolated from roots of 11-day-old seedlings subjected to 0 µM (control), 1 µM, 100 µM ABA at the indicated times, and assayed for relative expression ratio of *ZmPIP1-1* (A*), ZmPIP1-2*(B*), ZmPIP1-5* (C*)* and *ZmPIP2-4* (D) using real-time quantitative RT-PCR (black) and DNA array (white) analyses. The transcripts level of each *ZmMIP* in the roots was plotted as the expression value relative to the signals obtained for the non-stressed control plants. For qRT-PCR, two independent biological replicate (same material as used for array expression analyses) were assayed in duplicate.

One µM ABA induced *ZmPIP1-2* and *ZmPIP2-4* after 1 h treatment (Tab. 3). This specific reaction of a few *ZmPIP* genes was reminiscent of the early response to NaCl (Tab. 2). After 6 h and 24 h treatment by 1 µM ABA only the induction of the weakly expressed *ZmPIP1-2* was persistent. The highly expressed *ZmPIP2-4* showed a reduction after 1 h treatment with 1 µM ABA.

Real-time quantitative RT-PCR was performed to independently verify the DNA array expression patterns of *ZmPIP1-1*, *ZmPIP1-2*, *ZmPIP1-5* and *ZmPIP2-4*. *ZmPIP1-2* and *ZmPIP2-4* were induced by 1 µM ABA after 1 h and 24 h, whereas there was no effect on the expression of *ZmPIP1-1* and *ZmPIP1-5* (Fig. 20). Thus, the combination of both approaches pinpoints the specific induction of two *PIP* members by 1 µM external ABA, the higher expressed *ZmPIP2-4* as well as *ZmPIP1-2*.

Table 3. *ZmPIP* and *ZmTIP* genes expressed in maize roots in response to ABA. Expression ratios of three independent replicates are given. Inductions are highlighted in red (ratio = 2.0, p = 0.05), orange (ratio = 2.0, 0.05 <p =0.1), or light red (ratio = 1.67-2.0, p = 0.05). Reductions are indicated in aquamarine (ratio < 0.5, p = 0.05), green (ratio < 0.5, 0.05 < p= 0.10), or light green (ratio = 0.50-0.60, p = 0.05) (Materials & methods). Gene activities in unstressed roots are shown for comparison; n.d., not detected. Genes that were not detected in any experiment are not listed (Supplemental Tab. 2). Gene activities in unstressed roots are indicated for comparison, higher expression levels (>1.0 arbitrary units) are printed in bold.

Gene	Gene activity	1h 1µM			6h 1µM			24h 1µM			24h 100µM		
		mean	SD	p	mean	SD	p	mean	SD	p	mean	SD	p
ZmPIP1-1	**3.3**	**1.68**	0.53	0.05	**1.59**	0.09	0.00	**1.63**	0.31	0.02	**0.45**	0.22	0.05
ZmPIP1-2	0.57	**1.87**	0.30	0.01	**1.99**	0.95	0.07	**1.90**	0.42	0.02	**0.20**	0.07	0.03
ZmPIP1-3	0.41	**1.41**	0.67	0.22	**1.44**	0.63	0.19	**1.63**	0.31	0.09	**0.23**	0.09	0.06
ZmPIP1-5	**7.2**	**1.62**	0.51	0.07	**1.35**	0.56	0.20	**1.10**	0.27	0.32	**0.12**	0.05	0.01
ZmPIP1-6	0.37	**1.59**	0.03	0.01	**n.d**	n.d	n.d	**1.05**	0.32	0.47	**0.16**	0.14	0.11
ZmPIP2-1	**3.1**	**1.46**	0.24	0.03	**1.55**	0.36	0.05	**1.43**	0.34	0.07	**0.31**	0.14	0.03
ZmPIP2-2	0.42	**1.42**	0.08	0.004	**0.95**	0.15	0.36	**0.90**	0.22	0.24	**0.14**	0.10	0.08
ZmPIP2-3	0.58	**1.21**	0.16	0.14	**n.d**	n.d	n.d	**1.42**	0.16	0.07	**n.d**	n.d	n.d
ZmPIP2-4	**1.4**	**2.35**	0.34	0.005	**1.31**	0.56	0.23	**1.65**	0.72	0.16	**0.19**	0.07	0.01
ZmPIP2-5	**2.3**	**1.48**	0.43	0.10	**1.52**	0.94	0.24	**1.32**	0.50	0.21	**0.11**	0.04	0.004
ZmPIP2-6	**1.9**	**1.45**	0.45	0.09	**1.31**	0.58	0.31	**1.55**	0.43	0.06	**0.11**	0.08	0.03
ZmTIP1-1	**9.7**	**1.43**	0.21	0.02	**1.48**	0.39	0.06	**1.34**	0.22	0.04	**0.39**	0.18	0.03
ZmTIP1-2	0.25	**n.d**	n.d	n.d	**n.d**	n.d	n.d	**1.29**	0.08	0.05	**0.20**	0.11	0.07
ZmTIP2-1	**1.7**	**1.59**	0.76	0.19	**1.02**	0.17	0.47	**1.04**	0.34	0.48	**0.21**	0.16	0.05
ZmTIP2-2	**3.4**	**1.24**	0.12	0.03	**0.81**	0.23	0.16	**0.76**	0.22	0.12	**0.06**	0.05	0.02
ZmTIP2-4	**2.6**	**1.19**	0.10	0.04	**1.07**	0.46	0.49	**0.90**	0.39	0.30	**0.15**	0.06	0.01
rab17	0.09	**n.d**	n.d	n.d	**2.28**	1.69	0.14	**2.86**	1.74	0.05	**50.51**	27.18	0.003

The artificially high concentration of 100 µM ABA resulted in a similar induction of a few *ZmPIP* members when assayed by the *ZmMIP* DNA array. However, this induction of *ZmPIP1-1* and *ZmPIP2-4* could not be verified by several independent approaches analyses including Northern analyses, semi-quantitative as well as quantitative RT-PCR (data not shown). Interestingly, 100 µM ABA significantly repressed all detected *ZmMIP* members after 24 h (Tab. 3). The strong repression after 24 h was confirmed by

quantitative RT-PCR (Fig. 20). This general reduction resembles the response to 200 mM NaCl (Tab. 2), although it is extended to members such as *ZmPIP1-1*, which are not repressed by NaCl. Thus, both hormonal and unspecific, pharmacological effects of 100 µM ABA could be overlaid.

5. Response to the deficiency of K^+ and NO^-_3

Deficiencies of K^+ or NO^-_3 in nutrient solutions may influence the water flux of maize roots in young seedlings. In comparison with plants grown in complete medium, water flux in roots depleted by K^+ was increased threefold, but that of roots grown in medium without NO^-_3 was reduced by half (Schraut *et al*., 2005).

To examine whether the alteration in radial water flux was associated with variation of aquaporins at the transcriptional level, maize seedlings were cultivated hydroponically in complete nutrient medium and media without K^+ or NO^-_3 for 9 days. At 08:00 on 10th day K^+ and NO^-_3 were resupplied to the media without K^+ or NO^-_3 to study a potential recovery. Roots were sampled at 14:00 on the 8th, 9th, 10th and 11th day from control plants, from K^+- or NO^-_3 –depleted plants, or from K^+- and NO^-_3-resupplied seedlings.

Fig. 21. Growth of 9-day-old seedlings in complete nutrient medium, and K^+- or NO^-_3-deficient hydroponic solutions. Representative plants are shown. Bar indicates 5 cm.

5.1. Growth of plants affected by K^+- and NO^-_3-deficiency

The effects of K^+- and NO^-_3-deficiency on the growth of seedlings were observed in comparison with control seedlings. Control seedlings grew faster and had 4 leaves at the end of the experiment, whereas K^+- and NO^-_3-deficient seedlings had only 3 leaves (Fig. 21). Shoots of seedlings depleted by K^+ and NO^-_3 were shorter than those of control seedlings ($p < 0.05$). Resupply of K^+ seemed to accelerate the growth of shoots on day 11, but exhibited a similar pattern to control shoots. In contrast, the addition of NO^-_3 had no immediate effect on the growth of shoots (Fig. 22 A, B).

Roots of NO^-_3-deficient seedling grew faster in length. In contrast, roots of K^+-deficient seedlings were shorter (Fig. 21). After addition of K^+ at day 10 the growth of roots was accelerated and root length reached wild type levels (Fig. 22 C, D). Instead, the resupply of NO^-_3 was coincident with a deceleration of the previously enhanced root growth (Fig. 22 C, D).

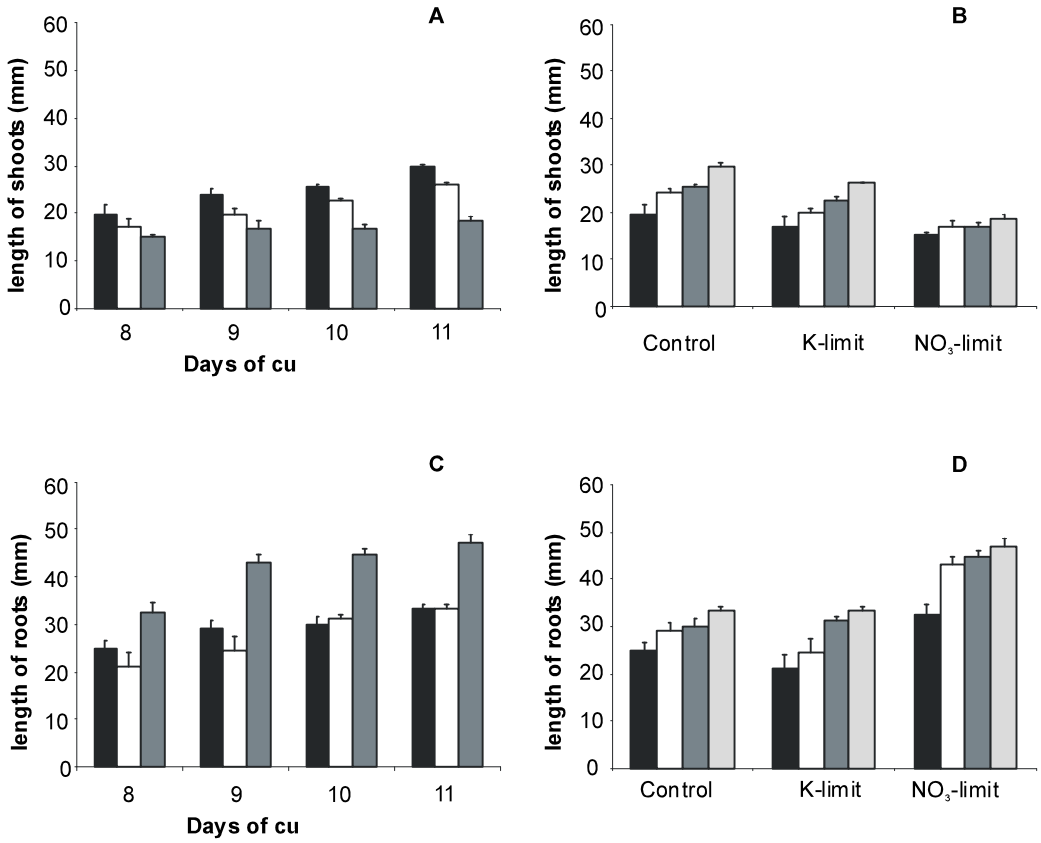

Fig. 22. Growth of seedlings cultured in the normal and K^+- and NO^-_3-deficient hydroponic solution. Length of shoots (A) and roots (C) were measured in the complete (black), K^+ (white)- and NO^-_3 (grey) - deficient hydroponic solution at indicated times. The length of shoots (B) and roots (D) were presented in control, K^+- and NO^-_3-deficient solution at day 8 (black), day 9 (white), day 10 (dark grey) and day 11 (light grey). K^+- and NO^-_3 were resupplied at day 10 and day 11. Each bar is the mean of three plants, the standard deviations are indicated.

5.2. Effects of nutrient limitation on the transcripts of ZmMIPs

A pilot study was performed to examine the alteration at transcriptional level under K^+- and NO^-_3-deficiency and after subsequent resupply of K^+- and NO^-_3 *ZmMIP*s transcripts were assayed using the *ZmMIP* DNA array. Only two separately cultivated materials were analyzed. Therefore, the results have to be regarded as preliminary. Nevertheless, interesting hints regarding ZmMIP regulation can be deduced.

After 8 days of K^+-deprivation the transcription of most highly expressed members of *ZmMIP*, such as *ZmPIP1-1*, *ZmPIP1-5*, *ZmPIP2-1*, *ZmPIP2-5*, *ZmTIP1-1*, *ZmTIP2-2* and *ZmTIP2-4* were suppressed. Surprisingly, on day 9 the repression was at least partially

released, which has to be confirmed independently (Tab. 4). However, it is clear from these preliminary data that there is no induction of either PIP or TIP genes in contrast to the observed increase in water flux upon K^+-starvation.

On the 10th day, 6 hr after resupply of K^+, all gene activities recovered to or even slightly above control levels. On the 11th day the relative gene activities remained high (Tab. 4).

Tab. 4. Effect of deficiency of and resupply of K^+- and NO^-_3 on expression of *ZmMIPs*. Maize seedlings were cultured in complete and K^+- or NO^-_3-deficient hydroponic solutions for 8 and 9 days. The deficient media were resupplied with the missing ions on day 10 six hours before sampling. The expression of *ZmMIPs* was analyzed by DNA array using *ZmMIP* array. There are no significant induction either at a higher or at a lower stringency (ratio = 2.0, $p < 0.05$ or $1.67 <$ ratio < 2.0, $p < 0.05$; compare Tab. 3). Reductions are indicated in green (ratio = 0.50, $p < 0.05$) and light green ($0.5 <$ ratio$=0.60$, $p < 0.05$ or ratio < 0.5, $p < 0.10$).
[1] Although there were only two replicates, a p-value was estimated using t-test; **: $p < 0.05$, *: $p < 0.1$, no star: $p > 0.10$.

K^+-deficiency	day 8		day 9		day 10		day 11	
gene name	mean	sd[1]	mean	sd[1]	mean	sd[1]	mean	sd[1]
ZmPIP1-1	**0.60**	0.07	**1.26**	0.38	**1.57**	0.48	**1.98**	0.36
ZmPIP1-5	**0.42**	0.03**	**0.66**	0.11	**1.43**	0.10	**1.07**	0.37
ZmPIP2-1	**0.46**	0.05**	**0.70**	0.20	**1.72**	0.35	**1.48**	0.41
ZmPIP2-4	**0.45**	0.16	**0.87**	0.02	**1.89**	0.18	**1.49**	0.14
ZmPIP2-5	**0.47**	0.03**	**0.98**	0.10	**1.55**	0.09	**1.14**	0.38
ZmPIP2-6	**0.54**	0.37	**1.13**	0.52	**2.18**	0.14	**0.91**	0.08
ZmTIP1-1	**0.44**	0.00**	**0.64**	0.06	**1.29**	0.11	**1.32**	0.72
ZmTIP2-2	**0.53**	0.03**	**0.63**	0.09	**1.29**	0.23	**1.70**	0.99
ZmTIP2-4	**0.39**	0.05**	**0.33**	0.12*	**1.33**	0.24	**1.16**	0.10
NO^-_3-deficiency	day 8		day 9		day 10		day 11	
gene name	mean	sd[1]	mean	sd[1]	mean	sd[1]	mean	sd[1]
ZmPIP1-1	**1.15**	0.13	**1.47**	0.83	**1.15**	0.12	**1.52**	0.45
ZmPIP1-5	**0.41**	0.03**	**0.44**	0.01**	**0.63**	0.21	**0.98**	0.61
ZmPIP2-1	**1.33**	0.58	**0.99**	0.39	**1.31**	0.03	**1.33**	0.30
ZmPIP2-4	**0.89**	0.11	**0.86**	0.29	**1.30**	0.31	**1.17**	0.51
ZmPIP2-5	**0.74**	0.14	**0.87**	0.22	**0.66**	0.13	**0.93**	0.53
ZmPIP2-6	**0.82**	0.22	**0.62**	0.28	**1.17**	0.23	**1.08**	0.57
ZmTIP1-1	**0.61**	0.05	**0.46**	0.11*	**1.27**	0.16	**1.43**	0.44
ZmTIP2-1	**0.76**	0.07	**0.86**	0.23	**0.99**	0.11	**1.40**	0.01
ZmTIP2-2	**1.06**	0.04	**1.04**	0.22	**1.61**	0.32	**2.36**	0.96
ZmTIP2-4	**0.60**	0.09	**0.52**	0.24	**0.81**	0.32	**1.30**	0.22

In the case of NO^-_3-deficiency, the transcripts of a single, major PIP isoform, *ZmPIP1-5*, and another TIP isoform *ZmTIP1-1*, were specifically repressed until day 9. Beginning at 6 hr after addition of NO^-_3 (day 10), all repressed gene activities resumed to control level until day 11 (Tab. 4). This repression was correlated with the reduced osmotic water flow, yet at the same time growth was enhanced. Therefore, the repressed isoforms could be associated specifically with transcellular permeability.

6. Antisera against ZmPIP1 and ZmPIP2

6.1. Selection of the epitopes with potential antigenicity

Because the level of mRNA may not always reflect the level of the corresponding protein, immunoblotting analyses were to be performed to investigate the abundance of aquaporins under treatment with salt and ABA and to estimate the relation of mRNA and protein. The study was focused onto ZmPIP that appear to play important roles in transporting water across the plasma membrane. In addition, some members of ZmPIPs are highly expressed in the maize roots at the transcriptional level and specifically responded to salt stress and ABA treatment. Due to the high homology of ZmPIP members, only subfamily-specific antigens representing ZmPIP1 and ZmPIP2 members were considered. An antiserum against ZmPIP1 was raised against an N-terminal ZmPIP1-1 peptide that is present in several ZmPIP1 members but absent from ZmPIP2 (Tab. 5).

Tab. 5. Selected sequences with antigenicity specific to ZmPIP1 and ZmPIP2. (a) Epitope are derived from ZmPIP1-1 (1N; H. Sieber and A. Schäffner, unpublished) or ZmPIP2-4 (E1, E2, E3). (b) According to the presence of homologous sequences, these members may be recognized by the various antisera.

Epitope[a]	Sequence	Location	Homologous sequences present in ZmPIPs[b]
1N	MEGKEEDVRLGANKFSERQPIGTAAQ GTDDKDYKEPPPAPLFEP	N-terminal	ZmPIP1-1, ZmPIP1-2, ZmPIP1-3,ZmPIP1-4, ZmpIP1-5
E1	MAKDIEASGPEAGEFSA	N-terminal	ZmPIP2-3, ZmPIP2-4
E2	KHQTDASASGPDAAQC	Extracellular loop A	ZmPIP2-1,ZmPIP2-2, ZmPIP2-3, ZmPIP2-4, ZmPIP2-5, ZmPIP2-6
E3	LRASATKLGSYRSNA	C-terminal	ZmPIP2-1, ZmPIP2-2, ZmPIP2-3, ZmPIP2-4, ZmPIP2-5, ZmPIP2-6, ZmPIP2-7

To raise antibodies against ZmPIP2 proteins, the amino acid sequence of ZmPIP2-4 was chosen because the corresponding gene is highly expressed in roots and it was shown to be responsive to NaCl and ABA (Result 3 and 4). In collaboration with the company Pineda (http://www.pineda-abservice.com) three peptide sequences from ZmPIP2-4 were chosen taking their antigenicity and their relative location within the predicted protein structure at the cytoplasmic N- and C-termini as well as within the extracellular loop A (Tab. 5).

6.2. Immunization of rabbits and chicken with GST-fusion proteins

A PCR fragment encoding the first 44 amino acids of ZmPIP1-1 was cloned in the GST fusion vector pGEX-2T (Pharmacia) using flanking BamHI and EcoRI restriction sites. The coding regions corresponding to ZmPIP2 peptides E1, E2 and E3 were amplified from cDNA with the addition of sequences amenable for GATEWAY cloning (Methods 2.1.8.2). The fragments were finally recombined into pDEST15 (Invitrogen). The fusion

proteins were expressed in *E. coli* BL-21 (DE3) upon induction with IPTG (Methods 2.7.1.2).

The proteins were affinity-purified using GST-Sepharose columns. Fractions showing GST activity were pooled (Methods 2.7.3) and analyzed by SDS-PAGE. All recombinant proteins migrated somewhat slower than a reference GST+23 protein carrying an extension of 23 amino acids due to flanking vector sequences (Fig. 23). However, it was not clear whether the weaker shift of GST-E3 was due to an abnormal electrophoretic behaviour or due to a degradation of the fusion protein.

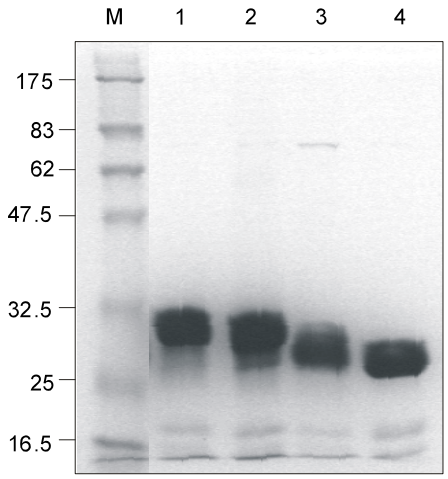

Fig. 23. Identification of GST fusion proteins. 5µg of fusion protein GST-E1 (lane 1, MW 29.53 kDa), GST-E2 (lane 2, MW 29.43 kDa), GST-E3 (lane 3, MW 29.55 kDa) and GST+23 (lane 4, MW 27.91 kDa) were loaded on the SDS-PAGE gel and visualized after staining with Coomassie brilliant blue. M, protein marker (kDa).

6.3. Antisera against ZmPIP epitopes

Fusion proteins E1 and E2 were used to immunize rabbits and chicken, respectively in collaboration with the company Pineda (Berlin). Pre-immune sera and antisera after 61 days were tested. Competition experiments with GST and with the respective GST-fusion proteins were performed to test the specificity of antibodies.

The rabbit anti-ZmPIP1 (1N) antiserum strongly and specifically reacted with 28 kDa and 53 kDa of ZmPIP1 proteins (Fig. 24). The band could be competed by pre-incubation of antiserum with fusion protein GST-ZmPIP1 but not with GST carrier protein alone. The chicken anti-ZmPIP2 (E1) antiserum specifically recognized a band with about 28 kDa and 53 kDa at the known electrophoretic mobility of ZmPIPs. The band could be competed by pre-incubation of the antiserum with the fusion protein GST-E1, but not with GST alone (Fig. 24). The reaction against a dimeric form is consistent with previous reports on PIP proteins (Kammerloher *et al*., 1994; Schäffner, 1998). No specific antibodies against GST-E1 and GST-E2 from rabbit were obtained (data not shown).

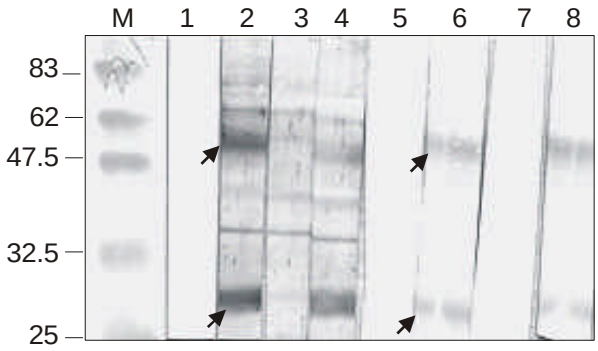

Fig. 24. Test of specificity of antisera. Microsomal fractions from maize roots were isolated and separated on the 12% SDS-PAGE, and blotted on nitrocellulose membrane. The membrane was probed with chicken anti-ZmPIP1 antiserum (1N, 1:1000) and rabbit anti-ZmPIP2 antiserum (E1, 1:500). For the competition experiment to test the specificity, the antisera were pre-incubated with 10 µg in a volume of 1 ml for 15 min. Bound antibodies were detected with alkaline-phosphortase-coupled anti-chicken or anti-rabbit secondary antibodies and BCIP/ NBT staining (Methods). M: protein marker (kDa); lane 1 and lane 5: negative controls for lane 2-4 and 6-8 (without primary antibody); lane 2: chicken antiserum against GST-E1; lane 3: antiserum against GST-E1 with 10µg fusion protein GST-E1; lane 4: antiserum GST-E1 with 10µg protein GST; lane 6: rabbit antiserum against GST-ZmPIP1; lane 7: rabbit antiserum against GST-PIP1 with 10 µg fusion protein GST-ZmPIP1; lane 8; rabbit antiserum against GST-PIP1 with 10µg protein GST. Arrow indicates the specific reaction against ZmPIP2 or ZmPIP1.

7. Effect of NaCl and ABA on ZmPIP1 and ZmPIP2 at the protein level

7.1. Amount of ZmPIP1 and ZmPIP2 proteins

As shown above (Chapter 3 and 4), *ZmPIP* transcripts responded to treatment with NaCl and ABA. Therefore, immunoblotting analyses were performed using antibodies raised against ZmPIP1 and ZmPIP2 to examine whether this was accompanied by changes in the amount of ZmPIP proteins. The antisera specifically reacted with isoforms of the ZmPIP1 and ZmPIP2 subfamily in maize. Anti-ZmPIP1 antibodies most probably cross-reacted with the homologous N-termini of ZmPIP1-1, ZmPIP1-2, ZmPIP1-3, ZmPIP1-4, and ZmPIP1-5. The anti-ZmPIP2 antiserum was more specific and should detect the homologous N-termini of ZmPIP2-3 and ZmPIP2-4, thus including ZmPIP2-4, whose transcript had been induced under several circumstances (Result 3 and 4). A cross-reaction with other PIP2 members of maize is less likely at least based on the primary structure of the amino acid sequence.

For parallel quantification of ZmPIP1 and ZmPIP2 two-color infrared fluorescent Western blots were used. The linear range of fluorescence detection had been confirmed for 2.5 - 10 µg microsomal proteins for both ZmPIP1 and ZmPIP2 antigens (Methods 2.7.7.2).

To analyze ZmPIP antigens after treatment with ABA microsomal fractions were isolated from roots of 11-day-old seedlings that were harvested 1 h and 24 h after addition of 1 or

100 µM ABA. The amount of ZmPIP1 and ZmPIP2 was assayed by two color infrared fluorescent immunoblots (Fig. 25). No detectable change of ZmPIP1 and ZmPIP2 proteins after application of ABA was found. Statistical testing was performed using ANOVA (Fig. 26).

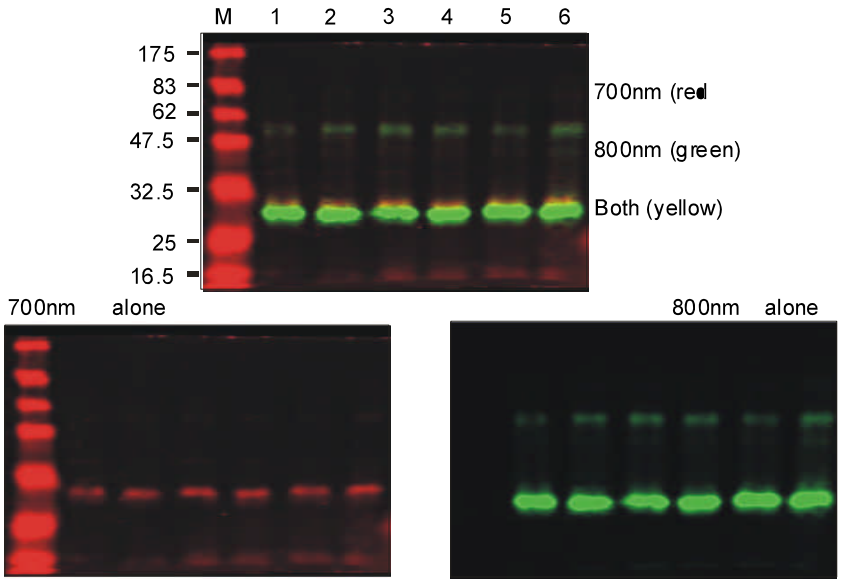

Fig. 25. Effect of ABA on the amount of ZmPIP1 and ZmPIP2. Microsomal fractions were isolated from roots treated with ABA. The fractions were separated on the 12% SDS-PAGE and blotted onto nitrocellulose. The membrane was probed with rabbit anti-ZmPIP1 (visible in green) and chicken anti-ZmPIP2 (visible in red). Antibodies bound on the membrane were detected with secondary IRDye800 goat anti-rabbit and Alexa647 goat anti-chicken (Methods). M: protein marker; lane 1: control at 1 h; lane 2: 1 µM ABA at 1 h; lane 3: 100 µM ABA at 1 h; lane 4: control at 24 h; lane 5: 1 µM ABA at 24 h; lane 6: 100 µM ABA at 24 h.

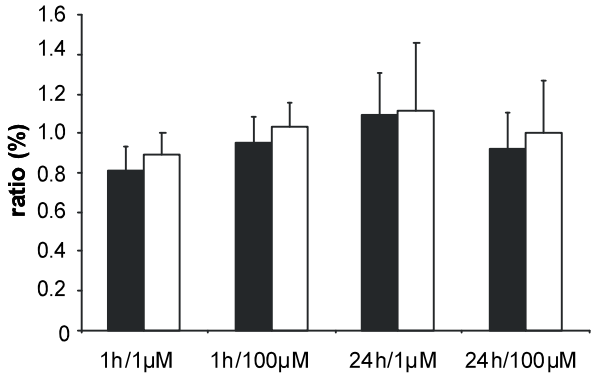

Fig. 26. Effect of ABA on the ZmPIP1 and ZmPIP2 proteins of maize roots. The amount of ZmPIP1 (black bar) and ZmPIP2 (white bar) were determined using two-color infrared fluorescent western blots. Means and standard deviations are shown for two independent experiments that were analyzed twice.

Similarly, microsomal fractions were analyzed to investigate whether the amount of ZmPIP aquaporins was affected by NaCl. 11-day-old seedlings were subjected to treatment with 100 and 200 mM NaCl. Microsomal fractions were isolated from roots collected after 2 h and 24 h.

Fig. 27 shows that the treatment with 100 and 200 mM NaCl scarcely changed the amounts of ZmPIP1 and ZmPIP2. The differences were not significant according to ANOVA tests.

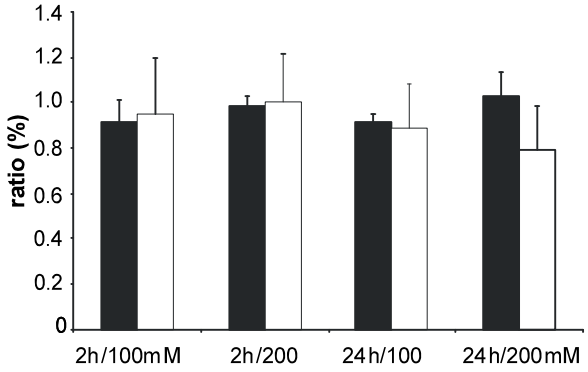

Fig. 27. Effect of NaCl on the ZmPIP1 and ZmPIP2 proteins of maize roots. The amount of ZmPIP1(black bar) and ZmPIP2 (white bar) were determined using two-color infrared fluorescent western blots. Means and standard deviations were shown for two independent experiments that were analyzed twice.

7.2. Phosphorylation of ZmPIP proteins

Water permeability of membranes mediated by aquaporin does not only depend on the amount but also on activity of the proteins. Phosphorylation is one important regulatory mechanism in many cellular processes (Kerk *et al*., 2002). Phosphorylation of aquaporin was reported as one possible mode to regulate their activity (Karlsson *et al*., 2003). Phosphorylation of the soybean PIP2 member PM28 at the conserved Ser 274 is reduced in response to lowered water potential in the apoplast (Johansson *et al.,* 1996).

Therefore, it was interesting to investigate whether maize aquaporins are phosphorylated and whether there was a change in their phosphorylation in response of salt stress and ABA. To detect phosphorylated proteins a direct in-gel stain of phosphate groups attached to tyrosine, serine or threonine residues after SDS-PAGE was applied (Pro-Q Diamond Phosphoprotein Stain, Molecular Probes, Eugene, USA).

Interestingly, two dominant Pro-Q-phospho-stained bands from microsomal fractions were observed among a background of phosphoproteins that migrated at about 28 kDa (lower band) and 53 kDa (upper band) (Fig. 28). This was reminiscent of the electrophoretic behaviour of aquaporins corresponding to dimeric and monomeric forms (Fig. 28). Thus, it was inferred that the bands could indicate or contain phosphorylated aquaporins. To confirm this assumption, microsomal fractions were treated with different concentrations of DTT, which results in a characteristic, progressive shift of PIP dimers into monomers during SDS PAGE (Fig. 29). Therefore, these samples were analyzed in parallel by quantitative immunoblotting for ZmPIP1 and ZmPIP2 antigens and by Pro-Q stain for phosphoproteins. A correlated, parallel shift from the upper/ dimeric into the lower/ monomeric forms for phospho-stained bands and antigens would indicate that phosphorylation was associated with the aquaporin antigen(s).

With increasing concentration of DTT, the intensity of the lower phospho-stained band became stronger at the expense of the upper band (Fig. 29). Both bands were quantified using a phosphoimager and MultiAnalyst. The signals were normalized by total protein content that was determined by subsequent Sypro-Ruby protein stain of the same gel (Methods).

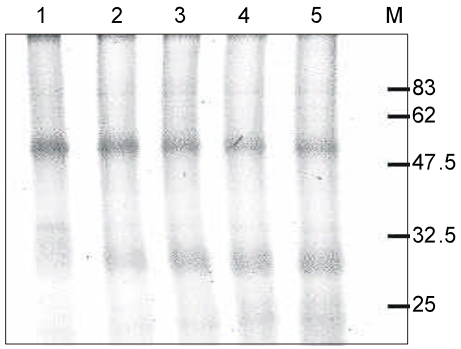

Fig. 28. **Effect of DTT on the phosphorylation state of microsomal fraction protein.** Microsomal fractions were extracted from roots and treated by 0 mM (lane 1), 10 mM (lane 2), 50 mM(lane 3), 100 mM (lane 4), 200 mM (lane 5) of DTT, and resolved on 12% SDS-PAGE, the gel was stained by Pro-Q Diamond. M: protein marker (kDa). Two bands at 28 and 53 kDa are distinguishable from the background at higher DTT concentrations.

In parallel, the shift from dimeric into monomeric forms for both ZmPIP1 and ZmPIP2 was recorded by quantitative two-channel infrared immunoblotting (Fig. 29). For ZmPIP2 the shift was more pronounced, mainly based on the observation that without DTT almost no monomeric form of ZmPIP2 was detected.

Phosphorylation signals for the upper and lower bands were separately plotted against the dimer signals of ZmPIP1 and ZmPIP2 (Fig. 30). The western signals showed a strong linear correlation with upper phospho-stained bands. The coefficient of determination of the linear correlation was 0.9352 and 0.9573 for ZmPIP1 and ZmPIP2, respectively (Fig. 30). According to Pearson this indicated a high significance of the correlation (ZmPIP1: $\alpha<0.01$, ZmPIP2: $\alpha<0.01$). The coefficient of determination of lower phosho-stained band with monomers of ZmPIP1 or ZmPIP2 were also high, yet somewhat worse at 0.8530 ($\alpha<0.05$ if considered according to Pearson correlation) and 0.8737 ($\alpha<0.01$) (data not shown). Thus, at least for the upper phosphorylated band quantitative co-segregation of ZmPIP2-3/ ZmPIP2-4 or ZmPIP1 antigens has been demonstrated exploiting the DTT-sensitive behaviour. This allowed studying changes of phosphorylation for these aquaporins. However, since it is presumed that other ZmPIP2 members, which are not detected by this antiserum, would show a similar DTT-sensitive shift, it cannot be excluded that the phosphorylation of those members is recorded as well. On the other hand, it is very unlikely that any other abundant protein of the microsomal fraction would show the identical dissociation from a 53 kDa form into the 28 kDa form upon treatment with increasing concentrations of DTT.

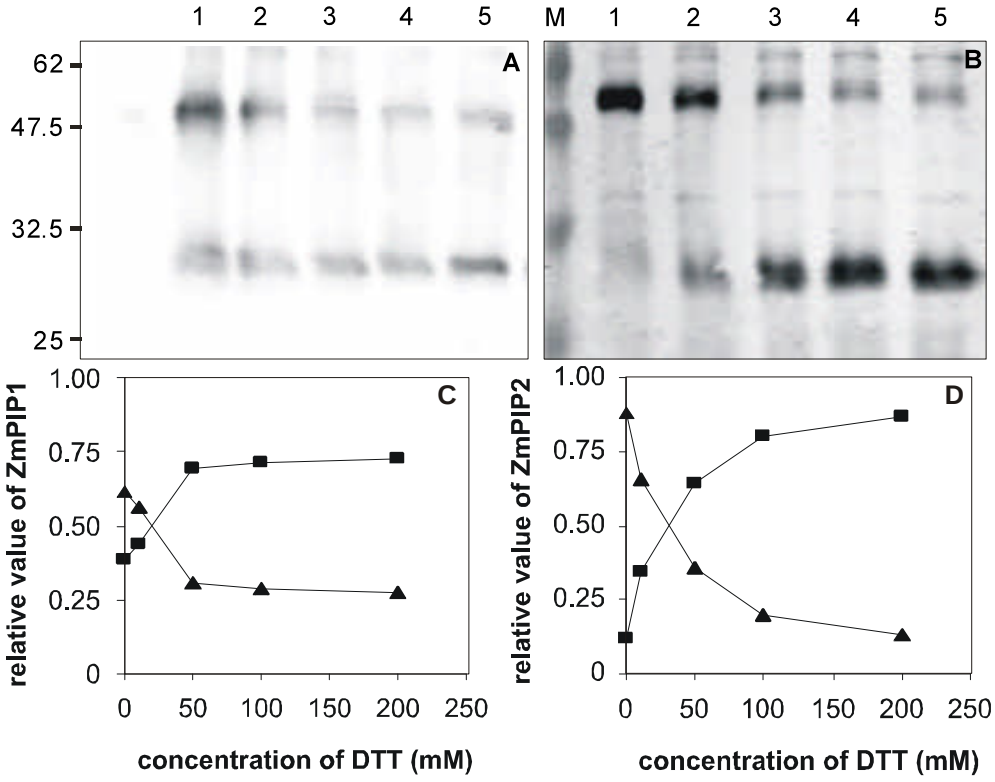

Fig. 29. Effect of DTT on the oligomeration of ZmPIP1 and ZmPIP2. Microsomal fractions were isolated from roots and assayed using two-color infrared fluorescent western blots. A. ZmPIP1. B. ZmPIP2. M: protein marker; lane 1: without DTT; lane 2: 10 µM DTT; lane 3: 50 µM; lane 4: 100 µM; lane 5: 200 µM. C and D show the plots of ZmPIP1 and ZmPIP2 dimers and monomers (▲) and (¦) after quantification from a representative experiment.

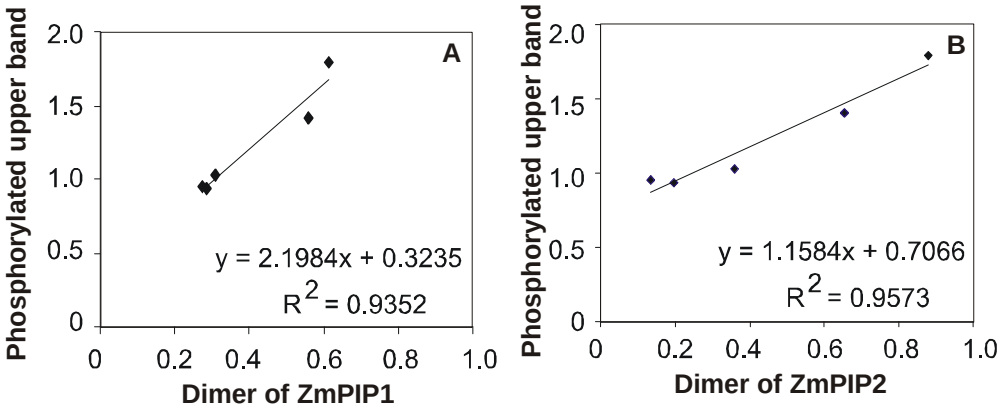

Fig. 30. Analysis on correlation between aquaporin and phosphorylation state. Microsomal fractions from maize roots were treated by different concentration of DTT, and fractioned on SDS-PAGE. The phosphorylation state and ZmPIP1 (A) and ZmPIP2 (B) were assayed by Pro-Q phosphor stain and quantitative two channel infrared immunoblotting.

According to these considerations the phosphorylation state in response to treatments with NaCl and ABA was studied. 11-day-old maize seedlings were treated with 0 mM, 100 mM, 200 mM NaCl for 2 h and 24 h or by 1 µM, 100 µM ABA for 1 h or 24 h; microsomal fractions were isolated from roots in the presence of kinase and phosphatase inhibitors (Methods), denatured in the presence of 100 mM DTT, and resolved on SDS-PAGE. Parallel gels were stained by Pro-Q for phosphorylation, by Sypro-ruby or Coomassie brilliant blue for total protein, or they were processed through immunological

detection of ZmPIP1 and ZmPIP2 antigens. Total protein was used for normalization. Two parallel samples from two independent treatments each were analyzed.

There were no detectable changes in phosphorylation state of aquaporins after treatment with both NaCl and ABA (Figs. 31, 32). This indicated that NaCl and ABA did not affect the phosphorylation state of ZmPIP1 and ZmPIP2-3/ 2-4 aquaporins and most probably, other ZmPIP2 members as well. Alternatively, an increased phosphorylation of only certain members could be paralleled by a dephosphorylation of others, thereby obviating the detection of changes.

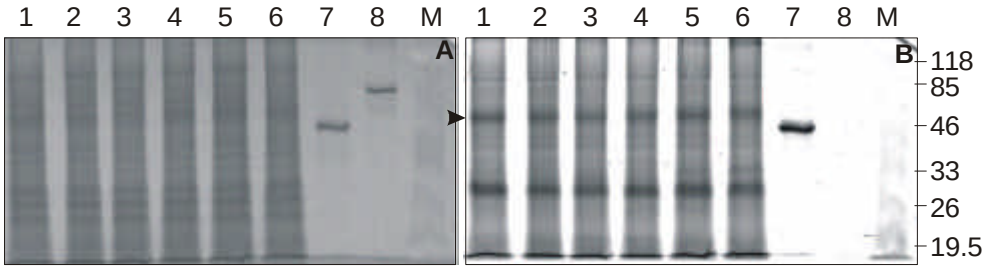

Fig. 31. Effect of NaCl on putative phosphorylated aquaporin using Pro-Q Diamond stain. Microsomal fractions were isolated from roots treated with NaCl. The fractions were separated on the 12% SDS-PAGE, the gel was stained by Sypro-ruby (A) and Pro-Q Diamond (B). M: protein marker; lane 1: control at 1 h; lane 2: 100 mM NaCl at 2 h; lane 3: 200 mM NaCl at 2 h; lane 4: control at 24 h; lane 5: 100 mM NaCl at 24 h; lane 6: 200 mM NaCl at 24 h. lane7: albumin; lane 8: BSA.

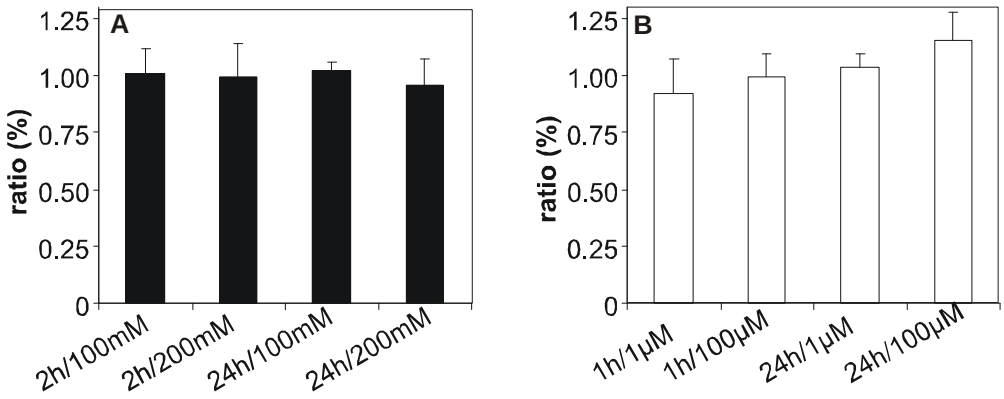

Fig. 32. Effect of NaCl and ABA on phosphorylation state of aquaporin. Microsomal fraction from roots of 11-day-old maize seedling treated by NaCl (A) and ABA (B) at indicated time were separated by SDS-PAGE and stained with Pro-Q Diamond for phosphorylation. The upper band was quantified and normalized by total protein amount. The ratio of treatment vs. controls is shown. Each bar is the mean of four experiments based on two replica each of two independent treatments. The standard deviations are indicated.

D. Discussion

1. Diversity and abundance of aquaporins in maize roots

Since the first aquaporin was characterized as water channel 11 homologues of the major intrinsic protein family have been found in mammals. In comparison, more members were identified in plants. *Arabidopsis* and maize possess more than 30 members of aquaporins (Chaumont *et al.*, 2001; Quigley *et al.*, 2001).

Mature root systems and primary roots of etiolated seedlings were analyzed for expression of aquaporins using the maize *MIP* array constructed in this study. Ten highly and six weakly expressed members were detected in mature root systems, the expression of other members of aquaporins were too low to be detected, whereas there were 15 aquaporin members detected in the primary roots of maize. Chaumont *et al.* (2001) identified total 31 aquaporin EST and 16 aquaporins EST in roots cDNA library. In comparison, this result of DNA array was basically in agreement with that of the previous analysis of maize EST sequences.

The difference lies in the weakly expressed members of aquaporins between two different methods. Two other weakly expressed members (*ZmTIP4-1* and *ZmNIP3-1*) were not detected by the array but identified in the cDNA library of maize roots. Whereas *ZmPIP1-6* and *ZmTIP1-2* were detected by the DNA array, but not present in the root cDNA sequences. In addition to difference of methods there might be difference of materials in different developmental stages of roots.

Both methods showed that 15-16 aquaporin homologues among 31 aquaporins were present in the maize roots, indicating the high diversity of aquaporins in roots, on the other hand, these results imply that the root is an important organ for uptake and transport of water if aquaporins involve the water transport across the membranes.

The highest intensities were observed for *ZmPIP1-1, ZmPIP1-5, ZmPIP2-1, ZmTIP1-1, ZmTIP2-1* and *ZmTIP2-2*. *ZmPIP2-4*, *ZmPIP2-5* and *ZmPIP2-6* were highly expressed at somewhat lower intensities. Other members including all *SIP*s and *NIP*s as well as *ZmPIP1-2, ZmPIP2-2, ZmPIP2-3* and *ZmTIP1-2* had low intensity in DNA array analysis. Chaumont *et al.* (2001) found that EST numbers *of ZmPIP1-1, ZmPIP1-5, ZmPIP2-1* and *ZmPIP2-4* were much more in *ZmPIP1* and *ZmPIP2* subfamily in maize roots. This indicates that DNA array could detect the relative abundance of aquaporin genes. The consistency in high diversity and high abundance of some members demonstrate validity of DNA array using newly constructed maize MIP array.

The presence of so many aquaporin members in roots raises the question, why do so many aquaporin members exist in the roots?

Plant cells differ from animal cells in their big central vacuole. Plant aquaporins are classified into PIPs, TIPs, NIPs and SIPs. The classification depended on the similarity of sequences. PIPs and TIPs reside in the plasma membrane and tonoplast, respectively, but the location of other two families NIPs and SIPs are unknown. The plasma membrane localization of PIP members has been confirmed for individual members in many species by biochemical and cytochemical approaches (Kammerloher *et al.,* 1994; Cutler *et al.,* 2000). In maize, the localization of ZmPIP1-2 has been confirmed by its enrichment in the plasma membrane fraction and by translational GFP fusion in transgenic maize root tips (Chaumont *et al.*, 2000).

Interestingly, Kirch *et al.* (2000) could also detect PIP antigens in membrane vesicles from the salt-tolerant *Mesembryanthemum crystallinum* that were distinct from plasma membrane and tonoplast, whereas detected TIP antigens were exclusively located to the tonoplast. There may be circumstances when these integral membrane proteins are shuttled into other membrane compartments such as internalized PM vesicles (Robinson *et al.*, 1996; Barkla *et al.*, 1999; Vera-Estrella, *et al.*, 2004).

In addition to the difference in subcellular localization, evidences are accumulating that individual aquaporin are differentially expressed in certain cell types, or tissues or organs (Daniels *et al.,* 1994, 1996; O'Brien *et al.,* 2002; Frangne *et al.,* 2001). The abundance or activities of aquaporins modulate the water flow across the membranes, which is important in many processes such as stomatal opening, phloem loading, pulvinar movement etc.

Heterologous expression in frog oocytes was most frequently used to characterize functions of MIPs. A few members from maize have been investigated. ZmPIP2-1, ZmPIP2-3, ZmPIP2-4, ZmPIP2-5, and ZmTIP1-1 displayed high water permeability, whereas these experiments failed to demonstrate a considerable aquaporin activity of ZmPIP1-1 and ZmPIP1-2 (Chaumont *et al.,* 2000, 1998; Fetter *et al.,* 2004). The issue has not yet been fully clarified, because PIP1 members from other species increased water permeability of oocytes (Li *et al.,* 2000). Thus, it may be a problem related to the heterologous expression system as long as homologous systems have not been applied to study this question. Interestingly, recent experiments indicated a synergistic effect of ZmPIP1 and ZmPIP2 proteins in enhancing water permeability (Fetter *et al.,* 2004). As forming heterologous tetramer with other member of ZmPIP2, ZmPIP1 members are also detected as water permeating, true aquaporins. On the other hand, it has to be considered that at least some aquaporins members were shown to be also permeable to other small and uncharged solutes such as glycerol, urea, NH_3, formamide, or CO_2 (Weig *et al.,* 2000; Gaspar *et al.,* 2003; Whittembury *et al.,* 1997; Uehlein *et al.,* 2003).

Thus, these diverse subcellular locations and functions of aquaporins may account for the diversity of aquaporins in plants.

2. Location of aquaporin members in primary roots

According to above result and Chaumont's EST numbers of aquaporin, 16 members of aquaporin are expressed in roots. The expression of aquaporin at tissue and cell level in the roots remains elusive.

Meristematic cells were congregated in root tip (0-3 mm), whereas zone 3-10 mm belongs to elongation zone. In the zone (10-50 mm) epidermis cells differentiated to root hair functioning as water uptake. In the zone (30 mm) from root tip Casparian bands developed in radial wall of endodermis and contained hydrophobic wax, they blocked radial apoplastic water flow.

Above mentioned various zones of primary roots were analysed for the expression of ZmMIPs using DNA array. 15 aquaporin members were detected in all zones of roots. Interestingly, *ZmNIP3-1* was found in all regions, which was not detected in mature root systems; *ZmPIP2-3* appeared in definite regions, in contrast to the aquaporin expression of mature root systems *ZmPIP1-6* and *ZmTIP1-2* in etiolated primary roots were expressed too weakly to be detected. This expression profile was also consistent with EST data (Chaumont *et al.*, 2001).

All detected aquaporin had a similar expression pattern. In zone 3-50 mm from root tip all detected members of aquaporin were expressed highly, the expression peaked in zone 10-20 mm. Some members of aquaporins were verified to have ability of water transport such as ZmPIP2-1, ZmPIP2-2, ZmPIP2-3, ZmPIP2-4, ZmPIP2-5, ZmTIP1-1 and ZmPIP2-3 in heterologous expression system (Chaumont *et al.*, 2001; Fetter *et al.*, 2004).

The similar expression pattern of aquaporin genes in primary roots let one to conceive whether there was an error in data normalization. The parallel analysed control gene KG10 (acyl-[acyl-carrier protein] desaturase) was expressed highly in root tips (0-3 mm), another control gene KG15 (putative ubiquitin-conjugating enzyme) was expressed in 10-50 mm; in other zone transcripts could not be detected. The results of control genes excluded artificial error. This indicated that high expression of aquaporin was associated with cellular growth and water uptake in the regions. In addition, semi quantitative RT-PCR showed the similar results to that of DNA array.

Hukin *et al.* (2002) analysed the expression pattern of three members of aquaporin in root tip and elongation zone. RT-PCR analysis showed a high transcripts level of *ZmPIP1-2* and *ZmPIP2-4* in the old region of root growth zone (5-6 mm) compared to the young region (1.5-2.5 mm), which was consistent with my results. But the expression pattern of *ZmTIP1-1* in roots in Hukin's experiment was different from my experiment. The discrepancy might result from sampling material for analysis. In my experiment zone 0-3 mm and zone 3-10mm were analysed for expression of *ZmTIP1-1* transcript, whereas zone 1.5-2.5 mm and zone 5-6 mm were analysed in Hukin's experiment. Other report

demonstrated that aquaporins were preferentially expressed in the region undergoing rapid elongation (Ludevid *et al.,* 1992; Javot *et al.,* 2002; Kirch *et al.,* 2000; Kaldenhoff *et al.,* 1995).

The cell growth involves enlargement and elongation of cells; the features of cell wall and cellular permeability affect the growth of cells. Hukin *et al.* (2002) investigated the inhibition of mercury on maize root growth and water permeability. 20 nM $HgCl_2$ inhibited the root growth on 4-11 mm from root apex but not on 0-3 mm zone and the inhibition could be reversed by 5 mM ß-ME, indicating root cell growth occurred on 4-11 mm from root apex. Addition of mercury inhibited water permeability of cells on zone 5-20 mm but not on root tips. This indicates correlation between water conductivity and growth of cells. The hydraulic conductivity depended on the expression of aquaporins. Therefore, high expression of aquaporin on the plasma membrane enhances permeability of cells and facilitates the growth of cells. Our result supports the inference.

The result in the study shows that not only *ZmPIP1-1* and *ZmPIP2-4* detected by Hukin *et al.* (2002), but also other members of *ZmPIPs* were required for cell expansion in the zone of root elongation. The high expression of aquaporin genes in the zone of root hair implied that aquaporin might mediate the transmembrane water transport to facilitate water uptake via cell-to-cell pathway. In the meristematic zone of root the transcripts of aquaporin genes were very low, indicating the less role of aquaporin in the water transport in the zone. Hukin *et al.* (2002) found that the plasmadesmata were connected and water transport occurred via symplast pathway in the meristematic zone, whereas in other zones of root was symplastic isolation via plasmadesmata closure, cell-to-cell pathway dominated, which ascribed to the high expression of aquaporin.

Interestingly not only *ZmPIPs* but also *ZmTIPs* have high transcripts in zone of elongation zone and root hair. *ZmTIPs* had higher water permeability than *ZmPIPs* in heterogous *xenopus oocytes* (Chaumont *et al.,* 1998; 2000). The plasmalemma but not tonoplast is greater barrier to transcellular water movement (Maurel, 1997). In fact cell expansion needs the vacuole expansion. The evidence demonstrated that the cells having defect in vacuole expansion did not expand (Schiefelbein & Somerville, 1990). High expression of *ZmTIPs* in the zone of elongation argued for entry of water into vacuoles and facilitated vacuole expansion and in turn the cell expansion.

On the other hand, cells differentiate in zone of elongation zone and root hair, small vesicles fused into central vacuole in cytosol. High expression of *ZmTIPs* favours the vacuolation of cells. TIP isoforms can be used as markers for different types of vacuoles (Neuhaus *et al.,* 1998; Maurel *et al.,* 1997, Jaun *et al.,* 1999).

In the case of root hair zone, high uptake of solutes and water led to transient water imbalance in the cells, high expression of aquaporins was necessary for rapid water transport and facilitated osmotic adjustment during radial transport of solutes and water.

The cells in the zones are differentiated to various functional cells such as epidermis, cortex, endodermis, pericycle and vascular parenchyma cells. To investigate the expression of aquaporin genes at cell level the cortex and stele were separated and analyzed.

The zone 10-50 mm from root tip was separated into stele and cortex that contained epidermis, cortex and endodermis. Stele and cortex were analysed for aquaporin expression. Analysis shows that some highly expressed members of aquaporin have higher abundance in cortex than in the stele; there are no difference of *ZmPIP1-2, ZmPIP1-3* and *ZmPIP2*-6 between cortex and stele. The result was verified by semi-quantitative RT-PCR and Northern analysis.

Baiges *et al.* (2001) has found similar distribution in cortex and stele of *Vitis-PIP1-1, Vitis-PIP2-1* and *Vitis-TIP1* in analysis of *Vitis* 3-5 cm from root tip for expression of aquaporins, no significant difference of *Vitis-PIP1-2* and *Vitis-TIP3* was observed between cortex and stele, but *VitisTIP3* and *Vitis-PIP1-3* has higher abundance in stele than in cortex.

There are reports suggesting that aquaporins were expressed highly in the endodermis (Barrieu *et al.,* 1998; Yamada *et al.,* 1995; Javot *et al.,* 2003). Expression data in cortex might not reflect that of aquaporin in endodermis. As endodermis cling to the pericycle of stele, we could not exclude the disruption of endodermis cells and leakage of RNA from endodermis cells during separation. In situ hybridization could show the expression of genes at cell level and confirm the expression of genes in endodermis. The expression of *ZmPIP1-1* was localized by the method. High signal was detected in cortex, which was consistent with the result of DNA array. No higher expression of *ZmPIP1-1* was found in endodermal cells than in other cortical cells.

As maize seedlings were grown in dark and covered with wetted tissue papers, there was no transpiration; the main driving force for water uptake was osmotic potential gradient, water was taken up via cell-to-cell pathway which contains symplastic pathway and transmembrane pathway. Symplastic connection occurs in root tips but not in zone of root growth (Hukin *et al.,* 2002). Therefore, aquaporins could be implicated in transmembrane water transport and high expression of aquaporins in the region of root growth accounted for their role in cell-to-cell pathway of water.

Lopez *et al.* (2003) measured the xylem water flux of detopped maize seedling during 48 h period and found that there were two peaks of xylem water flux in 16 h/8 h period, one was high maximal flow during the light period, at night the flux reached a less important peak, they concluded that in addition to transpiration, root pressure contributed to root water transport, and cell-to-cell and apoplastic pathway could occur simultaneously. The experiments using $HgCl_2$ revealed that aquaporins-mediated cell-to-cell pathway accounted for 60% to 80% of the root hydraulic conductivity (Maggio *et al.,* 1995; Wan *et al.,* 1999; Barrowclough *et al.,* 2000). The addition of $HgCl_2$ decreased the hydraulic conductivity

fourfold and twofold in epidermis/exodermis and cortex/endodermis, respectively. However, treatment with $HgCl_2$ had no significant effect on water transport in stele. This indicated that water transport through epidermis, exodermis, cortex and endodermis involved aquaporins whereas aquaporin was less involved in radial water transport through stele (North *et al.*, 2004).

The preferential expression of aquaporins in cortex in the study was consistent with the above analysis. In summary, higher expression in elongation region and root hair region suggests that expressions of these MIP members are related to capacity of root cell expansion and water uptake. Higher expression of aquaporins in cortical cells indicated their important role in water transport through cortex.

3. Effects of salt stress

Addition of NaCl to the hydroponic medium imposes osmotic and ionic stress onto plants and plant cells. Differential responses at the various levels have been observed after adding 100 mM or 200 mM NaCl. However, in both cases maize plants remarkedly managed to survive and to regain turgor and growth.

3.1. Immediate and early effects at the onset of salt stress (shock)

The osmotic potential of 100 mM and 200 mM NaCl were -0.49 MPa and -0.95 MPa, whereas that of the original growth medium was -0.04 MPa. The water potential of unstressed root cells of maize seedlings grown in this medium will be close to equilibrium, i.e. at about -0.04 MPa. In a similar setting a potential of -0.063 MPa had been determined for maize root cells; the turgor of young maize root cells was in the range of 0.5 to 0.7 MPa (Rodriguez *et al.*, 1997). Thus, for both NaCl concentrations root cells will lose water along the water potential gradient through plasma membrane and aquaporins. This will lead to a sudden drop in turgor and some initial decrease in the cellular osmotic potential due to the concentration of solutes upon water efflux and parallel Na^+ and Cl^- influx (Azaizeh *et al.*, 1991; Frensch & Hsiao, 1994; Munns, 2002; see below).

For 100 mM NaCl in the medium, the loss of turgor may already account for the most of the difference in water potential since the cellular osmotic potential will be around -0.5 MPa. Thus, equilibrium may be quickly reached although the plant has to initiate measures to regain turgor at the same time and to lower its osmotic potential to enable water uptake under these conditions (see below).

In contrast, the effects of 200 mM NaCl will be more severe. Even with a projected complete loss of turgor, a difference in water potential remains and drives water out of the root cells (-0.5 to -0.7 MPa *vs.* -0.95 MPa in the medium). Thus, the cells may lose water

even beyond this stage until the cellular water potential equalled the external -0.95 MPa. This scenario would lead to further shrinking of cells and to plasmolysis, i.e. the separation of the plasma membrane from the cell wall. Solution from the medium may fill the resulting gaps between membrane and cell wall, which may lead to an artefactual, extracellular flow of solution including salts across the root (Munns, 2002).

The initial efflux of water was also recorded at the the level of the relative water content (RWC) of roots. In a study with 150 mM NaCl added to dark-grown maize seedlings, RWC was reduced by 12% and 17% after 30 min in 0-5 mm and 5-10 mm zones of primary roots (Rodriguez *et al.*, 1997).

An immediate consequence of these effects is the sudden reduction of growth of roots and leaves (Rodriguez *et al*., 1997; Munns, 2002). The reduction of growth during salt stress could be prevented if plants were maintained at maximum water status using pressurization (Passioura & Munns, 2000). KCl and mannitol had similar effects like NaCl, indicating that these effects are entirely due to sudden osmotic changes and are not associated with nature of salt (Frensch & Hsiao, 1994). Under conditions preventing transpiration the reduction of growth could be rapidly released (Rodriguez *et al*., 1997), but it was prolonged if plants were transpiring and grown in the light (Neumann *et al*., 1994).

After exposure to saline solution Na^+ enters root cells along the electrochemical gradient because of the negative cytosol. In *Arabidopsis* it has been shown that Na^+ enter the root cells via potassium transporters such as HKT1 transports (Uozumi *et al.*, 2000), Na^+/K^+ symporter (Rubio *et al.*, 1995) or non-selective cation channels (Amtmann & Sanders, 1999; Demidchik & Tester, 2002). The measurement of Na^+ influx using radioactive tracer showed that Na^+ accumulation was linear with time and indicated unidirectional influx at the beginning of salt treatment (Essah *et al.*, 2003).

Although plant cells were subjected to these immediate and inevitable consequences of salt shock, several signals and active responses are triggered immediately and in an early phase to cope with this situation.

High concentration of NaCl immediately elevated cytoplasmic Ca^{2+} in *Arabidopsis* plants (Kiegle *et al.*, 2000) and in maize root protoplasts (Lynch *et al.*, 1989). The latter authors observed the dependence of cytosolic calcium on the concentration of NaCl; up to 90 mM NaCl there was no significant rise in intracellular calcium, however between 90 and 120 mM a sharp increase was provoked that sustained at 150 and 180 mM NaCl. Interestingly, this finding matches the differential responses to 100 mM and 200 mM NaCl shock in this study.

Ca^{2+} acts as a second messenger, transient increase of intracellular Ca^{2+} is perceived by various Ca^{2+} regulated proteins, among the phospholipase C enhancing the messenger

inositol (1, 4, 5) triphosphate, Ca^{2+}-dependent protein kinases (CDPK) and protein kinases of the SOS pathway.

Transient increase of cytosolic Ca^{2+} triggers protein phosphorylation cascades via CDPKs; these reactions activate transcriptional factors, which induced responsive genes, for example, enzymes for the biosynthesis of the phytohormone ABA, the synthesis of compatible solutes, ROS scavengers and osmoprotectants (Xiong *et al.*, 2002). ABA biosynthesis is rapidly induced in the roots from where it can be transported to aerial parts where it mediates the closure of stomata to reduce water loss and to reduce salt transport to the aerial parts (Leung *et al.*, 1998; Jia *et al.*, 2001; Schroeder *et al.*, 2001; Munns, 2002). Kawasaki *et al.* (2001) found the significant reduction of photosynthesis and stomatal conductance of two rice lines within 20 min after addition of 150 mM NaCl.

The SOS pathway has been established via mutant analyses in *Arabidopsis* (see introduction). The Ca^{2+}-dependent activation of SOS1, a Na^+/H^+ antiporter in plasma membrane has been identified to exclude Na^+ into root medium or export Na^+ to leaves via the xylem (Qiu *et al.*, 2002). Additional Na^+/H^+ antiporters residing in the tonoplast are responsible for vacuolar sequestration of Na^+, which not only lowers the concentration of Na^+ in cytosol but also contributes to osmotic adjustment (see below) to maintain water uptake from saline solution (Yokio *et al.*, 2002). Overexpression of vacuolar H^+-pyrophosphatase in *Arabidopsis* was reported to enhance plant salt tolerance substantially, indicating that a high proton gradient favoured the function of vacuolar Na^+/H^+ antiporter (Gaxiola *et al.*, 2001). Plants employ these mechanisms to lower the concentration of Na^+ in the cytosol, to minimize the damage from high salinity and to adapt to the salt stress.

Despite this efflux of Na^+ out of roots and export to the shoots via the xlyem stream, Na^+ concentration gradually elevated within 6 h treatment with 100 mM NaCl, in particular in the zone above 10 mm of maize roots (Rodriguez *et al*., 1997). Wang *et al.* (2003) found a gradual increase of Na^+ concentration in roots and shoots of maize treated with 150 mM NaCl. After prolonged salt stress this will eventually be detrimental. In particular, leaves may accumulate toxic levels of Na^+ in their vacuoles or cell wall (Munns, 2002); although there is also the ability to recirculate sodium ions via the phloem back to the roots (*Berthomieu et al.*, 2003).

Another consequence of high Na^+ may be the reduction of K^+-uptake into cells, which may negatively influence the activity of many enzymes (Munns *et al.*, 1988). Yet, in addition to Na^+ influx, Cl^- was also taken up from saline solution against the electrochemical potential. There was higher concentration of Cl^- in the 0-3 mm and 3-10 mm zones in response to 100 mM NaCl salt shock compared to control roots (Rodriguez *et al.*, 1997).

Although both Na^+ and Cl^- are toxic at high concentrations, they will also participate in osmoregulation and lowering the cellular water potential. As an additional measure to adjust the osmotic pressure cells synthesize compatible solutes and try to accumulate K^+

(which may be hampered by the excess in Na^+; see above). High concentrations of sucrose, glucose, fructose, and proline within 6 h treatment with 100 mM NaCl were measured (Rodriguez *et al.*, 1997), and genes involved in their biosynthesis like sucrose synthase and PEP carboxykinase were induced (Wang *et al.*, 2003). Interestingly, the distribution of the three sugars was different in the zone 0-3 mm and zone 3-10 mm, although the reason for this was not clear. Thereby, it is also important to consider the intracellular compartmentation of the ions, sugars or amino acids in the cytoplasm or the vacuole as well as the relative volumes of these compartments. With these measures, $?_s$ of root cells was reduced to -1.2 MPa, $?_w$ of roots was -0.6 MPa 2 h after addition of 100 mM NaCl (Rodriguez *et al*., 1997). Thus, the reduction of water potential allowed water uptake around this time point considering osmotic potential (-0.49 MPa) of the saline medium. Accordingly, the water content of leaves was not different after exposure to 100 mM NaCl vs. control in this study indicating water homeostasis was roughly achieved after 2 h treatment.

Right at this stage three highly expressed *ZmPIP* isoforms (*ZmPIP1-1*, *ZmPIP1-5*, *ZmPIP2-4*) were specifically induced at the transcriptional level. Interestingly, all of them were higher expressed in the cortex tissue of unstressed maize roots. Therefore, this finding can be interpreted as a reasonable measure to induce aquaporins around this time point during the acquisition of compatible solutes as soon as a minimal driving force was sufficient to regain water uptake. At later time points a further, slight reduction in the cellular osmotic potential (Frensch & Hsiao, 1994; Rodriguez *et al*., 1997) may supersede enhanced aquaporin expression. This may be the reason why aquaporins were transiently induced. Induction of aquaporins will also increase the cellular pathway of water uptake as long as the apoplastic pathway is reduced through ABA-mediated stomatal closure. This will limit the uptake of Na^+ into aerial parts via the apoplastic route.

At the same time point (2 h after 100 mM NaCl shock), ABA had accumulated in comparison with roots of seedlings grown in the control medium. With the roots regaining water uptake, the water status improved and cellular volume recovered, and the ABA content was gradually reduced towards later phase analyzed (9 h, 24 h).

The observed transient induction of *ZmPIP* members could be mediated by ABA. Indeed, exposure to 1 µM ABA also induced *ZmPIP2-4* and another member, ZmPIP1-2. Thus, the salt-induction of *ZmPIP2-4* was also provoked by ABA, whereas an ABA-independent pathway seems to activate the salt enhancement of *ZmPIP1-1* (and *ZmPIP1-5*, *ZmPIP2-6*). However, the same ABA level was determined after 2 h for the 200 mM NaCl experiment, and it was not associated with the transcriptional induction of any of the *ZmPIP* members. Thus, either other factors or pathways overrule the ABA regulation of *ZmPIP2-4* in the 200 mM NaCl experiment or the ABA-dependence of *ZmPIP2-4* induction is more complex and sensing the ABA concentration and/ or its changes. It has to be noted, that ABA is further enhanced after 200 mM NaCl application in contrast to 100 mM NaCl.

Therefore, a more detailed kinetic analysis of both transcription and ABA concentrations at this early phase will be necessary to resolve this question.

As indicated by several considerations (see above) and measured parameters, maize plants responded in a different way after the severe shock with 200 mM NaCl. Compared to the treatment with 100 mM NaCl and control, 200 mM NaCl salt stress significantly reduced the water content of leaves at 2 h. This lowered water content persisted until the end of treatment (48 h), indicating that stressed plants manifested a new water balance at a lower level. The reduced water status was also reflected by the ABA content of roots. At 2 h ABA accumulated significantly in the roots similar to the 100 mM NaCl experiment. However, this high level of ABA persisted until 24 h. Obviously, under these severe conditions with 200 mM NaCl no induction of aquaporins was observed in contrast to the 100 mM NaCl experiment.

The expression pattern of aquaporins after 2 h and 100 mM NaCl in maize was reminiscent to the salt-sensitive rice line IR29 (Kawasaki *et al.*, 2001). After treatment with 150 mM NaCl one PIP1 and one PIP2 member were transiently induced at 3 h time point in rice, but reduced to control levels after 6 h; a third MIP gene analyzed was slightly reduced after 6 h. In contrast, the salt resistant rice line Pokkali had a different expression pattern; the same three aquaporin genes were repressed at an early phase and then recovered; after a long term analysis (7 days) they were even induced. Thus, this contribution raised an important issue; the difference in response of aquaporins to salt stress could be related to the extent of the resistance to salt of the plant. Accordingly, maize cultivar used in this study displays the response like a moderately salt-sensitive species, which is in accordance to the general classification of maize (Blaylock, 1994).

In *Arabidopsis*, Kreps *et al*. (2002) showed that *AtPIP1-4* and *ZmNIP1-1* transcripts were induced after 3 h treatment with 100 mM NaCl using Affymetrix array harboring 8100 genes. Similarly, Affenzeller (2003) found the induction of *AtPIP1;4* after 5 h. A different scenario was described by Jang *et al.* (2004) who examined all 13 *AtPIP* genes by qRT-PCR. In their study the up-regulation of many members such as *AtPIP1-1*, *AtPIP1-2*, *AtPIP1-4*, *AtPIP2-3*, *AtPIP2-6* and *AtPIP2-7* by 100 mM NaCl was shown. However, they used hydoponic culture that included sucrose in the medium. These results implied that the up-regulation of aquaporins assists the subsequent uptake of water to maintain water homeostasis during the early stage of treatment with mild salt stress while the gradient of water potential was minor.

3.2. Later effects: 9 h until 24 h

After 9 h the concentration of ABA was strongly decreased in the 100 mM NaCl experiment. Thus, the inhibition of stomatal opening will be released allowing transpiration to drag water and ions into roots and to restart photosynthetic activity. Wang

et al. (2003) found that Na^+ content further increased in the root system and leaves from 6 h to 24 h after 150 mM NaCl shock. Rodriguez *et al.* (1997) reported that root expansion recovered 24 h after application of 150 mM salt shock, although Neumann *et al.* (1994) had found a more prolonged suppression of growth in light-grown and transpiring maize plants.

In contrast to the effect of 100 mM NaCl on ABA content in the roots, 200 mM NaCl further stimulated ABA accumulation beyond 2 h. This high level persisted until 24 h, indicating a persistent reduction of root cell volume during this period as suggested by Jia *et al.* (2001). This correlated with low water content of leaves indicating continued water deficiency. Indeed, there is previous evidence that the time taken for recovery of root growth during salt stress depends on the intensity of salt stress. With moderate level of osmotic stress (0.1- 0.4 MPa of mannitol or KCl) the recovery of growth by maize roots was essentially completed within 1 h. With a larger osmotic shock (0.6 MPa) there was a complete stop in elongation of roots for about 30 min and, afterwards, it commenced at a strongly reduced rate (Frensch *et al.*, 1994; 1995). One can infer that it took longer than 24 h for roots treated by 200 mM to recover growth.

This prolonged inhibition of growth may lead to the observed suppression of *ZmMIP*s at this stage after 200 mM NaCl shock. This response was much less specific than the transient upregulation of *ZmPIP*s after 2 h in the 100 mM NaCl experiment. Instead, a massive and broad repression was found. Interestingly, in addition to several *ZmPIP*s also *ZmTIP*s were repressed. The effect on the vacuolar members may indeed indicate a correlation to reduced cell expansion.

As outlined above, severe salinity could also cause root cells to plasmolyse. If they cannot recover, plasmolysed cells might die at the later phase. On the other hand, Huh *et al.* (2002) found 160 mM NaCl induce programmed cell death of *Arabidopsis* roots after 24 h indicating an active process that may be involved in adaptation. Sixty-nine percent of primary root cells were Tunel-staining positive indicating DNA fragmentation. The effected cells were distributed in the meristematic and elongation/ differentiation zones. Nevertheless, it is not clear whether such events would influence aquaporin expression in neighbouring, surviving cells.

High salinity (200 mM NaCl) repressed the expression of most aquaporin genes at later stage in this study. Wang *et al.* (2003) found that 7 *ZmPIPs* and 2 *ZmTIPs* transcripts were repressed after 12 h treatment with 150 mM NaCl in the maize roots. This corroborates my results but these authors could not discriminate different members because they used longer, cDNA clones that allowed crosshybridization (see Introduction). In barley roots *HvPIP2-1* was down-regulated after 24 or 48 h treatment with 200 mM NaCl (Katsuhara *et al.*, 2002). The amount of HvPIP2-1 protein was also reduced at 48 h.

3.3. After 48 h

Although water content of leaves of seedling treated by 200 mM NaCl was lower than that of control after 2 days, low water content remained at the definite level, indicating that water taken up from roots could balance by the loss from leaves; new water homeostasis was achieved during salt stress of 200 mM NaCl. The change in ABA concentration in roots supported this inference. In comparison with ABA concentration at 9 h and 24 h of treatment with 200 mM NaCl, ABA content was decreased significantly at 48 h. As ABA content was reduced, the processes inhibited by ABA such as photosynthesis and root growth regained (Munns, 2002). Accordingly, *ZmMIP* transcription recovered back to control level.

4. Effect of ABA on aquaporins

There are much informations about the effect of ABA on water flux and hydraulic conductivity. However, contradicting results were found that may depend on the different species and/ or conditions and techniques used. The studies by Fiscus (1981) and Markhart *et al.* (1979) show that ABA treatment reduced Lp_r. Similar results were obtained from the comparison of solute flow with water flux in xylem sap induced by ABA (Karmoket *et al.*, 1978; Van Steveninck *et al.*, 1988). On the other hand, ABA-induced Lp increase rather than a decrease was found by Glinka (1977; 1980) and Bassirad & Radin (1992). In maize, Freundl *et al.* (2000) measured hydraulic conductivity of roots and root cortical cells treated by ABA using root and cell pressure probe. Lp of roots cortical cells was stimulated by 7-27 folds after 1 h application of 100 nM and 1000 nM ABA, whereas Lp_r was increased by 3 folds at organ level. The reason for the difference lies in that there are several pathways for water movement across the root tissues according to composite water transport model. The relative flows in those pathways may change in response to the external conditions (Steudle & Peterson, 1998; Steudle, 2000). These water transport pathways comprise apoplastic pathway and cell-to-cell pathway. The latter pathway may involve aquaporins in the membranes.

Several previous reports indicated an effect of ABA on the transcription of aquaporins which did not give a consistent view (Kaldenhoff *et al.*, 1993; Gao *et al.*, 1999; Weig *et al.*, 1997; Hoth *et al.*, 2002; Jang *et al.*, 2004). One mM ABA induced aquaporin of seedling grown in the dark (Kaldenhoff *et al.*, 1993). In *Arabidopsis*, Jang *et al.* (2004) found that 100 µM ABA induced *AtPIP1-1*, *AtPIP1-2*, *AtPIP1-4*, *AtPIP2-3*, *AtPIP2-6* and *AtPIP2-7* but repressed *AtPIP1-5* in roots after 4 h. The induction *AtPIP1-2* was confirmed by global expression analysis (Hoth *et al.*, 2002), but Weig *et al.* (1997) reported that *AtPIP2-3* was repressed by 100 µM ABA.

However, in all these analyses high, unphysiological concentrations of ABA have been applied such as 50 µM, 100 µM and even 1000 µM. Although such exceedingly high

concentrations may facilitate the discovery of truly regulated genes, unspecific pharmaceutic effects cannot be excluded. Therefore, other researcher used much lower concentration of ABA for treatment of plants in physiological analyses (Freundl *et al.*, 2000; Ober *et al.*, 2003).

Nevertheless, I also applied a high ABA concentration of 100 µM. This treatment repressed the expression of all the aquaporins at 24 h arguing for an unspecific, non-hormonal effect although the transcripts of two control genes remained constant and a positive control gene, *rab17*, was strongly induced. *Rab 17* also responded to water deficit.

The inference of an unspecific effect is supported by the observation that application of 1 µM ABA, i.e. a much lower concentration, had only a more subtle effect. Specifically, *ZmPIP2-4* and *ZmPIP1-2* were transiently induced after 1 h (see above).

5. Effect of salt stress and ABA on aquaporin at protein level

The eventual function of genes depends on the amounts and activity of the encoded proteins and their subcellular localization, which are affected by several factors; namely the mRNA half-life, the translation rate, the rate of intracellular trafficking of membrane proteins and the protein stability. Although the transcription level of genes can provide important and valuable information on the function of genes, other levels such as protein amount, activity or metabolites will be necessary to fully interpret their function.

In addition to the analysis of the expression of aquaporins at mRNA level under treatment with salt stress and ABA, the amount of aquaporins (ZmPIP1 and ZmPIP2) has been also analyzed by two antisera detecting most ZmPIP1 members and ZmPIP2-4/ ZmPIP2-3. After application of high salinity or ABA (Fig. 26 and Fig. 27) no significant changes in ZmPIP1 and ZmPIP2 were observed. This was in contrast to the transcriptional analyses, where several aquaporin genes were repressed by 200 mM NaCl and 100 µM ABA or specifically induced (*ZmPIP1-1*, *ZmPIP1-2*, *ZmPIP2-4*). Apparently, the protein level of aquaporins was not correlated to the mRNA level.

There may be several reasons for this apparent or real discrepancy. Importantly, all transcriptional changes observed were transient. Therefore, changes may not be continuously transferred to the protein amount although the transcriptional regulations are clear-cut. Similar observations are e.g. frequent in circadian regulation of gene transcription. In addition, other isoforms detected by the antisera, but not altered at the transcriptional level might obviate the detection of altered protein amounts. The generation of isoform-specific antibodies could resolve this issue. Furthermore, only total membranes have been analyzed in this study. Thus, a possible translocation of e.g. PIPs from the plasma membrane, which would alter the membrane permeability accordingly, was not

differentiated. To investigate this question, detailed membrane fractionation will be necessary.

Nevertheless, the discrepancies could be real. In fact, there have been other reports showing that the transcript and protein levels of aquaporins are not necessarily correlated (Aroca *et al.,* 2005; Morillon *et al.,* 2002; Katsuhura *et al.,* 2002). In radish roots, for example some PIP1 isoforms were constitutively expressed in response to salt stress, yet the protein level was increased 1.5 fold (Suga *et al.*, 2001; 2002; 2003). Chilling of maize plants for three days, repressed all *PIP* genes except *ZmPIP1-6*, but PIP2 protein remained constant and PIP1 proteins even increased after the treatment (Aroca *et al.,* 2005). In contrast, Katsuhura *et al.* (2002) found that *PIP2-1* transcription was repressed in barley roots treated by 200 mM NaCl at 24 h and 48 h, and accordingly PIP2-1 protein was reduced at 48 h although not yet at 24 h.

6. Nutrient deficiency and *ZmMIP* expression

6.1. K^+-deficiency

K^+ is an essential macronutrient in plants. K^+ functions as an important osmoticum and a cofactor for enzymes, which affects protein synthesis and photosynthesis, regulation of pH and cation-anion balance. The partitioning of K^+ is a crucial driving force for growth, reversible osmotic changes such as stomatal movement, light-driven and seismonastic movement of organs, or phloem transport.

6.1.1. Effect of K^+ on hydraulic conductivity and water relation

There are differential reports on the effects of K^+-deficiency on water flux and/ or hydraulic conductivity of roots. Recently, Schraut *et al*. (2005) found that K^+-deficiency increased hydrostatic water flux threefold in excised maize roots using root pressure probe. A similar result was also described for excised sunflower roots (Quintero *et al*., 1998). This indicated a reduced resistance to water flux in the roots during K^+-starvation. Indeed, incomplete development of Casparian strips in the cell wall of the root endodermis has been observed during K^+-deficiency (Schraut *et al.,* 2005). It has been also reported that K^+ provides strength to plant cell wall and that it is involved in the lignification of scleremchyma tissue. Lignification of vascular bundles is also impaired during K^+-deficiency (Pissarek, 1973).

In contrast to the increase of the mostly hydrostatically driven water flux, osmotic water flux was reduced upon K^+-starvation in some species. A reduction of xylem water flux during K^+-deficiency was observed in tomato (Amor *et al.*, 2004). Seven days after starvation, xylem water flux was lowered and the K^+-concentration in the sap was reduced by 60%. Similarly, the hydraulic conductivity (Lp) of sunflower roots was reduced by a

factor of two (Graham & Ulrich, 1972), indicating that osmotic hydraulic conductivity was reduced by K^+-deficiency.

K^+ is also the dominant cation in root pressure exudation sap (Hsaio & Läuchli, 1986), indicating that K^+ plays a role in build-up of root pressure. K^+-deficiency reduced osmotic water flux not only by diminishing the osmotic gradient but also by reduction of cellular water permeability (see below).

Furthermore, K^+ is responsible for turgor changes in the guard cells to induce stomatal opening and closure. An increase in the K^+-concentration in the guard cells reduces osmotic potential and results in water uptake from apoplasm. The corresponding increase in turgor leads to swelling of the guard cell pair and thus stoma opening. Closure of the stomata in the dark is correlated with K^+-efflux and corresponding decrease in the osmotic pressure of guard cells. Under K^+-deficiency reducing sugars may substantially contribute to this osmotic regulation. However, this makes the stomates respond very slowly. This retarded response of sugar-loaded guard cells results in incomplete opening and closure in K^+-deficient plants (Hsiao & Läuchli, 1986). Thus, K^+-starvation reduces the transpiration of maize plants due to incomplete stomatal opening during daytime (Hsiao & Läuchli, 1986; Peaslee *et al.,* 1968). During the night, stomata did not close efficiently, thus leading to increased water loss through stomata. Consequently, during daytime the water flow driven by transpiration will be reduced – although complemented by other means (see above) and photosynthesis willl be hindered due to reduced gas exchange through stomata.

6.1.2. Effect of K^+ on growth

K^+-deficiency and reduced photosynthesis will indirectly retard growth. In addition, K^+ is directly involved in cell growth. It is transported actively across membranes and accumulates as an osmoticum to drive cellular expansion. High concentrations of K^+ can accumulate in cells and are not toxic like Na^+. Hsiao & Läuchli (1986) reported that K^+-concentration can vary in cytosol, vacuole and apoplasm in the range 10-200 mM, 100-200 mM and 100 mM, respectively.

Accordingly, cellular elongation might be hindered during K^+-deficiency. In *Avena* coleoptiles IAA–induced elongation ceased after a few hours in the absence of external K^+ (Haschke *et al*., 1975). The analysis of growth of the maize seedlings deprived of K^+ in this study showed that the growth of seedlings was retarded compared to control plants, but no change in the ratio of root to shoot was observed. A similar observation has been made for wheat in case of K^+-deficiency, which contrasted plants deprived of NO_3^- or PO_4^{3-} (Clarkson *et al*., 2000).

6.1.3. AQP expression

Preliminary observations indicate that *ZmPIP* members and *ZmTIP* members were repressed in K^+-deprived maize roots. For unknown reasons, there was a difference between the analysis after day 8 vs. day 9 of potassium starvation, which indicated at least a partial release from the suppression. Two days after re-supply of K^+, transcript activity of all repressed aquaporins recovered to control levels. The repressed members during K^+-deficiency are highly abundant PIP and TIP members; several of the affected members have been experimentally shown to transport water. They are expressed more highly in cortex than in stele and thus could be implicated in radial water transport in the roots.

Recently, similar results were found in roots of *Arabidopsis* (Armengaud *et al.*, 2004). Aquaporins such as *AtPIP1-4, AtPIP2-7, AtPIP2-8, AtTIP1-1, AtTIP1-2, AtTIP1-3, AtTIP2-1, AtTIP2-2* and *AtTIP4-1* were down-regulated during long-term K^+-starvation and up-regulated after K^+-resupply. This indicates that K^+-deficiency has similar effects on the expression of PIPs and TIPs in *Arabidopsis* and maize.Therefore, the transcriptional repression of aquaporins in response to K^+-deficiency may be a common feature in dicotyledonous and monocotyledonous species.

Although the repression of *ZmPIP* and *ZmTIP* genes was not consistent after day 8 and day 9, there is a tendency of reduced transcription for *ZmPIP1-1, ZmPIP1-5, ZmPIP2-1, ZmTIP1-1, ZmTIP2-1* and *ZmTIP2-4* and definitely no indication of induced expression of any of the *ZmMIP* members. Thus, K^+-deprivation led to a repression of several *PIP* and *TIP* isoforms in contrast to the observed increase in water flux. Apparently the increase in water flux was not related to the repression of PIPs and TIPs. Instead, the potential reduction may indicate a relation of these aquaporins to the retardation in growth observed upon K^+-deficiency.

According to the physiological functions of potassium ions, a reduced expression of PIP and TIP aquaporins in maize (and Arabidopsis) can be nicely correlated with two processes. First, the reduction may aim to reduce the water flow through root in parallel to the reduced transpiration. Thus, both factors counteract the enhanced water flow due to the lowered physical barriers for the hydrostatic water flow (Schraut *et al.*, 2005). Second, the repression of plasma membrane and tonoplast aquaporins suggests a correlation to the retarded growth under K^+-deficiency, which can be relieved upon resupply of the cation.

6.2. NO_3^- - deficiency

6.2.1. Effect of N-starvation on water relations

NO_3^--deficiency negatively affects hydraulic conductivity in maize (Barthes *et al.*, 1995; Hoarau *et al.*, 1996), in wheat (Carvajal *et al.*, 1996), and in cotton (Radin & Matthews, 1989). In maize, N-deficiency reduced hydraulic water flux of excised roots as measured

by root pressure probe indicating an increase of resistance to water flow and decrease of conductivity of roots (Schraut *et al.,* 2005). Barthes *et al.* (1995) and Hoarau *et al.* (1996) compared the effects of KCl and KNO_3 on the rate of xylem water flux and sap osmolarity. The KCl experiment may be regarded as a nitrate-deficient condition. Compared to KNO_3, five fold reduction of xylem water flux was observed with KCl, but the KCl conditions did not increase total osmolarity. No relationship was found between xylem sap osmolarity and xylem water flux, suggesting that reduction of xylem flux by NO_3^--limitation is mediated by a change in hydraulic conductivity rather than osmolarity (according to $J_v \sim \Delta\pi \times Lp$).

Furthermore, the lower value of hydraulic conductivity of wheat roots during N-deprivation was not sensitive to $HgCl_2$ (Carvajal *et al.*, 1996) arguing for reduction of Hg-sensitive water transport by N-deprivation that is usually attributed to aquaporin-mediated water permeability. Similarly, Larsson *et al.* (1987) analyzed the water permeability of plasma membrane vesicle from wheat roots using stopped-flow spectrophotometer. They found that the vesicles of N-deprived roots had lower and $HgCl_2$-insensitive water permeability in comparison with that of control vesicles. Measurements using cell pressure probe showed that the permeability of cortical cells of N-deficient cotton roots was lower than that of nutrient-sufficient control by 85% (Radin & Matthews, 1989). These experiments indicated that the osmotic hydraulic conductivity of roots and root cells was reduced by N-starvation in different plant species.

6.2.2. Influence of NO_3^--deficiency on growth

The shoots of maize seedlings deprived by NO_3^- were shorter than control plants; in contrast, the length of root was stimulated by N-deficiency. These results were comparable to experiments with barley (Karmoker *et al.*, 1991). Furthermore, the effect during N-deficiency was similar to that during P- or S-starvation (Robinson, 1994). The overlapping responses indicate some common sequence of events during these different nutrient deficiencies. Nutrient deficiency is perceived by roots and signals are transduced via the xylem to the shoot. There, stomata close and cause a reduction in transpiration, i.e. hydrostatic water conductivity, and in photosynthesis. As a consequence, the growth of leaves decreases and allocation of assimilates into roots increases: roots enlarge at a higher rate (Clarkson *et al.*, 2000). It appears that plants have evolved a strategy to maximize the capture of resources below ground to compensate for the nutrient deficiency.

6.2.3. Repression of aquaporin expression by NO_3^--deficiency

At transcriptional level, the preliminary results from two independent biological replicates show a single, highly expressed plasma membrane aquaporin, *ZmPIP1-5*, was specifically repressed along with *ZmTIP1-1*. Importantly, these genes had higher expression in cortex than in the stele as determined for primary roots. This means that repression of *ZmPIP1-5* and the two *TIP* members could be specifically responsible for a reduction of the cellular

water transport in the cortex, which may result in reduced osmotic hydraulic conductivity. Other MIPs were not affected. After resupply of nitrate, *ZmPIP1-5* recovered to control level, which is consistent with a report by Gaspar *et al*. (2003) who studied only this particular gene. Similarly, *TIP* mRNAs attained control levels.

The specificity of the response was surprising. However, one could speculate that this observation was related to isoform-specific functions of aquaporins and to two opposing effects of N-deficiency: reduction of osmotic permeability and enhanced growth of roots. The suppression of *ZmPIP1-5* could primarily target the transcelluar water flow, yet allow at the same time the enhanced root expansion. Therefore, a broad repression of different *PIP* and *TIP* isoforms that was correlated with a reduction in expansion growth in other cases was not found in this instance (compare 3.2., 6.1.3.).

A similar effect of N-starvation and N-resupply on aquaporin transcripts was also observed in tomato (Wang *et al*., 2001b) and *Arabidopsis thaliana* (Wang *et al*., 2000a). Using a microarray Wang *et al.* (2001b) reported that expression of several aquaporin genes was induced to 2-3 folds in roots by addition of nitrate to N-starved tomato plants, suggesting that N-deprivation repressed the expression of aquaporin, which was reversed by N-resupply.

An alternative explanation is posible on the basis of recent findings on additional permeabilities of MIP members to urea or ammonium. Gaspar *et al.* (2003) found that urea was transported by ZmPIP1-5; whether ammonium is permeating is not known. However, for two *Arabidopsis* TIP members, NH_3 permeation has been recently demonstrated (Loqué *et al*., 2005). Thus, the enhanced TIP or PIP gene expression upon nitrate resupply could be also associated with the transport of N-containing chemicals.

7. Perspectives

In this study indications were found that ABA could mediate the induction of *ZmPIP2-4*. However, obviously other signalling pathways are implicated in the regulation of aquaporin expression upon salt stress, nutrient deprivation or other environmental cues. Additional experiments including genetic approaches and signalling mutants should be employed to resolve these issues. E.g. the repression of aquaporins in response to the lack of nitrate may be indirect because nitrate functions as an osmoticum and important macronutrient involving growth, or it may employ signaling events that are more directly associated with the nitrogen source.

The analysis on protein amount in response to salt stress and treatment with ABA was included in this study. No significant change in protein amount was observed. In the study the proteins was from microsomal fractions. Recently, Vera-Estrella *et al.* (2004) reported the translocation of TIPs into different membrane fractions as one of mechanism for

regulation of aquaporin activity. A similar mechanisms for PIPs has not yet been demonstrated. Therefore, it will be interesting to investigated the presence and possible transfer of PIPs in the plasma membrane and putatitve internal vesicles (Robinson *et al.*, 1996) that are also known from mammalian regulation of aquaporin activity (Deen *et al.*, 1995).

The analysis on aquaporin transcription provides indirect information for the function and relevance of aquaporin in plants. To further investigate their functions, genetic approaches targeting specific aquaporin members RNAi or knock-out techniques will be helpful.

E. SUMMARY

Major intrinsic proteins (MIPs) are an ancient family that were found in various bacteria, fungi, amphibians, plants and animals. They are collectively called aquaporins (AQPs) because some members were found to transport water, and others were shown to be permeable to small uncharged molecules such as glycerol, urea, ammonium, or formamide. In the crop plant maize, 34 cDNA sequences encoding putative AQPs had been previously identified. They include 13 plasma membrane intrinsic proteins (ZmPIPs), 13 tonoplast intrinsic proteins (ZmTIPs), 5 NOD26-like intrinsic proteins (ZmNIPs) and 3 small basic intrinsic proteins (ZmSIPs).

Environmental cues such as increased salt concentration or nutrient deprivation affect root hydraulic conductivity. To examine an implication of AQPs in these processes, the expression of the maize *MIP* gene family was analyzed by a *ZmMIP* DNA array that harbored gene-specific sequences as targets for hybridization.

Eleven *ZmPIP* and 5 *ZmTIP* members were detected in roots of 11 day-old seedlings grown in hydroponic culture. Members of the other two subgroups were expressed weakly. *ZmPIP1-1*, *ZmPIP1-5*, *ZmPIP2-1*, *ZmPIP2-4*, *ZmPIP2-5*, *ZmPIP2-6*, *ZmTIP1-1*, *ZmTIP2-1*, *ZmTIP2-2* and *ZmTIP2-4* had the high abundance. Six day-old maize primary roots were further dissected to investigate the spatial expression pattern. High abundance of all detected *ZmMIP* members were observed in the elongation zone (3-10 mm) and root hair zone (10-20 mm), but less transcripts were detected in the root tip (0-3 mm) and mature zone (50-60 mm). Thus, the expression of aquaporins correlated with the region of enhanced water uptake. Analysis of aquaporin expression of longitudinally separated primary roots showed that higher transcription of *ZmPIP1-1*, *ZmPIP1-5*, *ZmPIP2-1*, *ZmPIP2-4*, *ZmPIP2-5*, *ZmTIP1-1*, *ZmTIP2-2* and *ZmTIP2-4* in cortex than in stele tissue. There was no difference of *ZmPIP1-2* and *ZmPIP2-6* transcript between cortex and stele. This indicated that aquaporin-mediated cellular pathway through cortex tissue played an important role for root water transport involving the identified isoforms.

Maize seedlings responded differentially to 100 *vs*. 200 mM NaCl treatments. Leaf water content was rapidly and persistently reduced after application of 200 mM NaCl in contrast to 100 mM NaCl. The stress hormone abscisic acid (ABA) strongly accumulated in roots after 2 h; it stayed at a highly elevated level for 48 h after addition of 200 mM NaCl, but ABA rapidly declined close to control levels in plants treated with 100 mM NaCl. The transcriptional responses of *ZmMIP* genes were also different in both szenarios. Two hours after addition of 100 mM, but not of 200 mM NaCl, two highly expressed plasma membrane isoforms *ZmPIP1-1* and *ZmPIP2-4* were transiently induced. In addition, the most highly expressed maize *PIP* gene in roots, *ZmPIP1-5*, showed a weak, yet significant induction. None of the *ZmTIP* genes was altered. The specific and transient induction was interpreted as a measure to enhance water uptake when plants were just regaining the capability of water uptake. In contrast, multiple *ZmPIP* and *ZmTIP* genes were specifically

reduced by 200 mM NaCl after 24 h. After 48 h, deregulations were overridden in both cases indicating homeostasis. One µM ABA exogenously applied to the roots transiently induced *ZmPIP2-4* similar to 100 mM NaCl as well as *ZmPIP1-2*. Previously, an increase in hydraulic conductivity had been observed upon ABA application. One hundred µM ABA, a high concentration frequently used in other studies, lead to a complete, possibly non-specific repression of all detected *ZmPIP* and *ZmTIP* genes after 24 h. It is inferred that the early induction of *ZmPIP2-4* by NaCl may be mediated by ABA, whereas other regulations are probably ABA-independent. Furthermore, transcriptional repression of aquaporins could be involved in the reduction of water permeability after treatment with 200 mM NaCl, but not after milder salt stress.

Aquaporin abundance was also investigated at the protein level in total microsomal fractions using antisera detecting ZmPIP2-3 and ZmPIP2-4 as well as the ZmPIP1 subgroup. Apparently, the protein level of aquaporins was not correlated to the transient changes in mRNA abundance. This may point to a real discrepancy of mRNA and protein levels. Alternatively, other detected isoforms, which were not altered, might obviate the resolution of changes, or a possible membrane translocation was not resolved when using microsomal fractions. Phosphorylation of aquaporins has been reported as another possible mechanism to regulate aquaporins. However, with respect to NaCl and ABA treatments no alterations in the degree of phosphorylation could be detected in this study, which, however, could not discriminate between different isoforms.

Finally, the implication of AQPs in changes of hydraulic conductivity provoked by K^+- and NO_3^--deprivation was examined in a preliminary study. K^+-deficiency reduced four *ZmPIP* and three *ZmTIP* members. This could be related to a reduced cellular water transport through roots as well as the retarded growth although overall water flux was increased. Surprisingly, *ZmPIP1-5* and *ZmTIP1-1* was specifically repressed after N-deprivation. This change may indicate that these isoforms are primarily involved in the transcellular water flow that is reduced under N-limitation; yet at the same time enhanced root growth is possible, which involves other isoforms that were not affected in this instance.

F. REFERENCES

Abe H, Yamaguchi-Shinozaki K, Urao T, Iwasaki T, Hosokawa D, Shinozaki K. 1997. Role of Arabidopsis MYC and MYB homologs in drought- and abscisic acid-regulated gene expression. *Plant Cell* **9,** 1859-1868.

Addicott FT, Lyon JL, Ohkuma K, Thiessen WE, Carns HR, Smith OE, Cornforth JW, Milborrow BV, Ryback G, Wareing PF. 1968. Abscisic acid: A new name for abscisin II (dormin). *Science* **159**, 1493-1498.

Affenzeller M. 2003. The transcription profile of MIP family and genes of stress- and secondary metabolism in *Arabidopsis thaliana* during water stress. Dissertation. Ludwig-Maximilians-Universität, München.

Agre P, Saboori AM, Asimos A, Smith BL. 1987. Purification and partial characterization of the Mr 30000 integral membrane protein associated with the erythrocyte Rh (D) antigen. *J. Biol. Chem.* **262**, 17497-17503.

Aharon R, Shahak Y, Wininger S, Bendov R, Kapulnik Y, Galili G. 2003. Overexpression of a plasma membrane aquaporin in transgenic tobacco improves plant vigor under favorable growth conditions but not under drought or salt stress. *Plant Cell* **15**, 439-447.

Amor FMD, Marcelis LFM. 2004. Regulation of K uptake, and growth of tomato during K starvation and recovery. *Sci. Horticult.* **100**, 83-101.

Amtmann A, Sanders D. 1999. Mechanisms of Na^+ uptake by plant cell. *Adv. Bot. Res.* **29**, 75-112.

Apse MP, Aharon GS, Snedden WA, Blumwald E. 1999. Salt tolerance conferred by overexpression of a vacuolar Na^+/H^+ antiport in Arabidopsis. *Science* **285**, 1256-1258.

Armengaud P, Breitling R, Amtmann A. 2004. The potassium-dependent transcriptome of Arabidopsis reveals a prominent role of jasmonic acid in nutrient signaling. *Plant Physiol.* **136**, 2556-2576.

Aroca R, Amodeo G, Fernandez-Illescas S, Herman EM, Chaumont F, Chrispeels MJ. 2005. The role of aquaporins and membrane damage in chilling and hydrogen peroxide induced changes in the hydraulic conductance of maize roots. *Plant Physiol.* **137**, 341-353.

Azad AK, Sawa Y, Ishikawa T, Shibata H. 2004. Phosphorylation of Plasma Membrane Aquaporin Regulates Temperature-Dependent Opening of Tulip Petals. *Plant Cell Physiol.* **45,** 608-617.

Azaizeh H, Gunse B, Steudle E. 1992. Effects of NaCl and $CaCl_2$ on water transport across root cells of maize (*Zea mays* L.) seedlings. *Plant Physiol.* **99**, 886–894.

Azaizeh H, Steudle E. 1991. Effects of salinity on water transport of excised maize (Zea mays L.) roots. *Plant Physiol.* **97**, 1136-1145.

Baiges I, Schäffner AR, Affenzeller MJ, Mas A. 2002. Plant aquaporins. *Physiol. Plant.* **115**, 175-182.

Baiges I, Schäffner AR, Mas A. 2001. Eight cDNA encoding putative aquaporins in Vitis hybrid Richter-110 and their differential expression. *J. Exp. Bot.* **52**, 1949-1951.

Baker ME, Saier MH. 1990. A common ancestor for bovine lens major intrinsic protein, soybean nodulin-26 protein, and *E. coli* glycerol facilitator. *Cell* **60**, 185-186.

Barkla BJ, Vera-Estrella R, Kirch HH, Pantoja O, Bohnert HJ. 1999. Aquaporin localization - how valid are the TIP and PIP labels? *Trends Plant Sci.* **4**, 86-88.

Barrieu F, Chaumont F, Chrispeels MJ. 1998. High expression of the tonoplast aquaporin ZmTIP1 in epidermal and conducting tissues of maize. *Plant Physiol.* **117**, 1153-1163.

Barrowclough DE, Peterson CA, Steudle E. 2000. Radial hydraulic conductivity along developing onion roots. *J. Exp. Bot.* **51**, 547-557.

Barthes L, Bousser A, Hoarau J, Deléens E. 1995. Reassessment of the relationship between nitrogen supply and xylem exudation in detopped maize seedlings. *Plant Physiol. Biochem.* **33**, 173–183.

Barthes L, Deléens E, Bousser A, Hoarau J, Prioul JL. 1996. Xylem exudation is related to nitrate assimilation pathway in detopped maize seedlings: use of nitrate reductase and glutamine synthetase inhibitors as tools. *J. Exp. Bot.* **47**, 485–495.

Bassirad H, Radin JW. **1992**. Temperature dependent water and ion transport properties of barley and sorgum roots. *Plant Physiol.* **99,** 34-37.

Beijer L, Nillson RP, Holmberg C, Rutberg L. 1993. The *glp* and *glpF* genes of the glycerol reglon in *Baillum subtilis. J. Gen. Micribiol.* **139,** 349-359.

Berthomieu P, Conejero G, Nublat A, Brackenbury WJ, Lambert C, Savio C, Uozumi N, Oiki S, Yamada K, Cellier F, Gosti F, Simonneau T, Essah PA, Tester M, Very AA, Sentenac H, Casse F. 2003. Functional analysis of AtHKT1 in Arabidopsis shows that Na^+ recirculation by the phloem is crucial for salt tolerance. *EMBO J.* **22,** 2004-2014.

Blaylock MJ, James BR. 1994. Redox transformation and plant uptake of Se resulting from root-soil interactions. *Plant Soil.* **158,** 1-17.

Bohnert HJ Su H, Shen B. Molecular mechanism of salinity tolerance In. Shinosaki K(ED), Cold, Drought, Heat, and Salt stress: Molecular Responses in Higher Plants, R.G. Landes, Austin, 1999, pp 29-60.

Bohnert HJ and members of the plant stress consortium. 2001. A genomics approach towards salt stress tolerance. *Plant Physiol. Biochem.* **39,** 295-311.

Bowling DJF, Edwards A. 1984. pH gradients in the stomatal complex of *Tradescantia virginiana*. *J. Exp. Bot.* **35,** 1641–1645.

Bowling DJF. 1987. Measurement of the apoplastic activity of K^+ and Cl^- in the leaf epidermis of *Commelina communis* in relation to stomatal activity. *J. Exp. Bot.* **38**, 1351-1355.

Carvajal M, Cooke DT, Clarkson DT. 1996. Responses of wheat plants to nutrient deprivation may involve the regulation of water-channel function. *Planta* **199,** 372-381.

Carvajal M, Martinez V, Alcaraz CF. 1999. Physiological function of water channels as affected by salinity in roots of paprika pepper. *Physiol. Plant* **105**, 95-101.

Chapin FS, Walter CHS, Clarkson DT. 1988. Growth response of barley and tomato to nitrogen stress and its control by abscisic acid, water relations and photosynthesis. *Planta* **173,** 352-366.

Chaumont F, Barrieu F, Herman EM, Chrispeels MJ. 1998. Characterization of a maize tonoplast aquaporin expressed in zones of cell division and elongation. *Plant Physiol.* **11**7, 1143-1152.

Chaumont F, Barrieu F, Jung R, Chrispeels MJ. 2000. Plasma membrane intrinsic proteins from maize cluster in two sequence subgroups with differential aquaporin activity. *Plant Physiol.* **122,** 1025-1034.

Chaumont F, Barrieu F, Wojcik E, Chrispeels MJ, Jung R. 2001. Aquaporins constitute a large and highly divergent protein family in maize. *Plant Physiol.* **125**, 1206-1215.

Chaumont F, Loomis, Chrispeels MJ. 1997. Expression of an *Arabidopsis* plasma membrane aquaporin in *Dictyostelium* results in hypoosmotic sensitivity and developmental abnormalities. *Proc. Natl. Acad. Sci. USA* **94**, 6202-6209.

Chrispeels MJ, Morillon R, Maurel C, Gerbeau P, Kjellbom P, Johansson I. 2001. Aquaporins of plants: Structure, function, regulation and role in plant water relations. *In Current Topics in Membrane, volume 51, pp279-334. Academic press.*

Clarkson DT, Carvajal M, Henzler T, Waterhouse RN, Smyth AJ, Cooke DT, Steudle E. 2000. Root hydraulic conductance: diurnal aquaporin expression and the effects of nutrient stress. *J. Exp. Bot.* **51**, 61-70.

Cramer G.R., Epstein E., Läuchli A. 1988. Kinetics of root elongation of maize in response to short-term exposure to NaCl and elevated calcium concentration. *J. Exp. Bot*. **25**, 1513–1522.

Cramer GR, Alberico GJ, Schidt C. 1994. Salt tolerance is not associated with the sodium accumulation of two maize hybrids. *Aust. J. Plant Physiol.* **25**, 675–692.

Cramer GR, Bowman DC. 1991. Kinetics of maize leaf elongation 1. Increased yield threshold limits short-term, steady-state elongation rates after exposure to salinity. *J. Exp. Bot*. **25**, 1417–1426.

Cramer GR., Läuchli A. 1986. Ion activities in solution in relation to Na^+–Ca^{2+} interactions at the plasmalemma. *J. Exp. Bot.* **25**, 321–330.

Crawford NM, Glass DMA. 1998. Molecular and physiological aspect of nitrate uptake in plants. *Trends Plant Sci.* **3**, 389-395.

Cutler SR, Ehrhardt DW, Griffitts JS, Somerville CR. 2000. Random GFP::cDNA fusions enable visualization of subcellular structures in cells of Arabidopsis at a high frequency. *Proc. Natl. Acad. Sci. USA* **97**, 3718-3723.

Daniels MJ, Chaumont F, Mirkov TE, Chrispeels MJ. 1996. Characterization of a new vacuolar membrane aquaporin sensitive to mercury at a unique site. *Plant Cell* **8,** 587-599.

Daniels MJ, Chrispeels MJ, Yeager M. 1999. Projection structure of a plant vacuole membrane aquaporin by electron cryo-crystallography. *J. Mol. Biol.* **294**, 1337-1349.

Daniels MJ, Mirkov TE, Chrispeels MJ. 1994. The plasma membrane of arabidopsis thaliana contains a mercury-insensitive aquaporin that is a homolog of the tonoplast water channel protein TIP. *Plant Physiol.* **106**, 1325-1333.

Daryll B, Javad Torabinejad D, Jones CR, Shope JC, Cangelosi AR, Thompson JE, Prestwich GD, Hama H. 2001. Rapid accumulation of phosphatidylinositol 4,5-bisphosphate and inositol 1,4,5-trisphosphate correlates with calcium mobilization in salt-stressed *Arabidopsis*. *Plant Physiol.* **126**, 759-769.

Davies WJ, Tardieu F, Trejo CL. 1991. How Do Chemical Signals Work in Plants that Grow in Drying Soil? *Plant Physiol.* **104**, 309-314.

Davies WJ, Wilkinson S, Loveys B. 2002. Stomatal control by chemical signalling and the exploitation of this mechanism to increase water use efficiency in agriculture. *New Phytol.* **153**, 449-460.

de Groot, BL, Grubmüller H. 2001. Water permeation across biological membranes: mechanism and dynamics of aquaporin-1 and GlpF. *Science **294***, 2353–2357.

Deen PMT, Croes H, van Aubel RA, Ginsel LA, van Os CH. 1995. Water channels encoded by mutant aquaporin-2 genes in nephrogenic diabetes insipidus are impaired in their cellular routing. *J. Clin. Invest.* **95**, 2291-2296.

Deen PMT, van Aubel RA, van Lieburg AF van Os CH. 1996. Urinary content of aquaporin 1 and 2 in nephrogenic diabetes insipidus. *J. Am. Soc. Nephrol.* **7**, 836-841.

Deen PMT, Verdijk MA, Knoers NVAM, Wieringa B, Monnens LAH, van Os CH, van Oost BA. 1994. Requirement of human renal water channel aquaporin-2 for vasopressin-dependent concentration of urine. *Science* **264**, 92-95.

Delauney AJ, Desh P, Verma S. 1993. Proline biosynthesis and osmoregulation. in plants. *Plant J* **4,** 215-224.

Dellaporta SL, Wood J, Hicks JB. 1983. A plant DNA mini-preparation: version II. *Plant Mol. Biol. Rep.* **1**, 19-21.

Demidchik V, Tester M. 2002. Sodium fluxes through nonselective cation channels in the plasma membrane of protoplasts from Arabidopsis roots. *Plant Physiol*. **128**, 379-387.

Dordas C, Chrispeels MJ, Brown PH. 2000. Permeability and channel-mediated transport of boric acid across membrane vesicles isolated from squash roots. *Plant Physiol.* **124**, 1349-1362.

Drew MC, Saker LR. 1975. Nutrient supply and growth of the seminal root system in barley. III. Localized, compensatory increase in growth of and rates of nitrate uptake when nitrate supply is restricted to only part of the root system. *J. Exp. Bot.* **29**, 435-451.

Essah PA, Davenport R, Tester M. 2003. Sodium Influx and Accumulation in Arabidopsis. *Plant Physiol.* **133,** 307-318.

Fabri CO, Schäffner AR. 1994. An *Arabidopsis thaliana* RFLP mapping set to localize mutations to chromosomal regions. *Plant J.* **5**, 149-156.

FAO. 1986. Production Year book. Vol. 34. Rome, Italy.

Fetter K, Van Wilder V, Moshelion M, Chaumont F. 2004. Interactions between plasma membrane aquaporins modulate their water channel activity. *Plant Cell* **16**, 215-228.

Fiscus EL. 1981. Effects of abscisic acid on the hydraulic conductance of and the total ion transport through *Phaseolus* root systems. *Plant Physiol.* **68**, 169-174.

Frangne N, Maeshima M, Schaffner AR, Mandel T, Martinoia E, Bonnemain JL. 2001. Expression and distribution of a vascular aquaporin in young and mature leaf tissues of *Brassica napus* in relation to water fluxes. *Planta* **212**, 270-278.

Fray RG, Wallace A, Grierson D, Lycett GW. 1994. Nucleotide sequence and expression of a ripening and water stress-related cDNA from tomato with homology to the MIP class of membrane channel proteins. *Plant Mol. Biol.* **24**, 539- 543.

Frensch J, Hsiao TC, Steudle E. 1996. Water and solute transport along developing maize roots. *Planta* **198**, 348–355.

Frensch J, Hsiao TC. 1994. Transient responses of cell turgor and growth of maize roots as affected by changes in water potential. *Plant Physiol.* **104**, 247-254.

Frensch J, Hsiao TC. 1995. Rapid response of the yield threshold and turgor regulation during adjustment of root growth to water stress in *Zea mays*. *Plant Physiol.* **108**, 303-312.

Freundl E, Steudle E, Hartung W. 1998. Water uptake by roots of maize and sunflower affects the radial transport of abscisic acid and the ABA concentration in the xylem. *Planta* **207**, 8-19.

Freundl E, Steudle E, Hartung W. 2000. Apoplastic transport of abscisic acid through roots of maize: effect of the exodermis. *Planta* **210**, 222-231.

Frink CR, Waggoner PE, Ausubel JH. 1999. Nitrogen fertilizer: retrospect and prospect. *Proc. Natl. Acad. Sci. USA* **96**, 1175-1180.

Gao YP, Young L, Bonham-Smith P, Gusta LV. 1999. Characterization and expression of plasma and tonoplast membrane aquaporins in primed seed of Brassica napus during germination under stress conditions. *Plant Mol. Biol*. **40,** 635-644.

Gaspar M, Bousser A, Sissoëff I, Roche O, Hoarau J , Mahé A. 2003. Cloning and characterization of *ZmPIP1-5b*, an aquaporin transporting water and urea. *Plant Sci.* **165**, 21-31.

Gaxiola R, **Li JS, Undurraga S, Dang LM, Allen GJ, Alper SL, Fink GR**. 2001. Drought- and salt-tolerant plants results from overexpression of the AVP1 H^+-pump. *Proc. Natl. Acad. Sci. USA* **98**, 11444-11449.

Glinka Z. 1977. Effects of abscisic acid and of hydrostatic pressure gradients on water movement through excised sunflower roots. *Plant Physiol.* **59**, 933-935.

Glinka Z. 1980. Abscisic acid promotes both volume flow and ion release to the xylem in sunflower roots. *Plant Physiol.* **65**, 537-540.

Graham RD, Ulrich A. 1972. Potassium deficiency-induced changes in stomata behavior, leaf water potential and root permeability in *Beta vulgaris* L. *Plant Physiol.* **49**, 213-218.

Greenway H, Munns R. 1980. Mechanisms of salt tolerance in nonhalophytes. *Annu. Rev. Plant Physiol.* **31**, 149-190.

Guardia DL, Benlloch MDM. 1980. Effects of potassium and gibberellic acid on stem growth of whole sunflower plants. *Physiol. Plant.* **49**, 443–448.

Guenther JF, Chanmanivone N, Galetovic MP, Wallace IS, Cobb JA, Roberts DM. 2003. Phosphorylation of soybean nodulin 26 on serine 262 enhances water permeability and is regulated developmentally and by osmotic signals. *Plant Cell* **15**, 981-991.

Guenther JF, Roberts DM. 2000. Water-selective and multifunctional aquaporins from *Lotus japonicus* nodules. *Planta* **21**0, 741-748.

Guerrero F, Mullet JE. 1986. Increased abscisic acid biosynthesis during plant dehydration requires transcription. *Plant Physiol.* **80,** 588-591.

Guerrero FD, Jones JT, Mullet JE. 1990. Turgor-responsive gene transcription and RNA levels increase rapidly when pea shoots are wilted. Sequence and expression of three inducible genes. *Plant Mol. Biol.* **15,** 11-26.

Guiltinan MJ, Marcotte WR, and Quatrano RS. 1990. A plant leucine zipper protein that recognizes an abscisic acid response element. *Science* **250,** 267–270.

Haake V, Cook D, Riechmann JL, Pineda O, Thomashow MF, Zhang JZ. 2002. Transcription Factor CBF4 Is a Regulator of Drought Adaptation in Arabidopsis *Plant Physiol.* **130**, 639–648.

Hartung W, Zhang J, Davies WJ. 1994. Does abscisic acid play a stress physiological role in maize plants growing in heavily compacted soil? *J. Exp. Bot.* 45, 221-226.

Haschka HP, Lüttge U. 1975.Stiochiometric correlation of malate accumulation with auxin-dependent K^+/H^+ exchange and growth in *Avena* coleoptiles segments. *Plant Physiol.***56**, 696-698.

Hasewaga PM, Bressan RA, Zhu J-K, Bohnert HJ. 2000. Plant cellular and molecular response to high salinity. *Ann. Rev. Plant Physiol. Plant Mol. Biol.* **51**, 263-499.

Henzler T, Steudle E. 1995. Reversible closing of water channels in *Chara* internodes provided evidence for a composite transport model of the plasma membrane. *J. Exp. Bot*. **46**, 199–209.

Hoarau J, Barthes L, Bousser A, Deléens E, Prioul JL. 1996. Effect of nitrate on water transfer across roots of nitrogen pre-starved maize seedlings. *Planta* **200,** 405-415.

Höfte H, Hubbard L, Reizer J, Ludevid D, Herman EM, Chrispeels MJ. 1992. Vegetative and seed-specific isoforms of a putative solute transporter in the tonoplast of *Arabidopsis thaliana*. *Plant Physiol.* **99,** 561-570.

Hose E, Clarkson DT, Steudle E, Schreiber L, Hartung W. 2001.The exodermis: a variable apoplastic barrier. *J. Exp. Bot.* **52,** 2245-2264.

Hose E, Steudle E, Hartung W. 2002. Abscisic acid and hydraulic conductivity of maize roots: a study using cell- and root-pressure probes. *Planta* **211,** 874-882.

Hoth S, Morgante M, Sanchez JP, Hanafey MK, Tingey SV, Chua NH. 2002. Genome-wide gene expression profiling in Arabidopsis thaliana reveals new targets of abscisic acid and largely impaired gene regulation in the abi1-1 mutant. *J. Cell Sci.***115,** 4891-4900.

Hoyos ME, Zhang S. 2000. Calcium-independent activation of salicylic acid-induced protein kinase and a 40-kilodalton protein kinase by hyperosmotic stress. *Plant Physiol.* **122,** 1355-1363.

Hsiao TC, Allaway WG, Evans LT. 1973. Action spectra for guard cell Rb^+ uptake and stomatal opening in *Vician faba*. *Plant Physiol.* **51,** 82-88.

Hsiao TC, Läuchli A. 1986. Role of potassium in plant-water relations. pages 281-312, Chapter 8. In: Advances in Plant Nutrition, Volume 2. B. Tinker and A. Lauchli (eds.), Praeger Publishers, New York, NY. 321.

Hukin D, Doering-Saad C, Thomas CR, Pritchard J. 2002. Sensitivity of cell hydraulic conductivity to mercury is coincident with symplasmic isolation and expression of plasmalemma aquaporin genes in growing maize roots. *Planta* **215,** 1047-1056.

Jang JY, Kim DG, Kim YO, Kim JS, Kang H. 2004. An expression analysis of a gene family encoding plasma membrane aquaporins in response to abiotic stresses in Arabidopsis thaliana. *Plant Mol. Biol.* **54,** 713-725.

Jauh GY, Phillips TE, Rogers JC. 1999. Tonoplast intrinsic protein isoforms as markers for vacuolar functions. *Plant Cell* **11**, 1867–1882.

Javot H, Lauvergeat V, Santoni V, Martin-Laurent F, Güçlü J, Vinh J, Heyes J, Franck KI, Schäffner AR, Bouchez D, Maurel C. 2003. Role of a single aquaporin isoform in root water uptake. *Plant Cell* **15,** 509-522.

Javot H, Marurel C. 2002. The role of aquaporins in root water uptake. *Ann. Bot.* **90**, 301-313.

Jia W, Zhang J, Liang J. 2001. Initiation and regulation of water deficit-induced abscisic acid accumulation in maize leaves and roots: cellular volume and water relations. *J. Exp. Bot.* **52,** 295-300.

Jia WS, Wang YQ, Zhang SQ, Zhang JH. 2002. Salt-stress-induced ABA accumulation is more sensitively triggered in roots than in shoots. *J. Exp. Bot*. **53,** 2201-2206.

Johanson U, Karlsson M, Johansson I, Gustavsson S, Sjövall S, Fraysse L, Weig AR, Kjellbom P. 2001 The Complete Set of Genes Encoding Major Intrinsic Proteins in Arabidopsis Provides a Framework for a New Nomenclature for Major Intrinsic Proteins in Plants. *Plant Physiol.* **126,** 1358-1369.

Johansson I, Karlsson M, Shukkla VK, Chrispeels MJ, Larsson C, KjellbomP. 1998. Water transport activity of the plasma membrane aquaporin PM28A is regulated by phosphorylation. *Plant Cell* **10,** 451-459.

Johansson I, Larsson C, Ek B, Kjellbom P. 1996. The major integral proteins of spinach leaf plasma membranes are putative aquaporins and are phosphorylated in response to Ca^{2+} and apoplastic water potential. *Plant Cell* **8,** 1181-1191.

Jung JS, Preston GM, Smith B, Guggino WB, Agre P. 1994. Molecular structure of the water channel through aquaporin CHIP - The hourglass model. *J. Biol. Chem.* **269,** 14648-14654.

Kaldenhoff R, Grote K, Zhu JK, Zimmermann U. 1998. Significance of plasmalemma aquaporins for water-transport in *Arabidopsis thaliana. Plant J.* **14,** 121-128.

Kaldenhoff R, Kölling A, Meyers J, Karmann U, Ruppel G, Richter G. 1995. The blue light-responsive *AthH2* gene of *Arabidopsis thaliana* is primarily expressed inexpanding as well as in differentiating cells and encodes a putative channel protein of the plasmalemma. *Plant J.* **7**, 87-95.

Kaldenhoff R, Kölling A, Richter G. 1993. A novel blue light- and abscisic acid-inducible gene of *Arabidopsis thaliana* encoding an intrinsic membrane protein. *Plant Mol. Biol.* **23,** 1187-1198.

Kammerloher W, Fischer U, Piechottka GP, Schäffner AR. 1994. Water channels in the plant plasma membrane cloned by immunoselection from a mammalian expression system. *Plant J.* **6,** 187-199.

Karlsson M, Fotiadis D, Sjovall S, Johansson I, Hedfalk K, Engel A, Kjellbom P. 2003. Reconstitution of water channel function of an aquaporin overexpressed and purified from Pichia pastoris. FEBS Lett**. 537,** 68-72

Karmoker JL, Clarkson DT, Saker LR, Rooney JM, Purves JV. 1991. Sulphate deprivation depresses the transport of nitrogen to the xylem and hydraulic conductivity of barley (*Hordeum vulgare* L.) roots. *Planta* **185**, 269–278.

Karmoket JL, von Stevenick RFM. 1978. Stimulation of volume flow and ion flux by abscisisc acid in excised root systems of *Phaseolus vulgaris L. cv*. Redland Pioneer. *Planta* **141**, 37-43.

Katsuhara M, Akiyama Y, Koshio K, Shibasaka M, Kasamo K. 2002. Functional analysis of water channels in barley roots. *Plant Cell Physiol.* **43**, 885-893.

Katsuhara M, Kawasaki T. 1996. Salt stress induced nuclear and DNA degradation in meristematic cells of barley roots. *Plant Cell Physiol.* **37**, 169-173.

Katsuhara M, Shibasaka M. 2000. Cell death and growth recovery of barley after transient salt stress. *J. Plant Research* **113**, 239-243.

Katsuhara M, Koshio K, Shibasaka M, Hayashi Y, Hayakawa T, Kasamo K. 2003. Over-expression of a barley aquaporin increased the shoot/root ratio and raised salt sensitivity in transgenic rice plants. *Plant Cell Physiol.* **44,** 1378-1383.

Katsuhara M. 1997. Apoptosis-like cell death in barley roots under salt stress. *Plant Cell Physiol.* **38**, 1091-1093.

Kawasaki S, Borchert C, Deyholos M, Wang H, Brazille S, Kawai K, Galbraith D, Bohnert HJ. 2001. Gene expression profiles during the initial phase of salt stress in rice. *Plant Cell* **13**, 889-905.

Kent LM, Läuchli A. 1985. Germination and seedling growth of cotton: salinity-calcium interactions. *Plant Cell Environ.* **8**, 155-159.

Kerk D, Bulgrien J, Smith DW, Barsam B, Veretnik S,Gribskov M. 2002. The complement of protein phosphatase catalytic subunits encoded in the genome of *Arabidopsis*. *Plant Physiol.* **129,** 908–925.

Kiegle E, Moore CA, Haseloff J, Tester MA, Knight MR. 2000. Cell-type-specific calcium responses to drought, salt and cold in the *Arabidopsis* root. *Plant J.* **23,** 267-278.

Kirch HH, Vera-Estrella R, Golldack D, Quigley F, Michalowski CB, Barkla BJ, Bohnert HJ. 2000. Expression of water channel proteins in *Mesembryanthemum crystallinum. Plant Physiol.* **123**, 111-124.

Kizis D, PagesM. 2002.Maize DRE-binding proteins DBF1 and DBF2 are involved in rab17 regulation through the drought-responsive element in an ABA-dependent path-way. *Plant J.* **30,** 679-689.

Kjellbom P, Larsson C, Johansson II, Karlsson M, Johanson U. 1999. Aquaporins and water homeostasis in plants. *Trends Plant Sci.* **4**, 308-314.

Kjellbom P. 2000. An abundant TIP expressed in mature highly vacuolated cells. *Plant J.* **21**, 83-90.

Knight MR. 2000. Calcium signalling during abiotic stress in plants. *Int. Rev. Cytol.* **195,** 269-324.

Kohler B, Blatt MR. 2002. Protein phosphorylation activates the guard cell Ca^{2+} channel and is a prerequisite for gating by abscisic acid. *Plant J.* **32,** 185-94.

Kreps JA, Wu Y, Chang H-S, Zhu T, Wang X, Harper JF. 2002. Transcriptome changes for *Arabidopsis* in response to salt, osmotic, and cold stress. *Plant Physiol.* **130,** 2129-2141.

Laegreid M, Bockman OC, Kaarstad O. 1999. Agriculture, Fertilizers and the Environment. CABI, Oxon, UK.

Laemmli UK. 1970. Cleavage of structural proteins during the assembly of the head of bacteriophage T4. *Nature* **227,** 680–685.

Larsson C, Widell S, Kjellbom P. 1987. Purification of high purity plasma membranes. *Methods in Enzymology* **148**, 558–568.

Läuchli A, Pflüger R. 1979. Potassium transport through plant cell membranes and metabolic role of potassium in plants. In Potassium Research-Review and Trends, pp.111-163.

Leigh RA, Jones RGW. 1984. A hypothesis relating critical potassium concentrations for growth to the distribution and functions of this ion in the plant-cell. *New Phytol*. **97**, 1–13.

Leung J, Giraudat J. 1998. Abscisic acid signal transduction. *Annu. Rev. Plant Physiol. Plant Mol. Biol*. **49,** 199-222.

Leung J, Merlot S, Gosti F, Bertauche N, Blatt MR, Giraudat J. 1998. The role of ABI1 in abscisic acid signal transduction: from gene to cell. *Symp. Soc. Exp. Biol.* **51,** 65-71.

Li L, Li S, Tao Y, Kitagawa Y. 2000. Molecular cloning of a novel water channel from rice: its products expression in *Xenopus* oocytes and involvement in chilling tolerance. *Plant Sci.* **154,** 43–51.

Lian HL, Yu X, Ye Q, Ding XS, Kitagawa Y, Kwak SS, Su WA, Tang ZC. 2004. The Role of Aquaporin RWC3 in Drought Avoidance in Rice. *Plant Cell Physiol.* **45,** 481-489.

Ligterink W. MAP kinases in plant signal transduction: How many, and what for? In: Hirt H, editor; MAP Kinases in Plant Signal Transduction. Berlin: Springer-Verlag; 2000. p. 11–27.

Liu LH, Ludewig U, Gassert B, Frommer WB, von Wirén N. 2003. Urea Transport by Nitrogen-Regulated Tonoplast Intrinsic Proteins in Arabidopsis. *Plant Physiol.* **133,** 1220-1228.

Liu Q, Umeda M, Uchimiya H. 1994. Isolation and expression analysis of two rice genes encoding the major intrinsic protein. *Plant Mol. Biol.* **26,** 2003-2006.

Lockhart JA. 1965. Cell extension. In: Bonner J, Varner JE, eds. Plant biochemistry. New York: Academic Press, 826–849.

Lopez F, Bousser A, Sissoeff I, Gaspar M, Lachaise B, Hoarau J, Mahe A. 2003. Diurnal regulation of water transport and aquaporin gene expression in maize roots: contribution of PIP2 proteins. *Plant Cell Physiol.* **44**, 1384-95.

Lopez F, Bousser A, Sissoëff I, Hoarau J, Mahé A. 2004. Characterization in maize of ZmTIP2-3, a root-specific tonoplast intrinsic protein exhibiting aquaporin activity. *J. Exp. Bot.* **55**, 539-541.

Loqué D, Ludewig U, Yuan L, von Wirén N. 2005. Tonoplast intrinsic proteins *AtTIP2;1* and *AtTIP2;3* facilitate NH_3 transport into the vacuole**.** *Plant Physiol.* **137**, 671-680.

Ludevid D, Höfte H, Himelblau E, Chrispeels MJ. 1992. The expression pattern of the tonoplast intrinsic protein γ-TIP in *Arabidopsis thaliana* is correlated with cell enlargement. *Plant Physiol.* **100**, 1633-1639.

Lynch J, Polito VS, Läuchli A. 1989. Salinity stress increases cytoplasmic Ca^{2+} activity in maize root protoplast. *Plant Physiol.* **90**, 1271-1274.

Maathuis FJ, Filatov V, Herzyk P, Krijger GC, Axelsen KB, Chen S, Green BJ, Li Y, Madagan KL, Sanchez-Fernandez R, Forde BG, Palmgren MG, Rea PA, Williams LE, Sanders D, Amtmann A. 2003. Transcriptome analysis of root transporters reveals participation of multiple gene families in the response to cation stress. *Plant J.* **35**, 675–692.

Maeda T, Wurgler-Murphy SM, Saito H. 1994. A two-component system that regulates an osmo-sensing MAP kinase cascade in yeast. *Nature* **36**9, 242–245.

Maggio, Joly RJ. 1995. Effects of Mercuric Chloride on the Hydraulic conductivity of Tomato Root Systems. Evidence for a Channel-Mediated Water Pathway. *Plant Physiol.* **109**, 331-335.

Malz S, Sauter M. 1999. Expression of two PIP genes in rapidly growing internodes of rice is not primarily controlled by meristem activity or cell expansion. *Plant Mol. Biol.* **4**0, 985-995.

Mariaux J-B, Bockel C, Salamini F, Bartels D. 1998. Desiccation- and abscisic acid-responsive genes encoding major intrinsic proteins (MIPs) from the resurrection plant *Craterostigma plantagineum. Plant Mol. Biol.* **38**, 1089-1099.

Markhart AH, Fiscus EL, Naylor AW, KramerPJ. 1979. Effects of abscisic acid on root hydraulic conductivity. *Plant Physiol.* **64**, 611-614.

Marschner H. 1995. Mineral Nutrition of Higher Plants, Ed 2. Academic Press, London.

Martínez-Ballesta MC, Aparicio F, Pallás V, Martínez V, Carvajal M. 2003. Influence of saline stress on root hydraulic conductance and PIP expression in *Arabidopsis*. *J. Plant Physiol.* **160**, 689-697.

Martínez-Ballesta MC, Martínez V, Carvajal M. 2000. Regulation of water channel activity in whole roots and in protoplasts from roots of melon plants grown under saline conditions. *Aust. J. Plant Physiol.* **27,** 685-691.

Maser P, Hosoo Y, Goshima S, Horie T, Eckelman B, Yamada K, Yoshida K, Bakker EP, Shinmyo A, Oiki S, Schroeder JI, Uozumi N. 2002. Glycine residues in potassium channel-like selectivity filters determine potassium selectivity in four-loop-per-subunit HKT transporters from plants. *Proc. Natl. Acad. Sci. USA* **99**, 6428-6433.

Maurel C, Kada RT, Guern J, Chrispeels MJ. 1995. Phosphorylation regulates the water channel activity of the seed specific aquaporin -TIP. *EMBO J.***14,** 3028–3035.

Maurel C, Reizer J, Schroeder JI, Chrispeels MJ, Saier MH. 1994. Functional characterization of the *Escherichia coli* glycerol facilitator, GlpF, in Xenopus oocytes. *J. Biol. Chem.* **269**, 11869-11872.

Maurel C, Reizer J, Schroeder JI, Chrispeels MJ. 1993. The vacuolar membrane protein gamma TIP creates water specific channels in *Xenopus* oocytes. *EMBO J.* **12,** 2241–2247.

Maurel C, Tacnet F, Güclü J, Guern J, Pierre Ripoche P. 1997. Purified vesicles of tobacco cell vacuolar and plasma membranes exhibit dramatically different water permeability and water channel activity. *Proc. Natl. Acad. Sci. USA* **94,** 7103-7108.

Maurel C. 1997. Aquaporins and water permeability of plant membranes. *Annu. Rev. Plant Physiol. Plant Mol. Biol*. **48**, 399-429.

Mengel K, Simic R. 1973. Effect of potassium supply on the aeropetal transport of water, inorganic acid and amino acid in young decapitated sunflower plants (*Helianthus annuus*). *Physiol. Plant.* **28**, 232-236.

Mikolajczyk M, Awotunde OS, Muszynska G, Klessig DF, Dobrowolska G. 2000. Osmotic stress induces rapid activation of a salicylic acid–induced protein kinase and a homolog of protein kinase ASK1 in tobacco cells. *Plant Cell* **12,** 165–178.

Milborrow BV. 2001. The pathway of biosynthesis of abscisic acid in vascular plants: a review of the present state of knowledge of ABA biosynthesis. *J. Exp. Bot.* **52,** 1145-1164.

Mizoguchi T, Nakajima K, Hatsuzawa K, Nagahama M, Hauri HP, Tagaya M, Tani K. 2000. Determination of functional regions of p125, a novel mammalian Sec23p-interacting protein. *Biochem. Biophys. Res. Commun*. **279,** 144-149.

Mizoguchi T. 1997. Environmental stress response in plants - the role of mitogen-activated protein kinases. *Trends Biotech*. **15,** 15-19.

Morillon R, Chrispeels MJ. 2001. The role of ABA and the transpiration stream in the regulation of the osmotic water permeability of leaf cells. *Proc. Natl. Acad. Sci. USA* **98,** 14138–14143.

Morillon R, Lassalles JP. 2002. Water deficit during root development: effects on the growth of roots and osmotic water permeability of isolated root protoplasts. *Planta* **214,** 392-399.

Moshelion M, Becker D, Biela A, Uehlein N, Hedrich R, Otto B, Levi H, Moran N, Kaldenhoff R. 2002. Plasma membrane aquaporins in the motor cells of Samanea saman: diurnal and circadian regulation. *Plant Cell* **14,** 727-739.

Munnik T, Ligterink W, Meskiene I, Calderini O, Beyerly J, Musgrave A, Hirt H. 1999. Distinct osmo-sensing protein kinase pathways are involved in signalling moderate and severe hyper-osmotic stress. *Plant J.* **20,** 381-388.

Munns R, Sharp RE. 1993. Involvement of abscisic acid in controlling plant growth in soils of low water potential. *Aust. J. Plant Physiol.* **20**, 425–437.

Munns R. 2002. Comparative physiology of salt and water stress. *Plant Cell Environ*. **25**, 239-250.

Munns R, Tonnet ML, Shennan C, Gardner PA. 1988. Effect of high external NaCl concentrations on ion transport within the shoot of *Lupinus albus*. II. Ions in phloem sap. *Plant Cell and Environ.* **11**, 291–300.

Murata K, Mitsuoka K, Hirai T, Walz T, Agre P. 2000. Structural determinants of water permeation through aquaporin-1. *Nature* **407,** 599–605.

Nakagawa H, Ohmiya K, Hattori TA. 1996. Rice bZIP protein, designated OSBZ8, is rapidly induced by abscisic acid. *Plant J*. **9,** 217-227.

Nakhoul NL, Davis BA, Romero MF, Boron WF. 1998. Effect of expressing the water channel aquaporin-1 on the CO_2 permeability of *Xenopus* oocytes. *Am. J. Physiol. Cell Physiol.* **43**, 543–548.

Neuhaus JM, Rogers JC. 1998. Sorting of proteins to vacuoles in plant cells. *Plant Mol. Biol.* **38,** 127-144.

Neumann PM, Azaizeh H, Leon D. 1994. Hardening of root cell walls: a growth inhibitory response to salinity stress. *Plant Cell Environ.* **17,** 303-309.

Nielsen S, Chou C, Marples D, Christensen EI, Kishore BK, Knepper MA. 1995. Vasopressin increases water permeability of kidney collecting duct by inducing translocation of aquaporin-CD water channels to plasma membrane. *Proc. Natl. Acad. Sci. USA* **92**, 1013-1017.

Niemietz CM, Tyerman SD. 1997. Characterization of water channels in wheat root membrane vesicles. *Plant Physiol.* **115,** 561-567.

Niemietz CM, Tyerman SD. 2000. Channel-mediated permeation of ammonia gas through the peribacteroid membrane of soybean nodules. *FEBS Lett.* **25**, 110–114.

North GB, Martre P, Nobel PS. 2004. Aquaporins account for variations in hydraulic conductance for metabolically active root regions of Agave deserti in wet, dry, and rewetted soil. *Plant Cell Environ.* **27**, 219-228.

O' Brien M, Bertrand C, Matton DP. 2002. Characterization of a fertilization-induced and developmentally-regulated plasma-membrane aquaporin expressed in reproductive tissues, in the wild potato *Solanum chacoense. Planta* **215,** 485-493.

O' Brien M, Kapfer C, Major G, Laurin M, Bertrand C, Kondo K, Kowyama Y, Matton DP. 2002. Molecular analysis of the stylar-expressed *Solanum chacoense* small asparagine-rich protein family related to the HT modifier of gametophytic self-incompatibility in *Nicotiana*. *Plant J.* **32,** 985-996.

Ober ES, Sharp RE. 2003. Electrophysiological responses of maize roots to low water potentials: relationship to growth and ABA accumulation. *J. Exp. Bot*. **54,** 813-824.

Oeda K, Salinas J, Chua NH. 1991. A tobacco bZip transcription activator (TAF-1) binds to a G-box-like motif conserved in plant genes. *EMBO J.* **10,** 1793-1802.

Okhuma K, Lyon JL, Addicott FT, Smith OE. 1963. Abscisin II, an abscission accelerating substance from young cotton fruit. *Science* **142**, 1592–1593.

Passioura J.B. 1988. Root signals control leaf expansion in wheat seedlings growing in drying soil. *Aust. J. Plant Physiol.* **15**, 687–693.

Passioura JB, Fry SC. 1992. Turgor and cell expansion beyond the Lockhart equation. *Aust. J. Plant Physiol*. **19,** 565-576.

Passioura JB, Munns R. 2000. Rapid environmental changes that affect leaf water status induce transient surges or pauses in leaf expansion rate. *Aust. J. Plant Physiol.* **27**, 941–948.

Peaslee DE, Moss DN. 1968. Stomatal conductivities in K-deficient leave of Maize (Zey mays L.). *Crop Science* **8,** 427-430.

Peaslee, DE, Moss DN. 1996. Photosynthesis in K- and Mg-deficient maize (Zea mays L.) leaves. *Soil Sci. Soc. Am. Proc.* **30,** 220-223.

Peuke AD, Jeschke WD, Hartung W. 1994. The uptake and flow of C, N and ions between roots and shoots in *Ricinus communis* L. III. Long distance transport of abscisic acid depending on nitrogen nutrition and salt stress. *J. Exp. Bot.* **45,** 741–747.

Pfaffl MW. 2001. A new mathematical model for relative quantification in real-time RT-PCR. *Nucleic Acids Res.* **29,** 2002-2007.

Phillips AL, Huttly AK. 1994. Cloning of two gibberellin-regulated cDNAs from *A. thaliana* by subtractive hybridization: expression of the tonoplast water channel γ-TIP is increased by GA3. *Plant Mol. Biol.* **24,** 603-615.

Pissarek HP. 1973. The development of potassium deficiency symptoms in summer rape. Z. *Pflanzenernährg. Bodenkunde* **136,** 1-96.

Plieth C, Hansen UP, Knight H, Knight MR. 1999. Temperature sensing by plants: the primary characteristics of signal perception and calcium response. *Plant J.* **18,** 491-497.

Prasad GV, Coury LA, Finn F, Zeidel ML. 1998. Reconstituted aquaporin 1 water channels transport CO_2 across membranes. *J. Biol. Chem.* **273**, 33123-33126.

Precht VM, Kraft M. 1993. Biostatitik 2. P11. R.Oldenbourg Verlag GmbH München.

Preston G, Jung SJ, Guggino WB, Agre P. 1994. Membrane topology of Aquaporin CHIP: analysis of functional epitope-scanning mutants by vectorial proteolysis. *J. Biol. Chem.* **269,** 1668-1673.

Preston GM, Jung JS, Guggino WB, Agre P. 1993. The mercury-sensitive residue at cysteine-189 in the CHIP28 water channel. *J.Biol.Chem.* **268,** 17-20.

Preston GM, Piazza-Carroll T, Guggino WB, Agre P. 1992. Appearance of osmotic water channels in *Xenopus* oocytes. *Science* **256,** 385-387.

Qiu QS, Guo Y, Dietrich MA, Schumaker KS, Zhu JK. 2002. Regulation of SOS1, a plasma membrane Na^+/H^+ exchanger in Arabidopsis thaliana, by SOS2 and SOS3. *Proc. Natl. Acad. Sci. USA* **99,** 8436-8441.

Quigley F, Rosenberg JM, Shachar-HillY, Bohnert HJ. 2001. From genome to function: the *Arabidopsis* aquaporins. *Genome Biol.* **3,** 1-17.

Quintero FJ, Ohta M, Shi HZ, Zhu JK, Pardo JM. 2002. Reconstitution in yeast of the Arabidopsis SOS signaling pathway for Na^+ homeostasis. *Proc. Natl. Acad. Sci. USA* **99,** 9061-9066.

Quintero JM, Fournier JM, Ramos J, Benlloch M. 1998. K^+ status and ABA affect both exudation rate and hydraulic conductivity in sunflower roots. *Physiol. Plant.* **102,** 279-284.

Radin JW, Ackerson RC. 1981. Water relation of cotton plants under nitrogen deficiency. *Plant Physiol.* **67,** 115-119.

Radin JW, Eidenbock MP. 1984. Hydraulic conductance as a factor limiting leaf expansion of phophorus-deficient cotton seedlings. *Plant Physiol.* **75,** 372-377.

Radin JW, Matthews MA. 1989. Water transport properties of cortical cells in roots of nitrogen- and phosphorus-deficient cotton seedlings. *Plant Physiol.* **89**, 264–268.

Radin JW. 1990. Responses of transpiration and hydraulic conductance to root temperature in nitrogen- and phosphorus-deficient cotton seedlings. *Plant Physiol.* **92**, 855–857.

Reisen D, Leborgne-Castel N, Ozalp C, Chaumont F, Marty F. 2003. Expression of a cauliflower tonoplast aquaporin tagged with GFP in tobacco suspension cells correlates with an increase in cell size. *Plant Mol. Biol.* **52,** 387-400.

Rhoades JD, Loveday J. 1990. Salinity in the irrigated agriculture in American society of civil engineer, irrigation of agriculture crops (Steward BA and Nielson DR.eds. Am. Soc. Agronomists, Monograph **30,** 1089-1142.

Robinson D. 1994. Tansley Review no. 73. The responses of plants to non-uniform supplies of nutrients. *New Phytol.* **127,** 635-674.

Robinson DG, Sieber H, Kammerloher W, Schäffner AR. 1996. PIP1 aquaporins are concentrated in plasmalemmasomes of *Arabidopsis thaliana* mesophyll. *Plant Physiol.* **111,** 645-649.

Rock CD, Zeevaart JAD. 1991. The aba Mutant of Arabidopsis thaliana is Impaired in Epoxy-Carotenoid Biosynthesis. *Proc. Natl. Acad. Sci. USA* **88,** 7496-7499.

Rock CD. 2000. Pathway to abscisic acid-regulated gene expression. *New Physiologist* **148,** 157-396.

Rodriguez HG, Roberts JKM, Jordan WR, Drew MC. 1997. Growth, Water Relations and Accumulation of Organic and Inorganic Solutes in Roots of Maize Seedlings during Salt Stress. *Plant Physiol.* **113,** 881-893.

Rubio F, Gassmann W, Schroeder JI. 1995. Sodium-driven potassium uptake by the plant potassium transporter HKT1 and mutations conferring salt tolerance *Science* **270,** 1660-1663.

Rus A, Yokoi S, Sharkhuu A, Byeong-ha Lee MR, Matsumoto TK, Koiwa H, Zhu JK, Bressan RA, Hasegawa PM. 2001. AtHKT1 is a salt tolerance determinant that controls Na^+ entry into plant roots. *Proc. Natl. Acad. Sci. USA* **98,** 14150-14155.

Ruth R. **Finkelstein, Lynch TJ**. 2000. The *Arabidopsis* abscisic acid response gene *ABI5* encodes a basic leucine zipper transcription factor. *Plant Cell* **12,** 599-610.

Salim M, Pitman MG. 1984. Water and solute flow through mung bean roots under applied pressure. *Physiol. Plant.* **61**, 263-270.

Salim M, Pitman MG. 1984. Pressure–induced water and solute flow through plants roots. *J. Exp. Bot*. **35,** 869-881.

Sarda X, Tousch D, Ferrare K, Legrand E, Dupuis JM, Casse-Delbart F, Lamaze T. 1997. Two TIP-like genes encoding aquaporins are expressed in sunflower guard cells. *Plant J*. **12**, 1103-1111.

Schachtman DP, Bloom AJ, Dvorak J. 1989. Salt-tolerant *Triticum lophopyrum* derivatives limit the accumulation of sodium and chloride ions under saline-stress. *Plant Cell Environ.* **12**, 47–55.

Schachtman DP, Kumar R, Schroeder JI, Marsh EL. 1997. Molecular and functional characterisation of a novel low-affinity cat-ion transporter (LCT1) in higher plants. *Proc. Natl. Acad. Sci. USA* **94,** 11079–11084.

Schachtman DP, Munns R. 1992. Sodium accumulation in leaves of *Triticum* species that differ in salt tolerance. *Aust. J. Plant Physiol.* **19**, 331–340.

Schiefelbein JW, Somerville C. 1990. Genetic control of root hair development in *Arabidopsis thaliana*. *Plant Cell* **2**, 235-243.

Schraut D, Heilmeier H, Hartung W. 2005. Radial transport of water and abscisic acid (ABA) in roots of zea mays under condition of nutrient deficiency. *J. Exp. Bot.* **57**, 1-8.

Schroeder JI, Allen GJ, Hugouvieux V, Kwak JM, Waner D. 2001. Guard Cell Signal Transduction. *Annu. Rev. Plant Physiol. Plant Mol. Biol.* **52**, 627-658.

Seki M, Narusaka M, Ishida J, Nanjo T, Fujita M, Oono Y, Kamiya A, Nakajima M, Enju A, Sakurai T, Satou M, Akiyama K, Taji T, Yamaguchi-Shinozaki K, Carninci P, Kawai J, Hayashizaki Y, Shinozaki K. 2002. Monitoring the expression of 7000 *Arabidopsis* genes under drought, cold and high-salinity stresses using a full-length cDNA microarray. *Plant J.* **31**, 279-292.

Seki M, Narusawa M, Abe H, Kasuga M, Y-Shinozaki K, Carninci P, Hayashizaki Y, Shinozaki K. 2001. Monitering the expression pattern of 1300 *Arabidopsis* genes under drought and cold stresses by using a full-length cDNA microarray. *Plant Cell* **13**, 61-72.

Sharp RE, Wu Y, Voetberg GS, Saab IN, LeNoble ME. 1994. Confirmation that abscisic acid accumulation is required for maize primary root elongation at low water potentials. *J. Exp. Bot.* **45**, 1743-1751.

Sheen J. 1996. Ca^{2+}-dependent protein kinases and stress signal transduction in plants. *Science* **274**, 1900-1902.

Shi H, Ishitani M, Kim C, Zhu JK. **2000**. The *Arabidopsis thaliana* salt tolerance gene *SOS1* encodes a putative Na^+/H^+ antiporter. *Proc. Natl. Acad. Sci. USA* **97,** 6896-6901.

Siefritz F, Tyree MT, Lovisolo C, Schubert A, Kaldenhoff R. 2002. PIP1 plasma membrane aquaporins in tobacco: from cellular effects to function in plants. *Plant Cell* **14**, 869-876.

Steudle E, Henzler T. **1995**. Water channels in plants: do basic concepts of water transport change? *J. Exp. Bot.* **46**, 1067-1076.

Steudle E, Murrmann M, Peterson CA. 1993. Transport of water and solutes across maize roots modified by puncturing the endodermis. Further evidence for the composite transport model of the root. *Plant Physiol.* **103**, 335-349.

Steudle E. 1993. Pressure probe techniques: basic principles and application to studies of water and solute relations at the cell, tissue, and organ level. In: *Water deficits: Plant responses from cell to community* (Smith, J.A.C. and Griffiths, H., eds), Bios Scientific Publishers Ltd., Oxford, UK, 5-36.

Steudle E. 1994 Water transport across roots. *Plant Soil* **167**, 79-90.

Steudle E. 1995. Trees under tension. *Nature* **378**, 663-664.

Steudle E. 2000. Water uptake by plant roots: an integration of views. *Plant Soil* **226**, 45-56.

Steudle E. 2001. The cohesion-tension mechanism and the acquisition of water by plant roots. *Annu. Rev. Plant Physiol. Plant Mol. Biol.* **52**, 847-875.

Steudle E. **Peterson CA**. 1998. How does water get through roots? *J. Exp. Bot.* **49**, 775-788.

Suga S, Imagawa S, Maeshima M. 2001. Specificity of the accumulation of mRNAs and proteins of the plasma membrane and tonoplast aquaporins in radish organs. *Planta* **212**, 294–304.

Suga S, Komatsu S, Maeshima M. 2002. Aquaporin isoforms responsive to salt and water stresses and phytohormones in radish seedlings. *Plant Cell Physiol.* **43**, 1229–1237.

Suga S, Murai M, Kuwagata T, Maeshima M. 2003. Differences in aquaporin levels among cell types of radish and measurement of osmotic water permeability of individual protoplasts. *Plant Cell Physiol.* **44**, 277–286.

Sun MH, XU W, Zhu YF, Su WA, Tang ZC. 2001. A simple method for *In Situ* hybridization to RNA in guard cells of *Vicia Faba* L.: The expression of aquaporins in guard cells *Plant Mol. Biol. Rep.* **19**, 129–135.

Tallman G, Zeiger E. 1988. Light quality and osmoregulation in *Vicia* guard cells. Evidence for involvement on three metabolic pathways. *Plant Physiol.* **88**, 887-895.

Tallman G. 2004. Are diurnal patterns of stomatal movement the result of alternating metabolism of endogenous guard cell ABA and accumulation of ABA delivered to the apoplast around guard cells by transpiration? *J. Exp. Bot.* **55**, 1963-1976.

Tan BC, Schwartz SH, Zeevaart JAD, McCarty DR. 1997. Genetic control of abscisic acid biosynthesis in maize. *Proc. Natl. Acad. Sci. USA* **94**, 12235-12240.

Taylor IB, Burbidge A, Thompson AJ. 2000. Control of abscisic acid synthesis. *J. Exp. Bot.* **51**, 1563-1574.

Tester M, Davenport R. 2003. Na^+ tolerance and Na^+ transport in higher plants. *Ann. Bot. (Lond).* **91**, 503-527.

Tester M, Leigh RA. 2001. Patitioning of transport process in roots. *J. Exp. Bot.* **52**, 445-457.

Thimm O, Essigmann B, Kloska S, Altmann T, Buckhout TJ. 2001. Response of *Arabidopsis* to iron deficiency stress as revealed by microarray analysis. *Plant Physiol.* **127,** 1030-1043.

Thompson´AJ, Jackson AC, Symonds RC, Mulholland BJ, Dadswell AR, Blake PS, Burbidge A, Taylor IB. 2000. Ectopic expression of a tomato 9-*cis*-epoxycarotenoid dioxygenase gene causes over-production of abscisic acid. *Plant J.* **23**, 363-374.

Uehlein N, Lovisolo C, Siefritz F, Kaldenhoff R. 2003. The tobacco aquaporin NtAQP1 is a membrane CO_2 pore with physiological functions. *Nature* **425**, 734-737.

Uno Y, Furihata T, Abe H, Yoshida R, Shinozaki K, Yamaguchi-Shinozaki K. 2000. *Arabidopsis* basic leucine zipper transcription factors involved in an abscisic acid-dependent signal transduction pathway under drought and high-salinity conditions. *Proc. Natl. Acad. Sci. US* **97**, 11632-11637.

Uozumi N, Kim EJ, Rubio F, Yamaguchi T, Muto S, Tsuboi A, Bakker EP, Nakamura T, Schroeder JI. 2000. The *Arabidopsis HKT1* gene homolog mediates inward Na^+ currents in *Xenopus laevis* oocytes and Na^+ uptake in *Saccharomyces cerevisiae*. *Plant Physiol.* **122**, 1249-1259

Urao T, Yakubov B, Satoh R, Yamaguchi-Shinozaki K, Seki M, Hirayama T, Shinozaki K. **1999**. A Transmembrane Hybrid-Type Histidine Kinase in Arabidopsis Functions as an Osmosensor. *Plant Cell* **11**, 1743-1754.

Urao T, Yakubov B, Yamaguchi-Shinozaki K, and Shinozaki K. 1998. Stress-responsive expression of genes for two-component response regulator-like proteins in *Arabidopsis thaliana*. *FEBS Lett.* **427**, 175-178.

Van Steveninck RFM, Van Stevenick ME, Läuchli A. 1988. The effect of abscisic acid and K^+ on xylem exudation from excised roots of *Lupinus luteus*. *Physiol. Plant.* **72**, 1-7.

Vera-Estrella R, Barkla BJ, Bohnert HJ, Pantoja O. 2004. Novel regulation of aquaporins during osmotic stress. *Plant Physiol.* **135**, 2318-2329

Wan XC, Zwiazek JJ. **1999**. Mercuric Chloride Effects on Root Water Transport in Aspen Seedlings. *Plant Physiol.* **121**, 939-946.

Wang H, Miyazaki S, Kawai K, Deyholos M, Galbraith D, Bohnert H. 2003. Temporal progression of gene expression responses to salt shock in maize roots. *Plant Mol. Biol.* **52**, 873-891.

Wang H, Qungang Q, Schorr P, Cutler AJ, Crosby WL, Fowke LC. 1998. ICK1, a cyclin-dependent protein kinase inhibitor from *Arabidopsis thaliana* interacts with both Cdc2a and CycD3 and its expression is induced by abscisic acid. *Plant J.* **15,** 501-510.

Wang J, Wu WS, Zuo KJ, Fei J, Sun XF, Lin J, Li XF, Tang KX. 2004. Isolation and characterization of a serine/thereonine protein kinase SOS2 gene from *Brassica napus. Cell. Mol. Biol. Lett.* **9**, 465–473.

Wang RC, Guegler K, Labrie ST, Crawford NM. 2000. Genomic analysis of a nutrient response in *Arabidopsis* reveals diverse expression patterns and novel metabolic and potential pegulatory genes induced by nitrate. *Plant Cell* **12,** 1491-1509.

Wang YH, Garvin D, Kochian L. 2001b. Nitrate-induced genes in tomato roots. array analysis reveals novel genes that may play a role in nitrogen nutrition. *Plant Physiol.* **127**, 345-359.

Wang Y-H, Garvin D, Kochian L. 2002. Rapid induction of regulatory and transporter genes in response to phosphorus, potassium, and iron deficiencies in tomato roots. evidence for cross talk and root/rhizosphere-mediated signals *Plant Physiol.* **130**, 1361-1370.

Wang, XQ, Ullah H, Jones AM, Assmann SM. 2001a. G protein regulation of ion channels and abscisic acid signaling in *Arabidopsis* guard cells. *Science* **292,** 2070-2072.

Weig A, Deswarte C, Chrispeels MJ. 1997. Major intrinsic protein family of arabidopsis has 23 members that form three distinct groups with functional aquaporins in each group. *Plant Physiol.* **114,** 1347-1357.

Weig AR, Jakob C. 2000. Functional characterisation of *Arabidopsis thaliana* aquaglyceroporins. In: *Molecular Biology and Physiology of Water and Solute Transport* (Hohmann, S. and Nielsen, S., eds), Kluwer Academic/Plenum Publishers, New York, pp 365-372.

Weig AR, Jakob C. 2000. Functional identification of the glycerol permease activity of *Arabidopsis thaliana* NLM1 and NLM2 proteins by heterologous expression in *Saccharomyces cerevisia*e. *FEBS Lett.* **48**1, 293-298.

Werner M, Uehlein N, Proksch P, Kaldenhoff R. 2001. Characterization of two tomato aquaporins and expression during the incompatible interaction of tomato with the plant parasite Cuscuta reflexa. *Planta* **213**, 550-555.

Whittembury G, Gonzalez E, Gutierrez AM, Echevarria M, Hernandez CS. 1997. Length of the selectivity filter of aquaporin-1. *Biol. Cell* **89**, 299-306.

Wu Y , Kuzma J, Maréchal E, Graeff R, Lee HC, Foster R, Chua NH. 1997. Abscisic acid signaling through cyclic ADP-ribose in plants. *Science* **278**, 2126-2130.

Xiong L, **Schumaker KS, Zhu JK**. 2002. Cell signaling during cold, drought, and salt stress. *Plant Cell* **14**, 165-183.

Xiong L, Zhu JK. 2001. Abiotic stress signal transduction in plants: Molecular and genetic perspectives. *Physiol. Plant.* **112**, 152-166.

Xiong L, Zhu JK. 2002. Molecular and genetic aspects of plant responses to osmotic stress. *Plant, Cell Environ.* **25**, 131-139.

Xu W, Bak S, Decker A, Paquette SM, Feyereisen R, Galbraith DW. 2001. Microarray-based analysis of gene expression in very large gene families: the cytochrome P450 gene superfamily of *Arabidopsis thaliana*. *Gene* **272**, 61-74

Yamada S, Bohnert HJ. 2000. Expression of a PIP aquaporin from the common ice plant in tobacco. *Plant Cell Physiol*. **41,** 719-725.

Yamada S, Katsuhara M, Kelly W, Michalowski CB, Bohnert HJ. 1995. A family of transcripts encoding water channel proteins: Tissue specific expression in the common ice plant. *Plant Cell* **7,** 1129-1142.

Yamada S, Katsuhara M, Kelly WB, Michalowski CB, Bohnert HJ. 1995. A family of transcripts encoding water channel proteins: tissue-specific expression in the common ice plant. *Plant Cell* **7,** 1129-1142.

Yamada S, Komori T, Myers PN, Kuwata S, Kubo T, Imaseki H. 1997. Expression of plasma membrane water channel genes under water stress in *Nicotiana excelsior*. *Plant Cell Physiol.* **3**8, 1226-1231.

Yamada S, Nelson D, Ley E, Marquez S, Bohnert HJ. 1997. The expression of an Aquaporin promoter from *Mesembryanthemum* c*rystallinum* in tobacco. *Plant Cell Physiol.* **38**, 1326-1332.

Yamcey Ph, Clark ME, Hang SC, Bowlus RD, Someno GN. 1982. Living with water stress: evolution of osmolyte system. *Science* **217**, 1214-1222.

Yeo AR, Flowers S. **A, Rao G, Welfare K, Senanayake N, Flowers T**. 1999. Silicon reduces sodium uptake in rice (Oryza sativa L.) in saline conditions and this is accounted for by a reduction in the transpirational bypass flow. *Plant Cell Environ.* **22**, 559-565.

Yokoi S, Quintero FJ, Cuber B, Ruiz MT, Bressan RA, Hasegawa PM, Pardo JM. 2002. Differential expression and function of Arabidopsis thaliana NHX Na^+/H^+ antiporters in the salt stress response. *Plant J*. **30,** 529-539.

Zhu JK. 2002. Salt and drought stress signal transduction in plants. *Annu. Rev. Plant Biol.* **53**, 247-273.

Zidan I, Azaizeh H, Neumann PM. 1990. Does salinity reduce growth in maize root epidermal cells by inhibiting their capacity for cell wall acidification? *Plant Physiol.* **93**, 7-11.

G. SUPPLEMENT

1. Oligonucleotide

1.1. Oligonucleotides for semi-quantitative RT-PCR

Name of genes	Accessory number	Forward-primer	Reverse-primer
ZmPIP1-1	X82633	CCTCGTCTACTGCACCGC	GAATTACAAGTCTGGGTTCGG
ZmPIP1-2	AF131201	CCTCGTCTACTGCACCGC	ACGCCCGTTCTTCGGACTG
ZmPIP1-3	AF131201	GGTTCGCGGTGTTCCTGG	TTAGTTATAAACCCACGTTTCC
ZmPIP1-5	AF326489	TCATGCAGTGCCTGGGC	CTGATGGCTAGCTGAACTGG
ZmPIP1-6	AF326490	TCATGCAGTGCCTGGGC	CGGAGTGATGGTCCATTGAG
ZmPIP2-1	AF326491	CGCCGAGATCATCGGCAC	GATTACATTGCAGGGGAACGAAAC
ZmPIP2-3	AF326493	CGCCGAGATCATCGGCAC	ATCACACTTTTTTTCCCCGTCAAGG
ZmPIP2-4	AF326494	GCAGAGCGCCTACTACGTG	TCCGAAGTAGAAAACAGCAGG
ZmPIP2-5	AF130975	CGCCGAGATCATCGGCAC	TGGCTAGAGGCAACCAACGAC
ZmPIP2-6	AF326495	CGCCGAGATCATCGGCAC	GGACACACAGACGCTGACC

Name of gene	Accessory number	Forward-primer	Reverse-primer
Beta 4 Tublin	X74655.1	CCAAGAACATGATGTGCG	GTGTACCAGTGCAAGAAAGC
Actin1(MAc1)	J01238	TTGTCAGGGACATAAAGGAG	AGGCATCTCGTAGCTCTTCT
Paw109		GTGTCTGAATCAGAAATCCT TCTATC	CATGTCAAATTTCACTGCTT CATCC
Rab17	X15994	GAAGGAAACGTAGCAGCATA	GAAGAAGGGAATCAAGGAGA
DBF1	AF493800	ACAGACCAGTACACCAATGC	CGACAGATGTGCTGTTGTAG

1.2. Oligonucleotides for control genes on MIPs DNA Array

Root expressed control genes and target sequences used for the *ZmMIP* array. Forward and reverse primers were used for amplification of target sequences of control genes expressed in the roots. Sequences were retrieved from TIGR database (http://www.tigr.org/tdb/tgi/zmgi/searching/ xpress_search.html).

Nr.	Accessory number.	Forward-primer	Reverse-primer
1	TC74462	CTCAGCCATCTACCACTACG	GGCAAGTTTGCTAATGGTTA
2	TC77795	ACTAACCAACGAGAGTGCAA	TTTGGTTGACCAAGAAGAGA
3	TC78020	ACAATGGACTGCACAATCTC	TACGCTTGTCTAGGACCAAA
4	TC71186	TCTGTTGCTTGTCCATCTTT	TTTCAGGGTTTTCCTAGCTC
5	TC74745	CATAGCATAGCTCCATTTGC	CGTGGTTCTGATCTTTTCTG
6	TC78183	ACTTTGTGTCGAGCATTTGT	AGGATGGATTATGGAGCAGT
7	TC11294	AAAGCACAAAACCTTGGACT	TACCAAAGCTGAACAAGGAA
8	TC71521	CGTTGTCTGATACACCCATT	AAAGTTCCAGAGGTCAAACC
9	TC71289	CATCGTGTGCAGATTACAGA	ATGCAGGAGTTCTTTGTTGA
10	TC71588	GGAAGGGTAACACATTCCTC	TTCTTCTGGGTGAGAAACAA
11	TC71118	CATACCCTCCACAACTTCAA	CAAAGTGACAATGGGTCCTA
12	TC68822	GTTTGGATGTTTGCGAATAG	GTTTGGATGTTTGCGAATAG
13	TC69252	TCAGGTGAGACACTTGGTTC	TCAAATTTCATGCCTTCTTG
14	TC69312	AAGAATCTATGCACCCGACT	TTTCTGAAATTTGTGGCTTG
15	TC71172	CCTCATAATACCGTCCATGA	ATTGCCCATCAGATTACACA
16	TC74278	TTCTAGTTGCGATTCTTGGA	GAAAGAAGGTAGCGGAAGAG
17	TC74471	CTGTGGAGGCACTACTTTCA	TATCGACCCAAAAACAAAAA
18	TC71084	GAATGTTGAGGCTACTGTGG	TCCTTCTCCTCCTTTTTGAC

19	TC71311-1	CCCCTTCGTATTTGGTACTC	AGAGTGAGACACAAATTGCAC
20	AF213455	TTGGAGACATGGAGCTTAAA	AAAGGCTTTCCTCTGTGTTT

1.3. Oligonucleotides for amplification of probes for *in-situ* hybridization

Name of genes	Name of probes	Forward-primer	Reverse-primer
ZmPIP1-1	Antisensense probe	gtaatacgactcactataggg ttacgtggagttccattcc	tgaactcttaaagcttgactcg
	Sense-probe	gttacgtggagttccattcc	gtaatacgactcactataggt gaactcttaaagcttgactcg
ZmPIP2-6	Antisensense probe	gtaatacgactcactatagg gctttcattcaggtcaagtg	ttgcattcgtccatctttat
	Sense-probe	gctttcattcaggtcaagtg	gtaatacgactcactatagg ttgcattcgtccatctttat
ZmPIP2-4	Antisensense probe	gtaatacgactcactatagg tcgctgctgttttctacttc	gtgatcggataaaaactcacg
	Sense-probe	tcgctgctgttttctacttc	gtaatacgactcactatagg gtgatcggataaaaactcacg
ZmTIP1-1	Antisensense probe	gtaatacgactcactatagg atgcatcgtcgactgtctc	aggcaaatgcacaaatctta
	Sense-probe	atgcatcgtcgactgtctc	gtaatacgactcactatagg aggcaaatgcacaaatctta

1.4. Oligonucleotides for amplification of antigen-coding fragments

Names of epitopes	Forward-primer	Reverse primer
epi_1_PIP2-4	GGGGACAAGTTTGTACAAAAA AGCAGGCTCCATGGCGAAGGA CATCG	GGGGACCACTTTGTACAAGAAAGC TGGG TCTACTTGGCCGAGAACTCG
epi_2_PIP2-4	GGGGACAAGTTTGTACAAAAA AGCAGGCTCCGGGTACAAGCA CCAGAC	GGGGACCACTTTGTACAAGAAAGC TGGG TCTAGCCGCACGCCGC
epi_3_PIP2-4	GGGGACAAGTTTGTACAAAAA AGCAGGCTCCTACGTGCTGAGG GCCA	GGGGACCACTTTGTACAAGAAAGC TGGG TTTAGGCGTTGCTCCG

1.5. The oligonucleotides of spiking control genes

Name	Annotation	Accession number	Primer	Sequence
Sp1	B-cell receptor-associated protein	AF126021	Sp1-F	CAATTAACCCTCACTAAAGGG CGCGAATCTGTGTTCACC
			Sp1-R	TTTTTTTTTTTTTTTTTTTTT AATGGACGGCAACACTCG
Sp3	Myosin light chain 2	M21812	Sp3-F	CAATTAACCCTCACTAAAGGG TCGGGGAGAAGCTCAAGGG
			Sp3-R	TTTTTTTTTTTTTTTTTTTTT AGGTCGGGCCGAACAGAAG
Sp4	Insulin-like growth factor II	X07868	Sp4-F	CAATTAACCCTCACTAAAGGG GATGCCATAGCAGCCACC
			Sp4-R	TTTTTTTTTTTTTTTTTTTTT CAGGCCAATGTGGGTTCC

1.6. General primers for amplification of target sequences.

Vector	primer	Sequences
pGEM˙-T Easy	M13 (22)-f	TCACGACGTTGTAAAACGACGG
pGEM˙-T Easy	M13 (25)-r	AAACAGCTATGACCATGATTACGCC
pGEM˙-T Easy	SP6	TATTTAGGTGACACTATAG
pGEM˙-T Easy	T7	TAATACGACTCACTATAGGG

2. DNA array

2.1. The expression of *ZmMIPs* in the different zones of maize primary roots.

Expression analysis of *ZmMIP*s in longitudinal zones of maize primary roots by DNA array. Total RNA were isolated from zone 0-3 mm (A), 3-10 mm (B), 10-20 mm (C), 20-50 mm (D), 50-60 mm (E). The gene activity of *ZmMIP*s was assayed by DNA array. Three independent experiments were performed, Sd, the standard deviation of the mean; n.d, not detected.

Name of genes	A	sd	B	sd	C	sd	D	sd	E	sd
ZmPIP1-1	**1.27**	0.16	**6.27**	1.17	**6.93**	1.66	**4.84**	0.62	**2.80**	1.00
ZmPIP1-2	**0.14**	0.02	**0.92**	0.24	**1.70**	0.22	**0.74**	0.22	**0.40**	0.14
ZmPIP1-3	**0.14**	0.10	**0.17**	0.02	**0.26**	0.04	**0.17**	0.04	**0.16**	0.02
ZmPIP1-5	**0.16**	0.01	**3.62**	0.99	**7.10**	1.06	**5.16**	0.25	**3.20**	0.91
ZmPIP1-6	**n.d**	n.d	**n.d**	n.d	**n.d**	n.d	**n.d**	n.d	**n.d**	n.d
ZmPIP2-1	**0.61**	0.10	**3.91**	0.04	**4.00**	0.99	**2.68**	0.74	**1.71**	0.91
ZmPIP2-2	**0.25**	0.08	**0.98**	0.40	**1.02**	0.09	**0.71**	0.19	**0.24**	0.10
ZmPIP2-3	**n.d**	n.d	**n.d**	n.d	**n.d**	n.d	**n.d**	n.d	**n.d**	n.d
ZmPIP2-4	**0.08**	0.03	**1.17**	0.14	**2.26**	0.56	**0.86**	0.36	**0.64**	0.20
ZmPIP2-5	**0.07**	0.03	**1.12**	0.36	**2.11**	0.43	**1.54**	0.12	**1.27**	0.34
ZmPIP2-6	**1.49**	0.03	**3.99**	1.11	**9.23**	3.07	**3.93**	0.74	**2.71**	0.62
ZmTIP1-1	**4.31**	1.02	**22.41**	6.81	**25.81**	6.88	**11.43**	1.09	**7.53**	2.99
ZmTIP1-2	**n.d**	n.d	**n.d**	n.d	**n.d**	n.d	**n.d**	n.d	**n.d**	n.d
ZmTIP2-1	**0.12**	0.04	**0.52**	0.12	**0.40**	0.11	**0.20**	0.01	**0.15**	0.01
ZmTIP2-2	**0.81**	0.38	**6.18**	1.22	**9.96**	0.97	**4.50**	0.89	**0.51**	0.33
ZmTIP2-4	**0.36**	0.10	**2.69**	1.47	**4.76**	0.57	**3.72**	0.91	**0.69**	0.15
ZmTIP3-1	**n.d**	n.d	**n.d**	n.d	**n.d**	n.d	**n.d**	n.d	**n.d**	n.d
ZmTIP3-2	**n.d**	n.d	**n.d**	n.d	**n.d**	n.d	**n.d**	n.d	**n.d**	n.d
ZmTIP4-1	**n.d**	n.d	**n.d**	n.d	**n.d**	n.d	**n.d**	n.d	**n.d**	n.d
ZmTIP4-2	**n.d**	n.d	**n.d**	n.d	**n.d**	n.d	**n.d**	n.d	**n.d**	n.d
ZmTIP4-3	**n.d**	n.d	**n.d**	n.d	**n.d**	n.d	**n.d**	n.d	**n.d**	n.d
ZmTIP4-4	**n.d**	n.d	**n.d**	n.d	**n.d**	n.d	**n.d**	n.d	**n.d**	n.d
ZmTIP5-1	**n.d**	n.d	**n.d**	n.d	**n.d**	n.d	**n.d**	n.d	**n.d**	n.d
ZmNIP1-1	**n.d**	n.d	**n.d**	n.d	**n.d**	n.d	**n.d**	n.d	**n.d**	n.d
ZmNIP2-1	**0.08**	0.03	**0.10**	0.01	**0.32**	0.06	**0.35**	0.05	**0.34**	0.08
ZmNIP2-2	**0.07**	0.01	**0.19**	0.03	**0.19**	0.04	**0.08**	0.01	**0.08**	0.01
ZmNIP3-1	**0.15**	0.03	**0.69**	0.12	**0.86**	0.22	**0.71**	0.04	**0.62**	0.12
ZmSIP1-1	**n.d**	n.d	**n.d**	n.d	**n.d**	n.d	**n.d**	n.d	**n.d**	n.d
ZmSIP1-2	**n.d**	n.d	**n.d**	n.d	**n.d**	n.d	**n.d**	n.d	**n.d**	n.d
ZmSIP2-1	**n.d**	n.d	**n.d**	n.d	**n.d**	n.d	**n.d**	n.d	**n.d**	n.d

2.2. The transcripts of *ZmMIPs* in the cortex and stele of maize primary roots.

Expression of *ZmMIPs* in cortex and stele of maize primary roots by DNA array. Total RNA were isolated from cortex and stele. The gene activity of ZmMIPs was assayed by DNA array. Three independent experiments were performed. Sd, the standard deviation of the mean; n.d, not detected.

Name of genes	Cortex	sd	Stele	sd
ZmPIP1-1	**8.91**	3.94	**1.26**	0.24
ZmPIP1-2	**0.80**	0.27	**0.50**	0.08
ZmPIP1-3	**0.27**	0.06	**0.13**	0.02
ZmPIP1-5	**6.88**	1.60	**1.57**	0.23
ZmPIP1-6	**n.d**	n.d	**n.d**	n.d
ZmPIP2-1	**3.77**	0.12	**1.97**	0.23
ZmPIP2-2	**1.02**	0.10	**0.54**	0.11
ZmPIP2-3	**0.31**	0.05	**n.d**	n.d
ZmPIP2-4	**1.32**	0.54	**0.17**	0.06
ZmPIP2-5	**2.50**	0.63	**0.93**	0.24
ZmPIP2-6	**4.20**	1.53	**3.59**	2.25
ZmTIP1-1	**20.49**	4.83	**2.19**	0.63
ZmTIP1-2	**0.13**	0.05	**n.d**	n.d
ZmTIP2-1	**0.32**	0.10	**n.d**	n.d
ZmTIP2-2	**7.52**	1.93	**1.75**	0.69
ZmTIP2-4	**5.95**	1.31	**0.38**	0.02
ZmTIP3-1	**0.03**	0.14	**n.d**	n.d
ZmTIP3-2	**n.d**	0.05	**n.d**	0.03
ZmTIP4-1	**n.d**	0.13	**n.d**	0.03
ZmTIP4-2	**n.d**	0.04	**n.d**	0.04
ZmTIP4-3	**n.d**	0.05	**n.d**	0.02
ZmTIP4-4	**n.d**	0.15	**n.d**	0.06
ZmTIP5-1	**n.d**	0.07	**n.d**	0.01
ZmNIP1-1	**0.02**	0.10	**n.d**	0.05
ZmNIP2-1	**0.45**	0.14	**n.d**	0.04
ZmNIP2-2	**0.24**	0.08	**n.d**	0.03
ZmNIP3-1	**0.91**	0.31	**n.d**	0.03
ZmSIP1-1	**n.d**	n.d	**n.d**	n.d
ZmSIP1-2	**0.13**	0.02	**0.12**	0.01
ZmSIP2-1	**0.14**	0.01	**n.d**	n.d

2.3. The effect of salt stress on the expression of *ZmMIPs* of maize roots.

ZmMIP transcripts in maize roots subjected to salt stress at different time points. Expression ratios of three independent replicates are given in comparison with unstressed plants. SD, the standard deviation of the mean; n.d., not detected; p, p-value of t-test.

Gene	2h/100NaCl			9h/100NaCl			24h/100NaCl			48h/100NaCl		
	Mean	sd	p	Mean	sd	p	Mean	sd	p	Mean	sd	p
ZmPIP1-1	**1.87**	0.32	0.014	**0.74**	0.15	0.060	**1.32**	0.48	0.179	**1.49**	0.69	0.157
ZmPIP1-2	**1.28**	0.61	0.349	**n.d**	n.d	n.d	**1.04**	0.12	0.316	**1.38**	0.55	0.261
ZmPIP1-3	**1.51**	0.18	0.013	**0.06**	n.d	n.d	**1.01**	0.52	0.397	**1.20**	0.45	0.344
ZmPIP1-5	**1.56**	0.10	0.004	**1.13**	0.27	0.254	**1.26**	0.37	0.194	**1.71**	0.95	0.141
ZmPIP1-6	**1.25**	0.10	0.021	**n.d**	n.d	n.d	**0.97**	0.38	0.379	**1.07**	0.20	0.319
ZmPIP2-1	**1.40**	0.13	0.012	**0.95**	0.30	0.360	**1.20**	0.47	0.291	**1.14**	0.24	0.220
ZmPIP2-2	**0.84**	0.04	0.013	**n.d**	n.d	n.d	**1.89**	0.86	0.103	**1.19**	0.66	0.413
ZmPIP2-3	**1.06**	0.15	0.331	**n.d**	n.d	n.d	**1.02**	0.40	0.478	**1.32**	0.65	0.332
ZmPIP2-4	**1.97**	0.67	0.037	**0.88**	0.30	0.246	**1.03**	0.28	0.487	**0.95**	0.04	0.174
ZmPIP2-5	**1.10**	0.31	0.352	**1.04**	0.39	0.489	**0.94**	0.38	0.340	**1.10**	0.26	0.309
ZmPIP2-6	**1.93**	0.74	0.063	**0.97**	0.47	0.371	**0.81**	0.52	0.217	**0.83**	0.25	0.161
ZmTIP1-1	**1.30**	0.04	0.003	**0.68**	0.07	0.012	**0.81**	0.23	0.145	**1.02**	0.56	0.420
ZmTIP1-2	**1.53**	0.45	0.067	**n.d**	n.d	n.d	**0.94**	0.30	0.390	**0.81**	n.d	n.d
ZmTIP2-1	**1.11**	0.33	0.375	**0.88**	0.07	0.116	**1.00**	0.43	0.414	**0.93**	0.22	0.276
ZmTIP2-2	**0.91**	0.27	0.282	**0.85**	0.27	0.212	**1.62**	0.71	0.144	**1.07**	0.06	0.093
ZmTIP2-4	**1.36**	0.17	0.027	**1.01**	0.07	0.394	**1.81**	0.56	0.049	**1.69**	0.39	0.037
ZmTIP3-1	**1.39**	0.38	0.180	**n.d**	n.d	n.d	**0.99**	n.d	n.d	**n.d**	n.d	n.d
ZmTIP3-2	**1.46**	0.34	0.136	**n.d**	n.d	n.d	**0.89**	0.12	0.221	**n.d**	n.d	n.d
ZmTIP4-1	**1.21**	0.39	0.307	**n.d**	n.d	n.d	**0.82**	0.22	0.226	**n.d**	n.d	n.d
ZmTIP4-2	**1.27**	0.04	0.031	**n.d**	n.d	n.d	**1.07**	0.77	0.450	**0.86**	n.d	n.d
ZmTIP4-3	**n.d**	n.d	n.d	**n.d**	n.d	n.d	**n.d**	n.d	n.d	**n.d**	n.d	n.d
ZmTIP4-4	**0.78**	1.03	0.294	**n.d**	n.d	n.d	**0.77**	0.22	0.202	**n.d**	n.d	n.d
ZmTIP5-1	**1.38**	0.47	0.221	**n.d**	n.d	n.d	**0.69**	n.d	n.d	**n.d**	n.d	n.d
ZmNIP1-1	**0.85**	0.23	0.259	**n.d**	n.d	n.d	**0.59**	n.d	n.d	**0.70**	n.d	n.d
ZmNIP2-1	**0.92**	0.19	0.255	**0.66**	0.12	0.030	**0.51**	0.05	0.003	**1.01**	0.46	0.463
ZmNIP2-2	**1.30**	0.38	0.222	**n.d**	n.d	n.d	**0.97**	0.48	0.414	**1.35**	n.d	n.d
ZmNIP3-1	**1.43**	n.d	n.d	**n.d**	n.d	n.d	**1.17**	n.d	n.d	**n.d**	n.d	n.d
ZmSIP1-1	**1.28**	n.d	n.d	**n.d**	n.d	n.d	**n.d**	n.d	n.d	**n.d**	n.d	n.d
ZmSIP1-2	**1.16**	0.45	0.385	**n.d**	n.d	n.d	**1.05**	0.22	0.425	**0.99**	0.20	0.444
ZmSIP2-1	**1.21**	0.53	0.364	**n.d**	n.d	n.d	**0.73**	0.06	0.062	**1.02**	0.05	0.304
RAB17	**1.41**	0.29	0.059	**n.d**	n.d	n.d	**2.50**	1.19	0.072	**n.d**	n.d	n.d

Gene	2h/200NaCl			9h/200NaCl			24h/200NaCl			48h/200NaCl		
	Mean	sd	p	Mean	sd	p	Mean	sd	p	Mean	sd	p
ZmPIP1-1	**1.31**	0.54	0.271	**1.02**	0.16	0.479	**0.91**	0.36	0.291	**1.70**	0.05	0.000
ZmPIP1-2	**1.33**	0.35	0.127	**n.d**	n.d	n.d	**0.58**	0.10	0.015	**1.47**	0.71	0.264
ZmPIP1-3	**1.10**	0.28	0.359	**0.72**	n.d	n.d	**0.72**	0.29	0.123	**1.14**	0.01	0.021
ZmPIP1-5	**0.87**	0.22	0.197	**0.92**	0.38	0.327	**0.50**	0.18	0.032	**1.14**	0.36	0.341
ZmPIP1-6	**0.93**	0.10	0.183	**n.d**	n.d	n.d	**0.31**	0.08	0.007	**0.83**	0.64	0.332
ZmPIP2-1	**0.96**	0.16	0.343	**0.74**	0.35	0.182	**1.01**	0.58	0.386	**0.99**	0.12	0.409
ZmPIP2-2	**0.86**	0.07	0.040	**n.d**	n.d	n.d	**1.20**	0.88	0.449	**1.60**	1.10	0.238
ZmPIP2-3	**0.87**	0.05	0.086	**n.d**	n.d	n.d	**0.81**	n.d	n.d	**1.45**	0.49	0.199
ZmPIP2-4	**1.07**	0.31	0.421	**1.00**	0.10	0.486	**0.32**	0.03	0.001	**1.00**	0.43	0.446
ZmPIP2-5	**0.92**	0.20	0.268	**0.64**	0.23	0.070	**0.31**	0.03	0.001	**0.68**	0.26	0.087
ZmPIP2-6	**1.09**	0.54	0.467	**1.10**	0.26	0.335	**0.53**	0.14	0.022	**0.71**	0.19	0.065
ZmTIP1-1	**0.76**	0.04	0.009	**0.92**	0.29	0.305	**0.55**	0.20	0.045	**0.77**	0.17	0.077
ZmTIP1-2	**1.11**	0.18	0.281	**n.d**	n.d	n.d	**0.52**	0.06	0.037	**1.15**	0.55	0.432
ZmTIP2-1	**0.93**	0.13	0.207	**0.69**	0.27	0.192	**0.35**	0.11	0.017	**0.67**	0.42	0.132

ZmTIP2-2	**0.80**	0.15	0.085	**0.33**	0.16	0.025	**0.12**	0.03	0.032	**0.56**	0.33	0.106
ZmTIP2-4	**0.96**	0.27	0.363	**1.07**	0.60	0.432	**0.59**	0.28	0.103	**1.14**	0.63	0.478
ZmTIP3-1	**0.80**	0.05	0.063	**n.d**	n.d	n.d	**0.07**	n.d	n.d	**0.87**	n.d	n.d
ZmTIP3-2	**1.10**	0.44	0.438	**n.d**	n.d	n.d	**n.d**	n.d	n.d	**0.83**	n.d	n.d
ZmTIP4-1	**1.04**	0.19	0.415	**n.d**	n.d	n.d	**0.69**	0.17	0.136	**1.06**	n.d	n.d
ZmTIP4-2	**0.87**	0.16	0.228	**n.d**	n.d	n.d	**0.76**	0.35	0.255	**0.79**	0.14	0.153
ZmTIP4-3	**0.81**	0.08	0.106	**n.d**	n.d	n.d	**n.d**	n.d	n.d	**n.d**	n.d	n.d
ZmTIP4-4	**1.01**	0.15	0.498	**n.d**	n.d	n.d	**0.88**	n.d	n.d	**0.68**	0.17	0.133
ZmTIP5-1	**0.80**	0.08	0.086	**n.d**	n.d	n.d	**n.d**	n.d	n.d	**n.d**	n.d	n.d
ZmNIP1-1	**0.93**	0.05	0.169	**n.d**	n.d	n.d	**0.74**	n.d	n.d	**1.00**	n.d	n.d
ZmNIP2-1	**0.96**	0.56	0.345	**0.38**	0.15	0.087	**0.10**	0.10	n.d	**0.63**	0.36	0.212
ZmNIP2-2	**1.09**	0.02	0.053	**n.d**	n.d	n.d	**0.53**	0.05	0.038	**1.12**	n.d	n.d
ZmNIP3-1	**1.08**	0.22	0.368	**n.d**	n.d	n.d	**0.60**	n.d	n.d	**n.d**	n.d	n.d
ZmSIP1-1	**0.97**	0.18	0.409	**n.d**	n.d	n.d	**n.d**	n.d	n.d	**n.d**	n.d	n.d
ZmSIP1-2	**1.07**	0.00	0.024	**0.27**	n.d	n.d	**0.31**	n.d	n.d	**1.38**	0.21	0.106
ZmSIP2-1	**0.93**	0.25	0.366	**n.d**	n.d	n.d	**0.47**	0.05	0.031	**1.19**	0.45	0.354
RAB17	**1.37**	0.77	0.375	**26.15**	9.54	0.026	**39.41**	26.94	0.011	**42.07**	32.89	0.070

2.4. The expression profile of ZmMIPs of maize roots after treatment with ABA.

ZmMIP genes expressed in maize roots in response to ABA. Expression ratios of three independent replicates are given in comparison with unstressed roots. Sd. the standard deviation of the mean; n.d. not detected; K. k-value of t-test.

Gene	1h/1µMABA			6h/1µM ABA			24h/1µM ABA		
	Mean	**sd**	**p**	**Mean**	**sd**	**p**	**Mean**	**sd**	**p**
ZmPIP1-1	**1.68**	0.53	0.052	**1.59**	0.09	0.002	**1.63**	0.31	0.025
ZmPIP1-2	**1.87**	0.30	0.012	**1.99**	0.96	0.074	**1.90**	0.42	0.018
ZmPIP1-3	**1.41**	0.67	0.222	**1.44**	0.63	0.191	**1.63**	0.31	0.089
ZmPIP1-5	**1.62**	0.51	0.065	**1.35**	0.56	0.205	**1.10**	0.27	0.318
ZmPIP1-6	**1.59**	0.03	0.009	**1.99**	n.d	n.d	**1.05**	0.32	0.469
ZmPIP2-1	**1.46**	0.24	0.034	**1.55**	0.36	0.046	**1.43**	0.34	0.065
ZmPIP2-2	**1.42**	0.08	0.004	**0.95**	0.15	0.361	**0.90**	0.22	0.245
ZmPIP2-3	**1.21**	0.16	0.142	**0.63**	n.d	n.d	**1.42**	0.16	0.072
ZmPIP2-4	**2.35**	0.34	0.005	**1.31**	0.56	0.233	**1.65**	0.72	0.156
ZmPIP2-5	**1.48**	0.43	0.098	**1.52**	0.94	0.244	**1.32**	0.50	0.215
ZmPIP2-6	**1.45**	0.45	0.093	**1.31**	0.58	0.306	**1.55**	0.43	0.064
ZmTIP1-1	**1.43**	0.21	0.025	**1.48**	0.39	0.062	**1.34**	0.22	0.045
ZmTIP1-2	**1.97**	n.d	n.d	**1.86**	n.d	n.d	**1.29**	0.08	0.053
ZmTIP2-1	**1.59**	0.76	0.187	**1.02**	0.17	0.470	**1.05**	0.34	0.479
ZmTIP2-2	**1.24**	0.12	0.034	**0.81**	0.23	0.157	**0.76**	0.22	0.116
ZmTIP3-1	**1.43**	n.d	n.d	**0.56**	n.d	n.d	**1.34**	n.d	n.d
ZmTIP3-2	**1.60**	n.d	n.d	**0.72**	n.d	n.d	**1.71**	n.d	n.d
ZmTIP4-1	**2.06**	n.d	n.d	**1.38**	n.d	n.d	**1.46**	n.d	n.d
ZmTIP4-2	**1.41**	n.d	n.d	**1.36**	n.d	n.d	**1.19**	n.d	n.d
ZmTIP4-3	**ND**	n.d	n.d	**n.d**	n.d	n.d	**n.d**	n.d	n.d
ZmTIP4-4	**1.76**	n.d	n.d	**0.84**	n.d	n.d	**1.71**	n.d	n.d
ZmTIP5-1	**1.52**	n.d	n.d	**0.87**	n.d	n.d	**1.42**	n.d	n.d

ZmTIP2-4	**1.19**	0.10	0.036	**1.07**	0.46	0.493	**0.90**	0.39	0.304
ZmNIP1-1	**1.05**	0.07	0.227	**0.77**	0.40	0.200	**0.76**	0.10	0.108
ZmNIP2-1	**0.92**	0.46	n.d	**0.43**	0.18	0.043	**0.61**	0.23	0.084
ZmNIP2-2	**n.d**	n.d	n.d	**1.69**	0.46	0.118	**1.43**	0.47	0.199
ZmNIP3-1	**n.d**	n.d	n.d	**1.01**	0.27	0.481	**1.42**	0.06	0.002
ZmSIP1-1	**n.d**	n.d	n.d	**n.d**	n.d	n.d	**n.d**	n.d	n.d
ZmSIP1-2	**1.57**	0.39	0.123	**1.54**	0.41	0.138	**1.09**	0.03	0.071
ZmSIP2-1	**1.30**	0.04	0.027	**1.77**	0.53	0.120	**1.40**	0.10	0.049
RAB17	**1.35**	n.d	n.d	**2.28**	1.69	0.137	**2.86**	1.74	0.050

Gene	**1h/100µM ABA**			**6h/100µM ABA**			**24h/100µM ABA**		
	Mean	**sd**	**p**	**Mean**	**sd**	**p**	**Mean**	**sd**	**p**
ZmPIP1-1	**2.09**	0.67	0.029	**1.30**	0.53	0.274	**0.45**	0.22	0.047
ZmPIP1-2	**1.65**	0.46	0.056	**1.07**	0.09	0.165	**0.20**	0.07	0.029
ZmPIP1-3	**1.66**	0.50	0.061	**0.54**	0.12	0.020	**0.23**	0.09	0.062
ZmPIP1-5	**1.65**	0.42	0.050	**0.61**	0.22	0.065	**0.12**	0.05	0.007
ZmPIP1-6	**1.36**	0.02	0.008	**0.45**	n.d	n.d	**0.16**	0.14	0.105
ZmPIP2-1	**1.54**	0.28	0.032	**0.72**	0.12	0.035	**0.31**	0.14	0.029
ZmPIP2-2	**1.26**	0.06	0.007	**0.70**	0.10	0.088	**0.14**	0.10	0.080
ZmPIP2-3	**1.13**	0.19	0.190	**0.15**	n.d	n.d	**0.09**	n.d	n.d
ZmPIP2-4	**2.35**	0.21	0.002	**0.63**	0.15	0.043	**0.19**	0.07	0.008
ZmPIP2-5	**1.43**	0.13	0.011	**0.41**	0.07	0.005	**0.11**	0.04	0.004
ZmPIP2-6	**1.44**	0.62	0.191	**0.28**	0.07	0.007	**0.11**	0.08	0.026
ZmTIP1-1	**1.21**	0.20	0.103	**1.61**	0.41	0.053	**0.39**	0.18	0.030
ZmTIP1-2	**1.30**	0.24	0.153	**0.78**	n.d	n.d	**0.20**	0.11	0.074
ZmTIP2-1	**1.40**	0.10	0.007	**0.57**	0.24	0.065	**0.21**	0.16	0.053
ZmTIP2-2	**0.92**	0.26	0.296	**0.25**	0.16	0.035	**0.06**	0.05	0.022
ZmTIP3-1	**1.09**	n.d	n.d	**0.32**	n.d	n.d	**0.30**	n.d	n.d
ZmTIP3-2	**1.40**	n.d	n.d	**n.d**	n.d	n.d	**0.52**	n.d	n.d
ZmTIP4-1	**1.43**	n.d	n.d	**n.d**	n.d	n.d	**0.29**	n.d	n.d
ZmTIP4-2	**1.13**	n.d	n.d	**1.27**	0.54	0.324	**0.60**	n.d	n.d
ZmTIP4-3	**1.24**	n.d	n.d	**0.41**	n.d	n.d	**n.d**	n.d	n.d
ZmTIP4-4	**0.79**	n.d	n.d	**0.37**	n.d	n.d	**0.26**	n.d	n.d
ZmTIP5-1	**1.11**	n.d	n.d	**0.35**	n.d	n.d	**0.26**	n.d	n.d
ZmTIP2-4	**1.06**	0.31	0.440	**0.48**	0.06	0.004	**0.16**	0.06	0.006
ZmNIP1-1	**0.85**	0.24	0.188	**0.37**	0.23	0.061	**0.09**	0.09	0.093
ZmNIP2-1	**0.71**	0.26	0.123	**0.11**	0.06	0.010	**0.11**	0.01	0.000
ZmNIP2-2	**1.28**	0.54	0.315	**0.91**	0.22	0.323	**0.23**	n.d	n.d
ZmNIP3-1	**1.00**	0.23	0.465	**0.76**	0.55	0.188	**0.24**	0.07	0.044
ZmSIP1-1	**n.d**	n.d	n.d	**n.d**	n.d	n.d	**n.d**	n.d	n.d
ZmSIP1-2	**1.35**	0.37	0.195	**0.62**	n.d	n.d	**0.06**	n.d	n.d
ZmSIP2-1	**1.01**	0.06	0.468	**1.12**	0.10	0.167	**0.58**	n.d	n.d
RAB17	**1.23**	0.16	0.132	**91.88**	69.51	0.004	**50.51**	27.18	0.003

2.5. The response of transcripts of *ZmMIPs* of maize roots to the deprivation and addition of K^+.

Maize seedlings were cultured in complete and K^+-deficient hydroponic solutions for 8 and 9 days. The deficient media were resupplied with the missing ions on day 10 six hours before sampling. The expression of *ZmMIPs* was analyzed by DNA array using *ZmMIP* array. Sd. the standard deviation of the mean; n.d. not detected.

Gene	Day 8	sd	Day 9	sd	Day 10	sd	Day 11	sd
ZmPIP1-1	**0.60**	0.07	**1.26**	0.38	**1.57**	0.48	**1.98**	0.36
ZmPIP1-2	**0.38**	0.03	**0.82**	0.38	**1.39**	0.05	**1.36**	0.17
ZmPIP1-3	**0.46**	0.13	**0.78**	0.08	**1.72**	0.50	**1.05**	0.17
ZmPIP1-5	**0.42**	0.03	**0.66**	0.11	**1.43**	0.10	**1.07**	0.37
ZmPIP1-6	**0.49**	0.21	**0.72**	0.02	**1.31**	0.17	**0.99**	0.14
ZmPIP2-1	**0.46**	0.05	**0.70**	0.20	**1.72**	0.35	**1.48**	0.41
ZmPIP2-2	**0.47**	0.06	**0.52**	0.13	**1.36**	0.32	**1.33**	0.43
ZmPIP2-3	**0.48**	0.18	**0.54**	0.30	**1.47**	0.05	**1.38**	0.00
ZmPIP2-4	**0.45**	0.16	**0.87**	0.02	**1.89**	0.18	**1.49**	0.14
ZmPIP2-5	**0.47**	0.03	**0.98**	0.10	**1.55**	0.09	**1.14**	0.38
ZmPIP2-6	**0.54**	0.37	**1.13**	0.52	**2.18**	0.14	**0.91**	0.08
ZmTIP1-1	**0.44**	0.00	**0.64**	0.06	**1.29**	0.11	**1.32**	0.72
ZmTIP1-2	**0.49**	0.28	**0.79**	0.11	**1.83**	0.17	**1.27**	0.12
ZmTIP2-1	**0.62**	0.07	**0.73**	0.02	**1.73**	0.44	**1.50**	0.40
ZmTIP2-2	**0.53**	0.03	**0.63**	0.09	**1.29**	0.23	**1.70**	0.99
ZmTIP2-4	**0.39**	0.05	**0.33**	0.12	**1.33**	0.24	**1.16**	0.10
ZmTIP3-1	**0.50**	0.16	**0.53**	0.22	**1.57**	0.26	**1.33**	0.30
ZmTIP3-2	**0.63**	0.25	**1.18**	0.24	**1.57**	0.43	**1.46**	0.30
ZmTIP4-1	**0.42**	0.01	**0.85**	0.31	**1.30**	0.07	**1.19**	0.23
ZmTIP4-2	**0.47**	0.03	**0.73**	0.16	**1.66**	0.06	**1.18**	0.27
ZmTIP4-3	**0.47**	0.17	**0.94**	0.03	**1.49**	0.26	**1.24**	0.19
ZmTIP4-4	**0.48**	0.14	**0.81**	0.10	**1.22**	0.21	**1.20**	0.07
ZmTIP5-1	**0.51**	0.18	**0.64**	0.09	**1.41**	0.31	**1.28**	0.02
ZmNIP1-1	**0.70**	0.00	**0.53**	0.35	**1.00**	0.00	**1.11**	0.37
ZmNIP2-1	**0.57**	0.10	**0.94**	0.32	**1.09**	0.10	**0.98**	0.30
ZmNIP2-2	**0.48**	0.08	**0.98**	0.00	**1.74**	0.57	**1.35**	0.03
ZmNIP3-1	**0.55**	0.25	**0.89**	0.15	**1.73**	0.45	**1.21**	0.17
ZmSIP1-1	**0.51**	0.22	**0.86**	0.21	**1.40**	0.29	**1.20**	0.18
ZmSIP1-2	**0.51**	0.20	**0.81**	0.15	**1.35**	0.32	**1.25**	0.12
ZmSIP2-1	**0.56**	0.12	**0.76**	0.05	**1.61**	0.48	**1.30**	0.01
Rab17	**0.64**	0.13	**0.78**	0.15	**1.60**	0.47	**1.52**	0.23

2.6. The response of transcripts of *ZmMIPs* of maize roots to the deprivation and addition of NO_3^-.

Maize seedlings were cultured in complete and NO^-_3-deficient hydroponic solutions for 8 and 9 days. The deficient media were resupplied with the missing ions on day 10 six hours before sampling. The expression of *ZmMIPs* was analyzed by DNA array using *ZmMIP* array. Sd. the standard deviation of the mean; n.d. not detected.

Gene	Day 8	sd	Day 9	sd	Day 10	sd	Day 11	sd
ZmPIP1-1	**1.15**	0.13	**1.47**	0.83	**1.15**	0.12	**1.52**	0.45
ZmPIP1-2	**1.17**	0.02	**1.30**	0.78	**1.60**	0.46	**1.29**	0.15
ZmPIP1-3	**0.82**	0.17	**0.66**	0.11	**1.00**	0.24	**0.95**	0.31
ZmPIP1-5	**0.41**	0.03	**0.44**	0.01	**0.63**	0.21	**0.98**	0.61
ZmPIP1-6	**0.64**	0.17	**0.56**	0.23	**0.83**	0.22	**1.11**	0.67
ZmPIP2-1	**1.33**	0.58	**0.99**	0.39	**1.31**	0.03	**1.33**	0.30
ZmPIP2-2	**0.80**	0.06	**0.81**	0.37	**1.23**	0.40	**1.71**	0.44
ZmPIP2-3	**0.68**	0.05	**0.74**	0.28	**1.10**	0.23	**1.90**	0.88
ZmPIP2-4	**0.89**	0.11	**0.86**	0.29	**1.30**	0.31	**1.17**	0.51
ZmPIP2-5	**0.74**	0.14	**0.87**	0.22	**0.66**	0.13	**0.93**	0.53
ZmPIP2-6	**0.82**	0.22	**0.62**	0.28	**1.17**	0.23	**1.08**	0.57
ZmTIP1-1	**0.61**	0.05	**0.46**	0.11	**1.27**	0.16	**1.43**	0.44
ZmTIP1-2	**0.86**	0.07	**0.92**	0.36	**1.06**	0.08	**1.29**	0.26
ZmTIP2-1	**0.76**	0.07	**0.86**	0.23	**0.99**	0.11	**1.40**	0.01
ZmTIP2-2	**1.06**	0.04	**1.04**	0.22	**1.61**	0.32	**2.36**	0.96
ZmTIP2-4	**0.60**	0.09	**0.52**	0.24	**0.81**	0.32	**1.30**	0.22
ZmTIP3-1	**0.76**	0.02	**0.74**	0.16	**1.26**	0.24	**2.01**	0.72
ZmTIP3-2	**0.96**	0.09	**1.05**	0.48	**1.19**	0.35	**1.47**	0.29
ZmTIP4-1	**0.87**	0.20	**0.83**	0.35	**1.06**	0.37	**1.03**	0.18
ZmTIP4-2	**0.76**	0.15	**0.68**	0.19	**1.12**	0.22	**1.08**	0.44
ZmTIP4-3	**0.74**	0.01	**0.86**	0.11	**1.23**	0.61	**1.16**	0.28
ZmTIP4-4	**0.77**	0.15	**0.89**	0.57	**1.18**	0.48	**1.24**	0.28
ZmTIP5-1	**0.80**	0.16	**0.64**	0.27	**1.13**	0.33	**1.14**	0.26
ZmNIP1-1	**0.58**	0.10	**0.50**	0.18	**0.85**	0.24	**1.55**	0.99
ZmNIP2-1	**0.76**	0.07	**0.73**	0.00	**0.76**	0.37	**0.83**	0.49
ZmNIP2-2	**0.98**	0.04	**1.11**	0.22	**1.11**	0.04	**1.23**	0.34
ZmNIP3-1	**0.89**	0.13	**0.87**	0.09	**1.32**	0.13	**1.44**	0.04
ZmSIP1-1	**0.78**	0.02	**0.52**	0.18	**1.10**	0.24	**1.26**	0.23
ZmSIP1-2	**0.87**	0.01	**0.89**	0.36	**1.11**	0.06	**1.26**	0.11
ZmSIP2-1	**0.80**	0.04	**0.87**	0.21	**1.31**	0.16	**1.55**	0.12
Rab17	**0.81**	0.12	**0.83**	0.39	**1.37**	0.34	**1.43**	0.11

ACKNOWLEDGEMENT

At first I would like to deeply thank my supervisor. PD Dr. A. R. Schäffner in the Institute of Biochemical Plant Pathology in GSF Research Centre for Environment and Health for giving me the opportunity to pursue the doctoral degree of Biochemistry in his laboratory and challenge myself in the field of molecular biology. I thank him for confidence. encouragement and supervision during my stay and for discussion, correction and review of this manuscript.

I would express my profound gratitude and deep appreciation to Prof. Dr. H. Sandermann for accepting me as a member of “BIOP”.

I would like to express my sincere gratitude to Prof. Dr. Stefan Weiss at the Institute of Biochemistry of the Ludwig-Maximilians-University Munich for accepting to be my second referee.

I appreciate Dr. Burkhard Messner for suggestions and correction of this manuscript. On the other hand. with his help I have gone a short way and saved much time in usage of Gateway technique and isolation, purification and characterization of fusion proteins.

I am thankful to Dr. Henrik Buschmann for direction on isolation and purification of total RNA and plasmid DNA and for help in accommodation.

I show much gratitude to Dr. Matthias Affenzeller for discussing aquaporin with me and helping in using the program “Haruspex” for analysis of DNA array data.

Special thanks to Dr. M. Götz for his kind help in statistic analysis of DNA array data and discussion of technical problem.

I am also grateful to Dr. Oliver Thulke and Dr. Olaf Neuschaefer-Rube for technical assistance in printing DNA probes on the membrane.

Cordial thanks to Dr. Xi Huang for his kindly technical direction in performing Northern analysis.

My sincere thanks go to Dr. Christian Lindermayr. Dr. Sebastian Grün. and Olivier Da Ines for analysis of proteins and discussion of aquaporins.

Thanks very much to Dr. Mohamed Sathik for discussion and critical readings of this manuscript.

I am grateful to Dr. Hagen Scherb in Institute of Biomathematics for selection of statistic methods and statistic analysis of data.

I wish to express my gratitude to Prof. Dr. U. Heinzmann and Ms. Elenore Samsone in Institute of Pathology for cutting and pre-treatment of materials for in situ hybridisation.

I sincerely thank my colleagues Birgit Geist, Elke Gerstner and Susanna Holzinger for their friendly technical assistance and collaboration.

My thanks go to the staffs of BIOP for their help during the period of this work.

I wish to express my special gratitude to Prof. Wolfram Hartung and Daniela Schraut at the University Würzburg for fruitful cooperation and discussions

Many thanks to Prof. Ernst Steudle at the University Bayreuth for chance of practice by which I could learn to measure the hydraulic conductivity of cells in vivo using cell pressure probe.

I am indebted to my wife and my child for their support and assistance.

Finally, I thank the “Deutsche Forschungsgemeinschaft (DFG)” for financial support.

CURRICULUM VITAE

PERSONAL DETAILS

Name:	Chuanfeng Zhu
Date of birth:	May 15, 1965
Place of Birth:	Henan. P.R. China
Nationality:	Chinese
Marital status:	Married
Parents:	Xiurong Kang and Jialiu Zhu

EDUCATION

1972-1977:	Primary School in Zhaolou. Henan. P.R. China
1977-1981:	Middle School in Zhecheng. Henan. P.R. China
1981-1985:	Henan Normal University. P.R. China
Sep. 1985:	Bachelor of Science
1985-1988:	Lanzhou University. P.R. China
Jul. 1988:	Master of Science
2001- to date:	Ludwig-Maximilians University Munich. Germany GSF-National Research Centre for Environment and Health Institute of Biochemical Plant Pathology. Under the Supervision of PD Dr. Anton R. Schäffner. "Effects of abiotic stimuli and the phytohormone ABA on aquaporin gene family in maize roots"

PROFESSIONAL TRAINING

1999-2000:	University of International Business and Economics (UIBE) AfDS (Ausbildung für Deutsche Sprache) center
2000-2001:	Practice of "Urban environmental protection 2000/2001" in Germany. Financed by Carl Duisberg Gesellschaft e.V.

WORK EXPERIENCE

1988-1991:	Lanzhou University. Institute of Plant Physiology. Lecturer/Research Assistant.
1991-1999:	Gansu Provincial Environmental Monitoring Centre. P.R.China, Engineer/Technical President.

PUBLICATION

Chuanfeng Zhu, Daniela Schraut, Wolfram Hartung, Anton R. Schäffner. 2005. Differential response of maize MIP genes to salt stress and ABA. *J. Exp. Bot.* (submitted).